



FITTING THE EXTINCTION CURVES OF GRB HOST GALAXIES USING DUST MODELS

MASTER THESIS

Written by *Kristina S. Jepsen, lpt586*
30. juni 2021

Supervised by
Anja C. Andersen

UNIVERSITY OF COPENHAGEN

A large, abstract geometric design in the bottom right corner, consisting of several overlapping circles and lines in a light gray color.



UNIVERSITY OF
COPENHAGEN

NAME OF INSTITUTE: Niels Bohr Institutet

NAME OF DEPARTMENT: Niels Bohr Institutet

AUTHOR(S): Kristina S. Jepsen, lpt586

EMAIL: lpt586@alumni.ku.dk

TITLE AND SUBTITLE: Fitting the extinction curves of GRB host galaxies using dust models

-

SUPERVISOR(S): Anja C. Andersen

HANDED IN: 30.06.2021

DEFENDED: 08.07.2021

NAME Kristina Sundgaard Jepsen

SIGNATURE *Kristina S Jepsen*

DATE 30/06/2021

Abstract

Extinction curves of the Milky Way (MW), Large Magellanic Cloud (LMC) and Small Magellanic Cloud (SMC) have given us a unique possibility to gain insight into the dust compositions of these three galaxies. For many years these were the only galaxies where we had a direct way to measure the interstellar dust composite. Recently it has become possible to obtain extinction curves of gamma-ray bursts (GRBs) host galaxies, which has opened the possibility to study the interstellar dust within distant early-type galaxies in great detail.

In this thesis I am examining the extinction curves of the MW, the LMC, the SMC and 10 different GRB host galaxies to identify possible ideal interstellar dust combination which can explain the observed extinction in these galaxies. To obtain the dust combinations, I have reproduced the observed extinction curves using laboratory measurements of the individual extinction of a select group of carbon and silicate dust grains expected to be good representatives for the average interstellar dust composition in galaxies.

Combining different dust grain size combinations and different materials I find that the MW and LMC are best represented by a dust composition consisting of a mix of carbon and silicate dust. However, for the SMC and the different GRB host galaxies, the dust composition which best represents the observations contains only silicate dust. Both of these dust combination types are reasonable because they are consistent with dust composition found in other studies of the extinction curves.

Resumé

Ekstinktionskurver fra Mælkevejen, den Store Magellanske Sky og den Lille Magellanske Sky har givet os en unik mulighed for at få indsigt i støvindholdet i de tre galakser. I mange år var disse de eneste galakser hvor vi havde mulighed for at måle støvsammensætningen direkte. For nyligt er det blevet muligt at få ekstinktionskurver fra gamma-ray bursts host galaxies. Dette har åbnet op for at støv sammensætningen også kan undersøges i fjerntype galakser i stor detalje.

I dette speciale vil jeg undersøge ekstinktionskurverne fra Mælkevejen, den Store Magellanske Sky, den Lille Magellanske Sky og 10 forskellige GRB host galaxies for at identificere ideelle støvkombinationer, som kan forklare de observerede ekstinktionskurver. For at finde disse støvkombinationer har jeg reproduceret de observerede ekstinktionskurver ved hjælp af laboratorie målinger af den individuelle ekstinktion fra udvalgte silikat og karbon støv korn, som forventes at være en god repræsentation af støvet i galakserne.

Ved at kombinere forskellige støv korn størrelser og støv af forskelligt materiale finder jeg at Mælkevejen og den Store Magellanske Sky bedst kan repræsenteres af en støvkombination bestående af silikat og karbon støv. For den Lille Magellanske Sky og de 10 GRB host galaxies er det dog kun støv bestående af silikat der er den bedste støvkombination. Begge disse kombinationer er rimelige da de stemmer overens med hvad andre studier af de forskellige ekstinktionskurver finder er de bedste støvkombinationer.

Contents

1	Introduction	1
2	Extinction	2
3	Interstellar dust	3
4	Host galaxies	5
4.1	The Milky Way galaxy	6
4.2	The Magellanic Clouds	7
4.2.1	The Large Magellanic Cloud	8
4.2.2	The Small Magellanic Cloud	9
4.3	Gamma-ray burst	9
5	Extinction curves	10
5.1	Milky Way	11
5.2	Large Magellanic cloud	12
5.3	The Small Magellanic Cloud	13
5.4	Gamma-ray bursts	13
5.5	Supernova like extinction	14
6	Dust grains	15
6.1	Grain sizes	15
6.2	Complex refractive index	16
6.3	DDSCAT	17
6.4	Grain shape	20
6.5	Carbon	24
6.6	Silicates	25
7	Fitting routine	26
7.1	Finding the average particle density	27
7.2	Loop setup	27
7.3	Bins vs computation time	28
7.4	Interpolation	30
7.5	Picking best fit	30
7.6	How to bin the grain sizes	32
8	Fitting routine tests	32
8.1	Position of bins	32
8.2	Which dust grains dominate the extinction curves	33
9	Results	36
9.1	Milky Way extinction fit	36
9.2	Large Magellanic Cloud average extinction fit	40
9.3	Large Magellanic Cloud supershell extinction fit	44
9.4	Small Magellanic Cloud extinction fit	48
9.5	GRB host galaxy extinction fits	53
9.6	GRB 090313A extinction fit	56

9.7	GRB 100219A extinction fit	57
9.8	GRB 100418A extinction fit	58
9.9	GRB 100901A extinction fit	59
9.10	GRB 111008A extinction fit	60
9.11	GRB 111209A extinction fit	61
9.12	GRB 120119A extinction fit	62
9.13	GRB 120815A extinction fit	63
9.14	GRB 121024A extinction fit	64
9.15	GRB 130427A extinction fit	65
10	Discussion	66
10.1	Why can't the 2175Å bump fitted?	66
10.2	Why is it silicate dust that gives the best dust combination?	67
11	Conclusion and outlook	70
12	Litterateur	I
A	Fitting routine raw code	VI
B	Mixed dust combination fits of GRB's	XV

1 Introduction

When looking up at the dark night sky it is possible to see the belt of the Milky Way. This belt is filled with faraway stars, gas and dust. In all its glowing glory it is easy to overlook the dark spots giving a sharp contrast to the light. These dark spots are just as important for the galaxy as the light. The dark spots contain the gas and dust which can be used to make new stars and planets form. But just like the dust can be helpful, it can also be a hindrance. When trying to determine distances to objects within the galaxy, the dust blocks the light making the object appear further away. This effect is called extinction. The extinction is a measurement of how much light the dust absorbs and scatters. For the Milky Way (hereafter MW) the interstellar extinction curve has been known for some time and is characterised by a bump at 2175\AA [1]. Besides the MW it is possible to determine the extinction of the Large and Small Magellanic clouds (hereafter LMC, SMC). Both of these differ from the MW curve. The LMC has a smaller bump and a steeper rise in smaller wavelengths, and the SMC is a step featureless curve [2]. For some time these were the only galaxies it was possible to determine the extinction for. Within the last 10-15 years, it has become possible to determine the extinction curve of gamma-ray burst (hereafter GRB) host galaxies using the deviations from the normal power-law spectral energy distribution.

As mentioned earlier the extinction can be a hindrance in some cases, but it can also be useful. Since extinction is a measure of how much light is absorbed and scattered by the dust, we can use it to determine what kind of dust caused the extinction. In 1977 Mathis, Rumpel and Nordsieck (hereafter MRN) came up with a power-law fit that took the natural abundance of the elements into account when fitting different size distribution and dust combinations, to the observed extinction curves. They found that to get a good fit for the 2175\AA feature they had to make a combination of carbon dust and some other material. If they hadn't used a mix of dust materials they would not be able to fit the entire extinction curve well according to their criteria. They got the best fits when using a combination of carbon and some form of silicate dust [3]. This combination has been explored in numerous articles, most of which agrees with the outcome of the MRN interpretation. It is therefore possible from the extinction curves to gain knowledge of the dust composition of the galaxy in which the extinction curve originates. In this thesis I will examine the extinction curves of the MW, LMC, SMC and ten GRB host galaxies. I will try to fit combinations of different dust materials and dust grain sizes to the observed extinction curves. I will do this to examine if it is possible to recreate the extinction using the single dust grain sizes unique extinction. Thereby I will be showing that the extinction is caused by certain types of grains of certain materials for the specific galaxy. This will indicate whether or not the simple carbon and silicate dust model proposed by MRN is viable for all galaxies. It will also provide insight into the host galaxies of the GRBs which may not always be resolved when observing the burst. This method can therefore tell what the dust in the galaxy most likely is made of without having a direct measurement of the host galaxy.

2 Extinction

Before I start examining the different extinction curves I have to understand what causes the extinction in the first place. The extinction is a measurement of how dust in the line of sight absorbs and scatters light, thereby obscuring the light source behind it. If I assume that the extinction goes to zero when the wavelength $\lambda \rightarrow \infty$ and I have observations of the object at long wavelengths where the extinction is very small, it becomes possible to determine the dimming of the light caused by the dust. This dimming effect caused by the dust, the extinction A_λ at wavelength λ is measured in magnitudes and is defined the following way

$$\frac{A_\lambda}{mag} = 2.5 \log \left(\frac{F_\lambda^0}{F_\lambda} \right). \quad (1)$$

Here F_λ is the observed flux and F_λ^0 is the non extinguished flux of the object [4].

The extinction curves I am going to examine in this thesis are mostly observed in the visual wavelengths and partly in UV and IR wavelengths. I will therefore normalise the measured extinction A_λ with the extinction in the visual band A_V . The visual extinction is 1 at $1.8\mu m^{-1}$ because $1.8\mu m^{-1}$ it is the centre of the V band filter. As an example, the normalised MW extinction curve is displayed in figure 1.

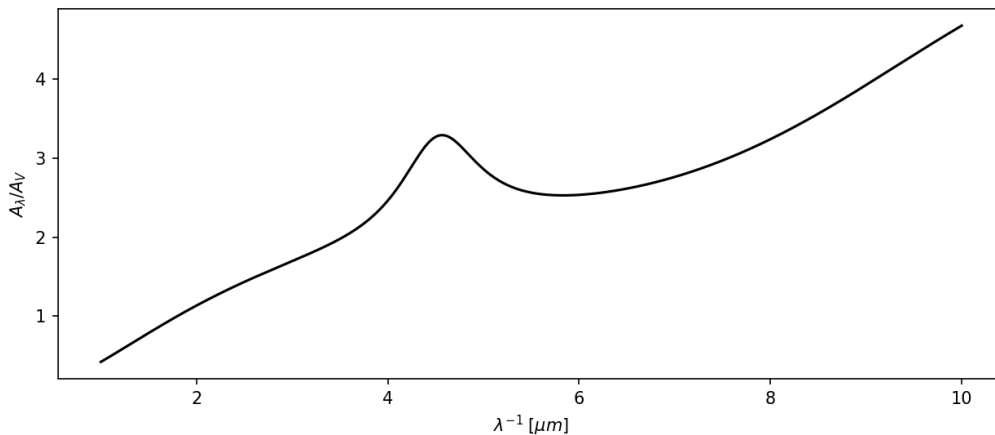


Figure 1: The normalised extinction curve of the MW, with $R_V = 3.1$ as a function of inversed wavelength [1].

Besides absorbing and scattering light dust can also polarise it. The polarisation arises from nonspherical grains that somehow are aligned by the interstellar magnetic field. The polarisation of dust grains has the biggest effect on the extinction around the V band, approximately at 5500 \AA . Here it can become as much as $0.03A_V/mag$. The polarisation tends to be larger when the reddening $R_V = \frac{A_V}{A_B - A_V}$ is large. For the extinction curves examined in this thesis, most have an R_V smaller or similar to that of the MW extinction curve in figure 1. It is therefore fair to assume that a limited amount of extinction is caused by polarisation from the dust grains in these cases [4].

3 Interstellar dust

In order to fit the dust grain sizes to the observed extinction curves, I first have to establish what a typical dust grain is. Interstellar dust is normally much smaller than the dust we are used to here on Earth. A typical lower bound on the transition from molecule to dust grain is ≈ 50 atoms corresponding to a grain radius of 3.5\AA [4]. These grains are very small even for interstellar grains that can become as large as $0.4\mu\text{m}$, with very few grains exceeding this size [5].

What exactly the dust is made of is a more complicated story. The only way to know for certain is by examining spectral features in extinction, scattering and emission [6]. One of the most characteristic features of extinction curves is that of the 2175\AA bump, which can be seen in figure 1. The bump is now thought to be caused by large polycyclic aromatic hydrocarbon (hereafter PAH) molecules, based on interstellar abundances and their ability to fit the varying full width half maximum (hereafter FWHM) of the bump, in different sightlines. In earlier models, the bump was thought to occur from graphite or even large silicate grains. This has since been ruled out due to lack of fitting the varying FWHM and interstellar abundances [6].

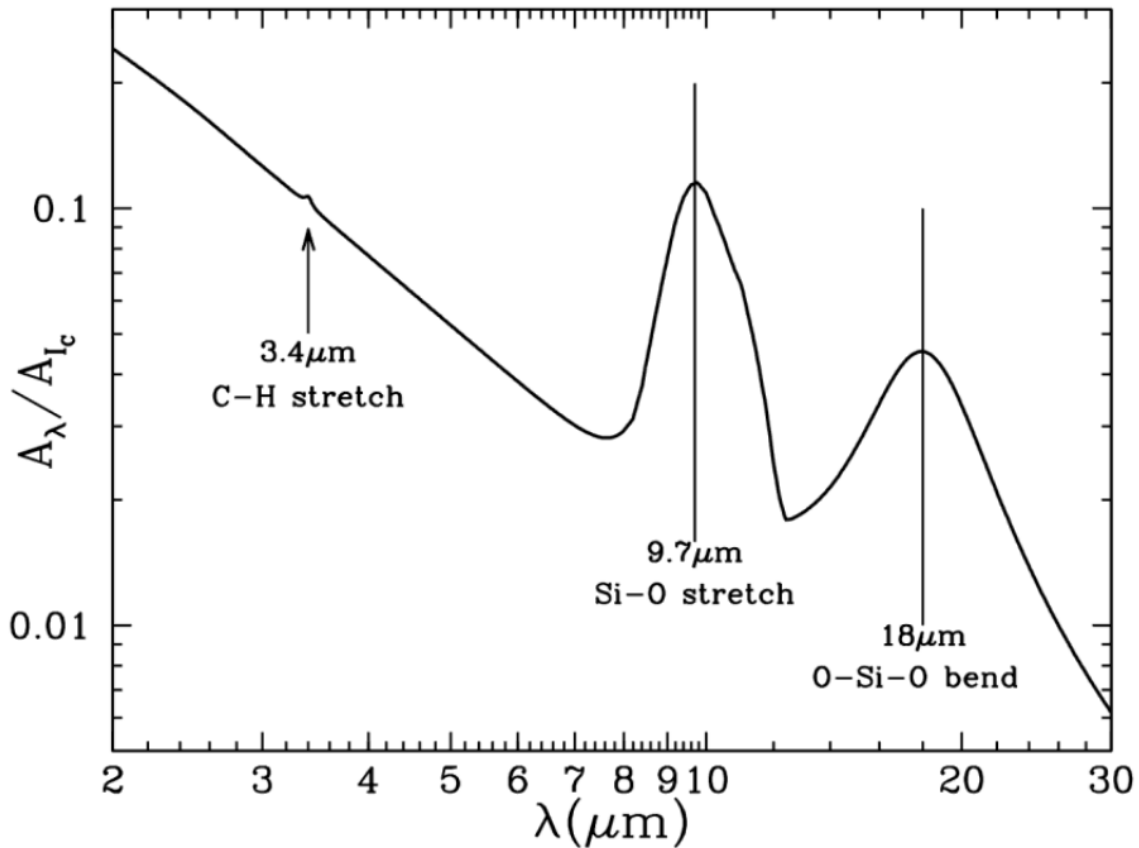


Figure 2: The $9.7\mu\text{m}$ Si-O stretching feature and $3.4\mu\text{m}$ C-H stretching feature. Credit: [7].

Other prominent features of extinction curves are the absorption feature at $\sim 9.7\mu m$, which can be seen in figure 2. This feature is similar to those of silicate materials. Silicates often have absorption features near $10\mu m$, originating from the Si-O stretching mode. It is therefore very unlikely that the $9.7\mu m$ could be caused by some other material. This is backed up by several observations of outflows from cool oxygen and carbon-rich stars. When observing cool oxygen-rich stars the $10\mu m$ absorption feature is present, which is expected, since they are expected to condense silicate dust. On the other hand, the $10\mu m$ feature is not present when observing carbon-rich stars. This too is expected because carbon-rich stars don't form silicate dust [6].

Besides the two features described above there are a lot of smaller features that also contribute to our understating of interstellar dust. There are a lot of interstellar diffuse bands (hereafter DIBs), though none of them has been properly identified. There is some evidence that some of the many DIBs could come from PAHs or even ultrasmall grains of various materials. What exactly is the source of the DIBs remain unknown [6]. Other features are contributed to different ice coatings of the dust grains such as H_2O , CO_2 and NH_3 just to mention a few [6]. Also present is a feature at $3.4\mu m$, which is due to stretching of C-H in aliphatic a type of chain-like hydrocarbon [6]. This feature can be seen in figure 2. Furthermore, there are a lot of features contributed to the stretching of different modes in PAHs, some of these can be seen in figure 3 [6]. Most of these features will not be present in the extinction curves I am going to fit because I am only looking at the extinction in the interval $0.1 - 1\mu m$. The features that fall within this interval are either too narrow or too weak to be resolved. However, the 2175\AA bump will be present in some of the curves.

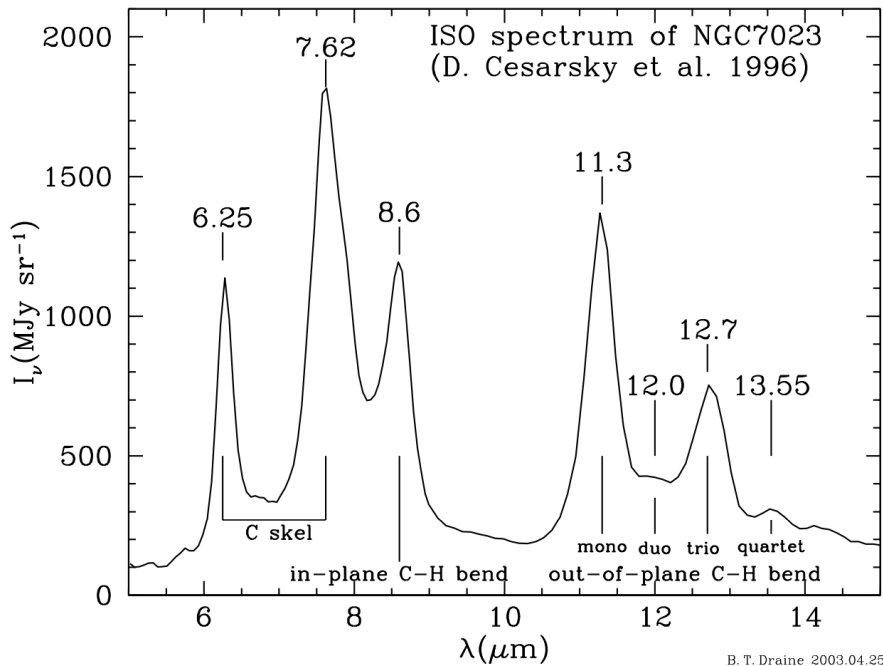


Figure 3: Example of PAH features. Credit: [6].

Based on the features described above it is possible to narrow down the list of materials the dust is most likely made of. There is strong evidence that silicates make up a large fraction of the interstellar dust mass $\sim 95\%$. However, the exact composition of the silicate dust grains remains unknown. The most likely metals to be part of the silicate dust is Mg and Fe, based on interstellar abundances. They are expected to either be pyroxenes $(\text{Mg}_x, \text{Fe}_x)\text{SiO}_3$ or olivines $(\text{Mg}_{2x}, \text{Fe}_{2x})\text{SiO}_4$. The ratio of pyroxenes to olivines, as well as the ratio of Mg-rich to Fe-rich silicates, is unknown [6]. Another Si material thought to be part of interstellar dust is SiC, silicon carbide. SiC has been found in meteorites and have an emission feature at $11.3\mu\text{m}$. However, the absence of the feature in extinction curves suggests that SiC only make up $\sim 5\%$ of the Si abundance in silicates. SiC, therefore, don't play an important role in interstellar extinction [6].

Besides silicates there is strong evidence for carbon-rich materials to be part of the dust. Some examples are diamond, graphite and PAHs. Most of these are connected with the 2175\AA bump [6]. Another group of carbon dust thought to be part of the dust is carbonates. Carbonates have been found in dusty disks, but are estimated to make up less than 1% of the dust mass. They are therefore not important when dealing with the extinction [6]. The last groups of possible grains are metallic iron or iron oxides. How many of these are found in the interstellar dust depends on whether or not there is iron in the silicates. It is therefore not possible to rule out their existence [6].

Based on the above sections, it is, therefore, most likely that the interstellar dust is made up of a combination of silicates and carbon-rich materials. Here $\sim 95\%$ of the mass is found in silicates and the remaining $\sim 5\%$ is made up of the different carbon materials.

4 Host galaxies

Another thing to consider before I start fitting the different extinction curves is the galaxies in which the extinction origins. For the GRBs, the galaxies themselves may not always be resolved when the burst is observed. It is therefore important to understand what a GRB is in order to understand how the extinction curves are derived. The MW is a large spiral galaxy whereas the LMC and the SMC are smaller irregular dwarf galaxies. Because the galaxies are different in nature their possible dust composition and thereby extinction may also vary a lot from galaxy to galaxy. One, therefore, has to keep in mind the environment of the host galaxy when determining the dust composition, so that one doesn't end up with a composition that is unlikely due to the host galaxy's local environment.

4.1 The Milky Way galaxy

The Milky Way galaxy is a large spiral galaxy though to be of the galaxy type Sb-Sbc, meaning that its spiral arms are tightly wound around the centre of the galaxy, with some space between containing less dust and gas [8]. The MW is fairly large in size and mass since it measures 282 ± 30 kpc in virial radius and have a virial mass of $1.3 \pm 0.3 \times 10^{12} M_{\odot}$ [8]. Like other galaxies, the MW is made of a central supermassive black hole, a bulge, a stellar disk and a halo. In this thesis I am most interested in the stellar disk part of the galaxy since it is here we find the dust and most of the stars [8]. It is also in this disk we find the solar system. The disk, therefore, plays an important role when it comes to extinction in different directions, because we most of the time have to look through parts of the disk when making observations, thereby getting obscured light sources.

Because the solar system is located in the MW it is not possible for us to get a complete picture of the galaxy itself. We, therefore, have to approach the MW differently than other galaxies, when wanting to observe the entire galaxy at once. An example of this could be something as simple as taking a picture of the galaxy face on to help determine the number of spiral arms. This is not possible because we sit in the plane of the galaxy. Our picture would therefore end up looking like figure 4, which shows the plane of the MW. In figure 4 we can also see the LMC and SMC in the lower right corner.

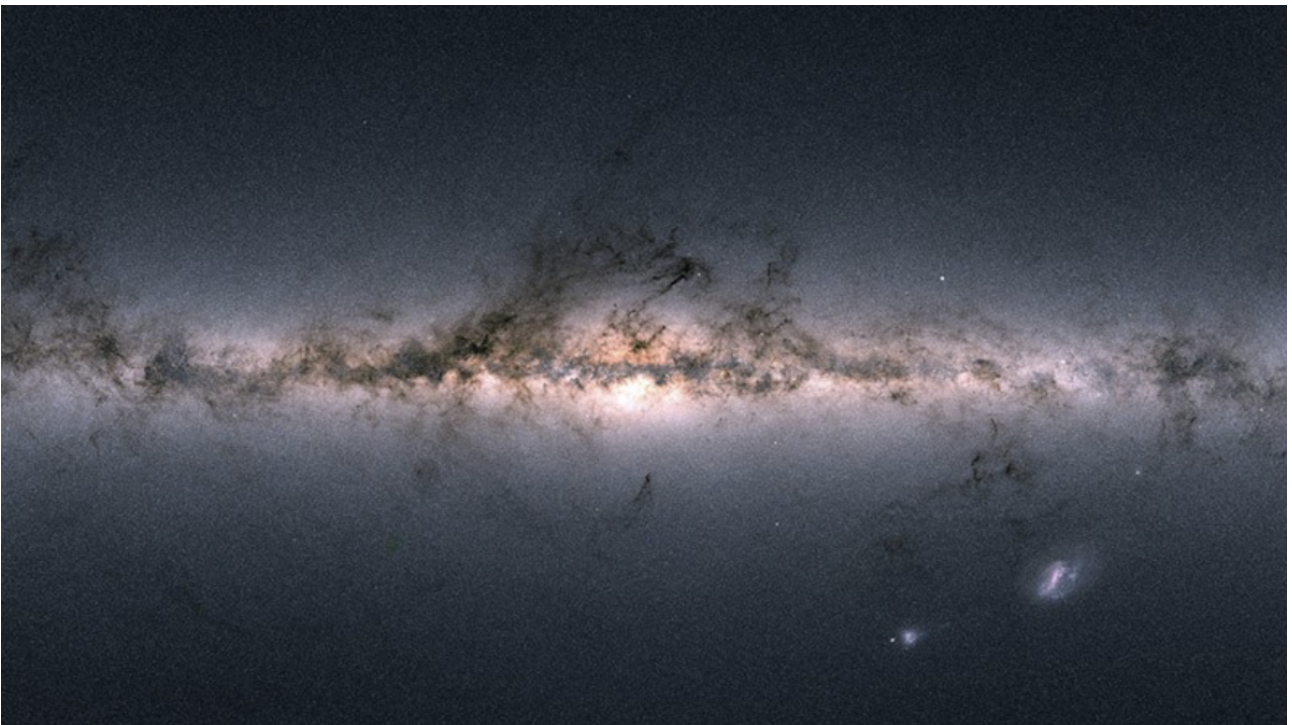


Figure 4: The Milky way galaxy. Credit: [9].

Just like there are some measurements that become more difficult because we are in the plane of the galaxy, others are only possible because we are close to the galaxy. Such an example is observing the extinction in different sightlines. Before I go into more detail about how the extinction is determined in the MW, let's first talk about where we find the dust and what it is thought to be made of, since this is the cause of the extinction.

As seen in figure 4 there are many dark areas when observing the MW. This is the dust. In the MW most of the dust is found in the plane or stellar disk as can be seen in figure 4. Based on numerous studies of absorption lines the most likely elements that make up the dust are C, O, Si, Fe, Mg, S, Al, Ni and Ca [5]. How exactly they combine into different grain materials is still unknown, but as described earlier the two main groups of grains are the carbon grains and the silicates. Here the silicates contain most of the other metals mentioned as likely dust components.

In the beginning of this thesis I described how extinction is determined in general. Now in reality this may sometimes be a bit more tricky than just figuring out how much light isn't coming through the dust. In the MW there are two ways to go about determining the extinction. The first method is called the pair method. In this method, one compares two stars of the same spectral class. One star is hidden behind dust and the other one is in a sightline with no dust. By comparing the spectra of the two stars one then gets a measurement of how much dust there is in the obscured sightline, which in turn give us the extinction of that line [6]. If one on the other hand can't measure the extinction of a sightline in all the desired wavelengths, it is possible to approximate the extinction using a seven-parameter function. One thing worth noting is that this function is normalised after the I band and not the V band extinction, as is usually used for normalisation. The function is as follows:

$$\frac{A_\lambda}{A_I} \approx f(\lambda; R_V, C_1, C_2, C_3, C_4, \lambda_0, \gamma) . \quad (2)$$

Here C_3 , λ_0 and γ determines the strength of the 2175Å bump and C_1 , C_2 and C_4 determines the slope and curvature of the curve at $\lambda < 3030\text{Å}$. At $\lambda > 3030\text{Å}$ it is R_V that determines the extinction [6].

4.2 The Magellanic Clouds

Orbiting the MW are two smaller irregular galaxies. In figure 4 these are seen as the two light spots in the lower right quarter. These are the Magellanic Clouds. Because the LMC and SMC are orbiting the MW, they are some of the only galaxies in which it is possible for us to find the extinction for individual stars, such as it is done in the MW [6]. But as we shall see in the following sections this is one of the few similarities there is to the MW.



Figure 5: The Large and Small Magellanic Clouds. Credit: [10].

4.2.1 The Large Magellanic Cloud

The Large Magellanic Cloud is as its name suggest the larger of the two galaxies in figure 5 and it is located ~ 50 kpc from the MW. The LMC is a lot smaller than the MW and measures 8.9 kpc in radius including its halo. Because it is smaller in size it also makes sense that it is a lot smaller in its mass. The LMC have an estimated mass of $8.7 \pm 4.3 \times 10^9 M_{\odot}$ [11]. Like the MW the LMC has a disk and a halo, but there don't seem to be any significant structure in the disk, like the obvious spiral arms in the MW [11].

Like many other galaxies the LMC contains dust. The dust in the LMC is like the dust in the MW, dominated by the following elements; C, O, Mg, Si and Fe [12]. In the LMC we again don't know how the elements combine in the specific dust groups, but as for the MW, we find that the most likely combination is carbon and silicate dust [1]. One major difference between the two galaxies is the metallicity. The metallicity is a measurement of the amount of metals in the galaxy. Here the LMC is only half of what we find in the MW, meaning that there are half as many of the different elements available to make the dust from [12]. As we shall see later this produces a slightly different extinction curve than the one we normally see in the MW.

4.2.2 The Small Magellanic Cloud

The Small Magellanic cloud is likewise as the name suggests the smaller of the two galaxies in figure 5. The SMC is a bit further away from the MW than the LMC. The SMC is located ~ 60 kpc from the MW [13]. Since the SMC is smaller than the LMC it also makes sense that the SMC has a smaller radius. The SMC is 3.1 kpc in radius and has a mass of $1.8 \times 10^9 M_{\odot}$ [14]. The SMC is therefore clearly the smallest of the three galaxies.

The dust in the SMC is similar to both that of the MW and the LMC. The dust in the SMC is like the MW and the LMC dominated by the following elements; C, O, Mg, Si and Fe [12]. The exact combinations of the elements in the different dust grain groups are again unknown. When examining the SMC the most likely dust combination seem to be just silicates or silicates with very little carbon [1]. The SMC should therefore have an extinction curve that is different from that of the MW and LMC. As we shall see later this is indeed the case. One reason for this could be the SMC's lower metallicity. The SMC have a metallicity that is 1/5 of the metallicity found in the MW [12]. There are therefore way less of the different elements available to make up the dust, giving rise to a different dust grain combination and hence different extinction curve.

4.3 Gamma-ray burst

Unlike the MW, LMC and SMC gamma-ray bursts are not connected to one galaxy. There are therefore not one specific host galaxy all the GRBs originate from and neither is there one universal GRB extinction curve. This does however not mean that I can't say anything about the dust composition in the GRB host galaxies. To understand how I am still able to use the GRBs to examine the dust in their host galaxies, I first have to establish what a GRB is and how it behaves.

GRBs are explosions in galaxies far away that sends out a ton of low energy gamma rays. There are two classes of GRBs, long and short duration GRBs. Short duration GRBs are less than 2 seconds long and are primarily found at low redshifts. What is the course of the short duration GRBs are not well known. It has been speculated that they may occur from compact binary mergers, such as a neutron star and a black hole [15]. Long-duration GRBs can on the other hand last as long as 2000 seconds. Unlike the short duration bursts, there is a fairly good idea of what causes the long duration bursts. The long duration bursts seem to come from the death of massive stars [15]. Figure 6 shows an overview of the GRBs observed with *Swift*, which is a space telescope that has observed most of the GRBs I am going to look at. In this thesis, I am only interested in the long duration bursts because they have some interesting properties that allow me to find their extinction curves. Normally GRB spectre is smooth, featureless and intrinsic power-law in nature, any deviation from this can therefore be contributed to dust, gas

and metals in the host galaxies. If one, therefore, has the spectral energy distribution of the GRB it is possible to fit the observed extinction of the host galaxy using either the MW, LMC or SMC as a model for the observed extinction [16].

Since all the information I have about the host galaxy comes from the GRB, I can not say anything about what dust compositions I would expect the specific GRB host galaxy to have. If the observed extinction of a GRB host galaxy is fitted using for example the MW as a model, I would of cause expect the dust in this host galaxy to be similar to that of the MW.

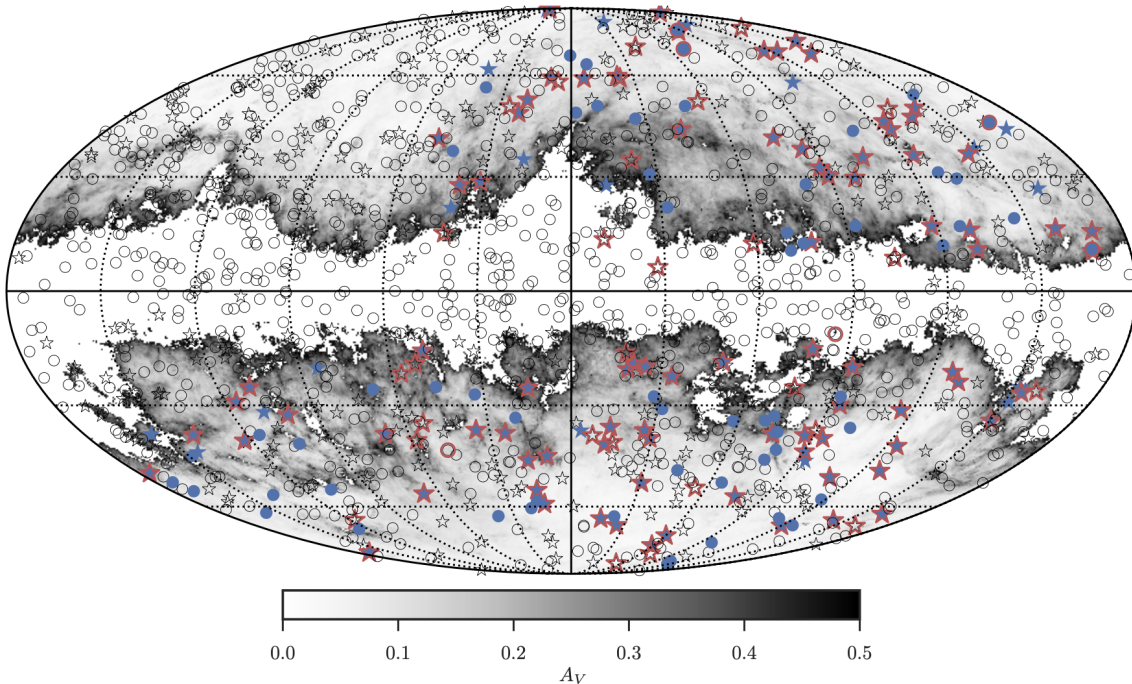


Figure 6: Overview of the 1266 GRBs detected by Swift until 31/03/17. Here the circles represent burst without a known redshift and the stars are burst with known redshift. The blue and red stars on the map represent the sample examined in [17]. Credit: [17].

5 Extinction curves

Now that I finally have explained what extinction is and where it originates, I can start looking at the extinction curves that I want to fit the dust compositions to. So far the only well studied extinction curves are those of the MW, the LMC and the SMC. Extinction curves have been found for a handful of GRB host galaxies [18], but none of them is as well studied as the MW, LMC and SMC curves. Meaning that we may have observed the curve but we don't know much about the dust in the GRB host environment, whereas we are fairly certain that the MW contains at least 33 % silicate dust [1]. As we shall see in the following section the three curves have very different characteristics.

5.1 Milky Way

When looking at the MW extinction curve there is not one universal curve, but multiple depending on the sightline one has chosen to observe. These curves vary quite a lot depending on the sightline. Some lines have a small R_V values indicating that there are primarily small grains in the sightline and others have large R_V indicating that the sightline contains larger grains. The larger the reddening R_V is the flatter the extinction curve will become [6]. An example of the observed extinction in different sightlines can be seen in figure 7.

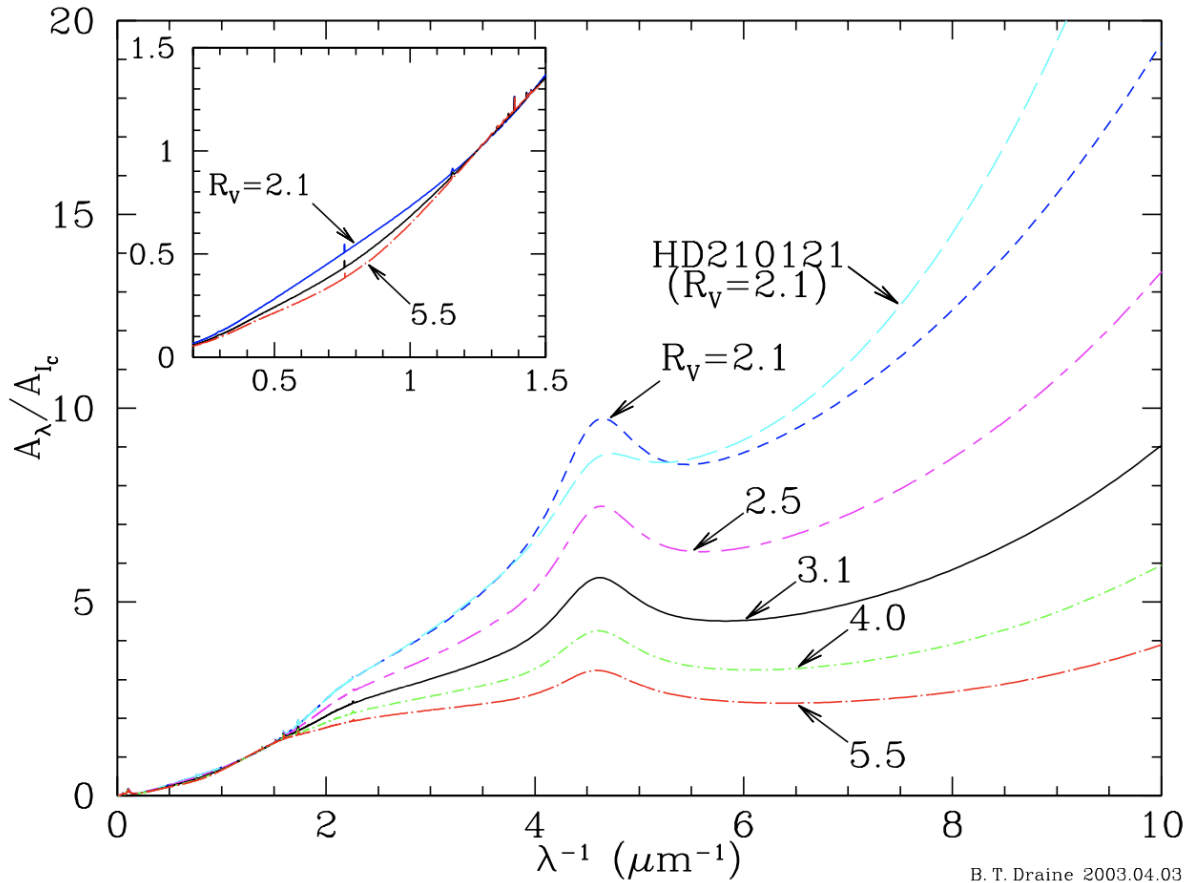


Figure 7: Milky Way extinction curves, with different reddening. Credit: [6].

The average MW extinction curve has an R_V of 3.1 [6]. When examining the extinction curve of the MW I will therefore use this curve and not one of the other more extreme cases. When looking at the curve the biggest feature, the 2175 Å bump, is attributed to PAHs. This is not the only part of the extinction curve that is connected with certain grains. The rise of the extinction curve into the UV wavelengths is most likely coming from small carbon grains and the longer wavelengths are most likely large silicate grains [19]. The MW curve, therefore, looks like it fits with the prediction from section 3 that the interstellar dust is made up of silicate and carbon dust. This is also the conclusion of [1], from which I have my observed MW extinction data.

5.2 Large Magellanic cloud

Like the MW the LMC to have different extinction curves depending on the chosen sightline. For the LMC there are two extinction curves representing two different sightlines. One that takes the average extinction of the dwarf galaxy and one that is called the supershell extinction. The supershell is the extinction measured near the massive star-forming region 30 Dor [12]. This specific extinction curve is also sometimes referred to as the LMC2 extinction curve or the LMC2 supershell extinction curve. The average extinction of the LMC does on the other hand not include the 30 Dor area. The average extinction of the LMC is very similar to that of the average extinction of the MW and has a similar reddening of $R_V = 3.41 \pm 0.28$. The supershell is on the other hand a more steep curve with a much smaller bump at 2175\AA . This can also be seen in figure 8. The supershell has a reddening of $R_V = 2.76 \pm 0.09$ [12].

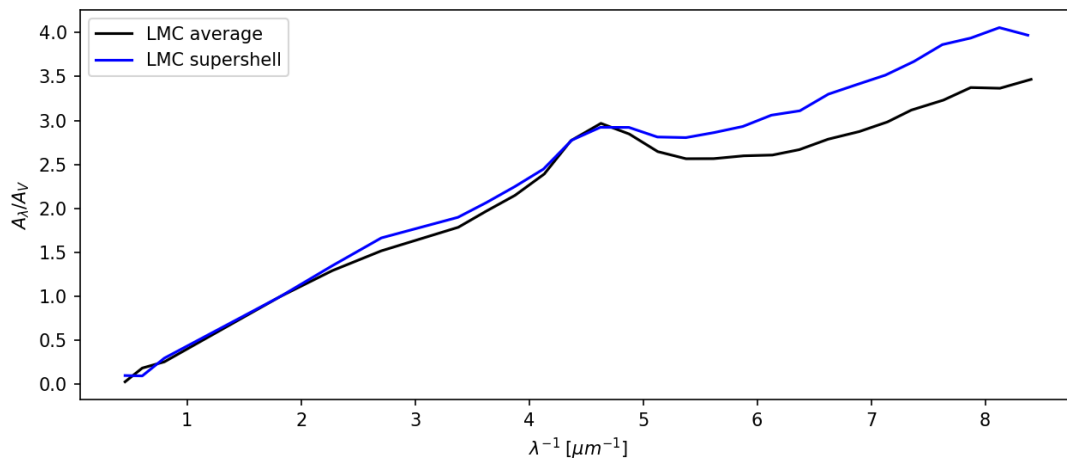


Figure 8: The Large Magellanic cloud extinction curves [2].

When examining the LMC curves it is also possible to connect these curves to certain grain types. As for the MW, the bump in the LMC curves is thought to come from PAHs. The difference in the two LMC curves is attributed to fewer small grains in the average extinction sightline [12]. This is consistent with the observation from the MW curves that a larger R_V equal a smaller amount of small grains. In [1] they have examined the average extinction curve of the LMC and find that it also fits well with a combination of silicate and carbon grains, though not with the same combination used to fit the MW curve. This is consistent with the dominant elements in the dust of the LMC and the lower LMC metallicity, that I mentioned earlier in the thesis.

5.3 The Small Magellanic Cloud

Unlike the MW and the LMC, the SMC doesn't have multiple extinction curves depending on how it is observed. For the SMC there is one curve that is observed in the SMC bar region. This extinction varies from that of the average MW curve and the two LMC curves since it doesn't have the characteristic 2175Å bump. Instead the SMC extinction is a step featureless curve with an $R_V = 2.74 \pm 0.13$ [12]. The SMC extinction curve is shown in figure 9.

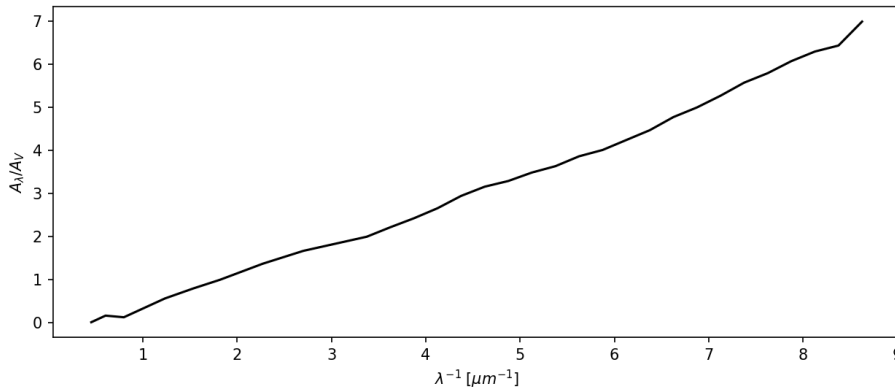


Figure 9: The Small Magellanic cloud extinction curve [2].

For the SMC it would also seem most likely that the extinction is caused by silicate and carbon dust based on the abundances of the different elements present in the galaxy. Besides this, the R_V is similar to that of the LMC supershell meaning the two should contain grains of similar sizes. If one goes to the literature different studies have shown that the presence of at least small carbon grains is unlikely. In [19] they find that the extinction of the SMC can be recreated without carbon dust smaller than $\lesssim 0.02\mu m$ and in [1] they find that the best fit to the SMC curve is found using pure silicate dust. It can therefore be questioned how big a role the extinction from carbon grains plays in the SMC. When fitting the curve it will therefore be interesting to see what combination of grain materials gives the best results.

5.4 Gamma-ray bursts

One major difference between the MW, LMC, SMC and the GRBs is that there is not one specific curve that you can pinpoint and say that's a GRB extinction curve, because all the GRB host galaxies don't contain the same amount of metal and hence dust composition (see table 6 in the discussion section). The GRB curves are instead found to be different variations of the MW, LMC and SMC extinction curves. In [16] they have examined 22 GRBs with redshift larger than $z = 4$. Here they find that the majority of the GRB host galaxies have extinction curves that fit the SMC curve and few curves that fit the LMC and MW curve. Likewise, [18] have found 10 cases where the GRB host galaxy extinction fits well with that of the SMC. Eight out of the 10 cases have a redshift $z < 4$. It would therefore seem that

the GRB host galaxies tend to behave more like the SMC extinction curve, than the MW and LMC. I would therefore expect the extinction from the GRB host galaxies in the majority of the cases to be a steep featureless curve.

5.5 Supernova like extinction

Besides the three standard extinction curves for the MW, LMC and SMC, there is also a supernova like extinction curve. The supernova (hereafter SN) extinction curve is mainly found in high redshifts, typically at $z > 4$. Here the SN extinction curve represents dust thought to be formed in SN ejecta rather than dust evolved in stars [20]. The SN curve is only relevant for $z > 4$ since the stars responsible for producing the dust wasn't available in high enough numbers to be solely responsible for the dust production before $z \approx 5 - 6$. The dust at $z > 4$ therefore mainly have to come from the SN ejecta, giving rise to a different extinction curve [16]. This extinction curve can be seen in figure 10. Further examination of the SN like extinction curve has shown that is most likely not responsible for the dust production at $z > 4$ [16]. The validity of the SN extinction curve can therefore be debated.

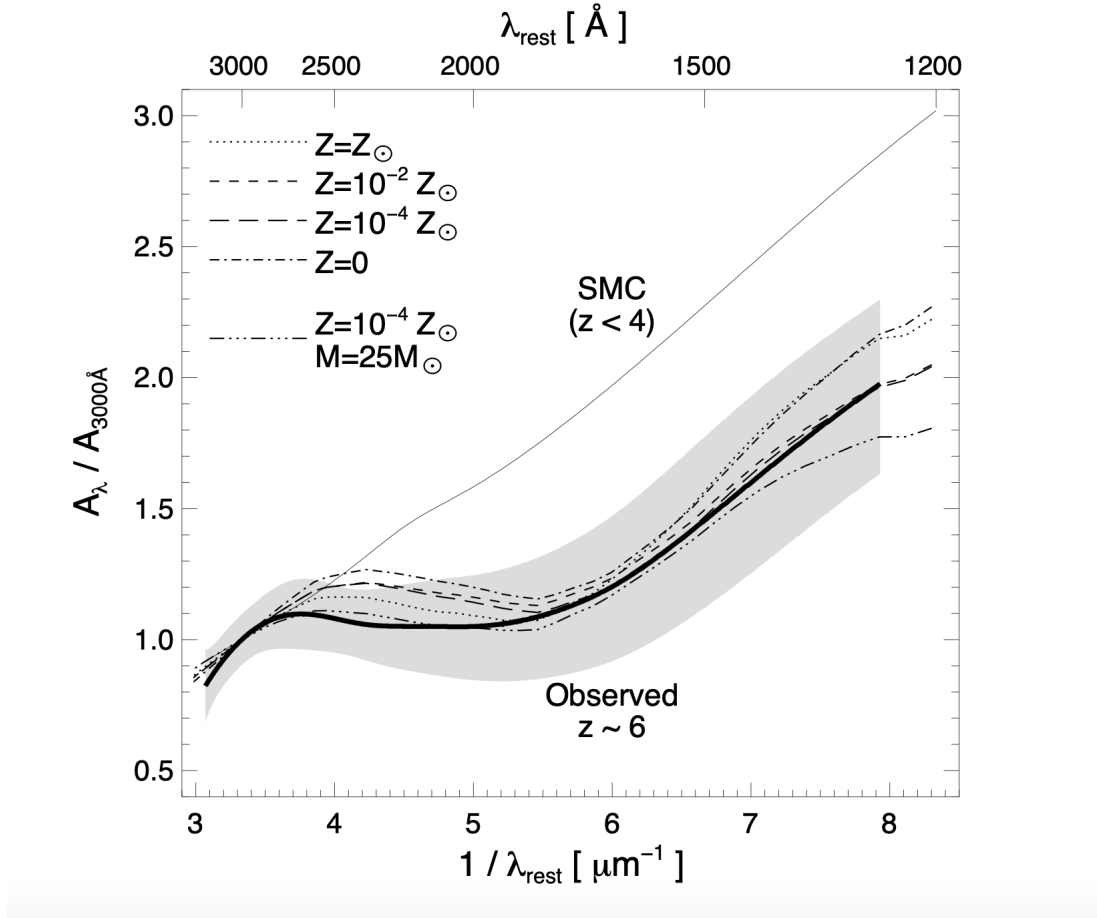


Figure 10: Example of an SN like extinction curve at $z \sim 6$. The dashed lines represent the extinction with different metallicities. Credit: [20]

Like for the other extinction curves there are specific grain properties connected with the SN curve. Generally the grains are smaller in the SN curve and the flat part of the curve is contributed to amorphous carbon grains and Fe_3O_4 [20].

I will not be fitting dust combinations to the SN curve because the MW, LMC, and SMC all have redshifts smaller than 4. Likewise, most of the GRB host galaxies I will look at also have $z < 4$ and will therefore not be "supernova like" in their extinction. I, therefore, have no need to fit the dust composition to the SN extinction curve for comparison purposes.

6 Dust grains

The final thing to consider before I start fitting the different observed extinction curves are which dust grains to use during the fit. In the sections above I have described how the different extinction curves all are best fitted by a combination of silicate and carbon dust, as well as why we think these are the most likely species to make up the dust in the different cases. It would therefore be a good place to start by trying to use silicates and carbon grains.

6.1 Grain sizes

The next thing to consider besides the materials is which grain sizes to use. In the article by Mathis, Rumpl and Nordsieck [3], where they try to find the dust grain sizes distribution of the MW, they have examined graphite, silicon carbide, pyroxene/enstatite, olivine, iron and magnetite. They find that the best fit is obtained using graphite and one of the silicate materials (pyroxene/enstatite or olivine). They specifically used grains in the size range $0.005\mu m$ to about $1\mu m$ for graphite and $0.025\mu m$ to $0.25\mu m$ for all other materials [3]. Since they also conclude that silicate and carbon grains give the best fit, which fits with the other studies namely [1, 19], I am going to use the MRN grain sizes as a base for the grain size range I will use to fit the extinction.

In the section about interstellar dust I wrote that you would rarely find grains larger than $0.4\mu m$ in the dust [5]. I have therefore decided not to use any grains larger than this for both materials. Choosing these sizes as an upper bound on the grains sizes, cover the upper bound from the MRN article for all materials except graphite. Here they go a bit larger but they do not specify exactly what their largest graphite size is, just that it is about $1\mu m$. It will therefore be interesting to see how many of the large carbon grains I end up needing when fitting the observed extinction curves. For all other grain types, I have picked a size that is larger than the MRN upper bound and I should therefore be able to see if $0.4\mu m$ or their estimate of $0.25\mu m$ is a reasonable upper bound.

For the lower bound the MRN article uses $0.005\mu m$ for graphite and $0.025\mu m$ for all other materials. Earlier when I looked at the SMC extinction curve I talked about a study that had found that the observed extinction could be reproduced without using carbon grains [1] and one where carbon grains smaller than $0.02\mu m$ weren't needed [19]. It would therefore be interesting to see how small the silicate grains need to be in order to fit the entire SMC extinction curve. If I remove all carbon grains smaller than $0.02\mu m$, as suggested in [19], I will have to have dust of some other material to fit the part of the SMC extinction curve the carbon grains with the sizes $0.005 - 0.02\mu m$, was otherwise responsible for in the MRN grain size distribution. Because I only have silicate and carbon dust it would therefore be natural to substitute the carbon dust sizes with silicate dust of a similar size to see if they can give a good fit to the observed extinction curve. I would therefore need silicate dust of the sizes $0.005 - 0.02\mu m$ in order to test if the SMC extinction curve really can be reproduced without carbon grain smaller than $0.02\mu m$. The other study of the SMC extinction curve found that it could be reproduced using only silicate dust [1]. To test if this is true I would need the widest possible silicate dust grain size range, to be sure that I have grains that cover the entire observed extinction curve. The smallest grain I can make is $0.001\mu m$ because if I were to pick a smaller size the dust grain would become a molecule [4]. In order to examine the SMC extinction curve, I would therefore need silicate dust grains with the size range $0.001 - 0.40\mu m$.

Based on the above paragraphs I am therefore going to fit all the extinction curves with silicate and carbon grains in the size range $0.001 - 0.4\mu m$.

6.2 Complex refractive index

Before I start looking at how to get the synthetic extinction of the individual grains, there is one final thing I have to consider. The code, DDSCAT, that I will be using to generate my synthetic dust grains with need an input material file of a dielectric material. Dielectric means that the material has no free electrons that can move around inside the material [21]. The dielectric material file has to contain the complex refractive index of the material in order for DDSCAT to compute the synthetic extinction of the individual dust grains made from the chosen material. To understand how DDSCAT can take a material and find the synthetic extinction, one first has to understand what the complex refractive index is. The complex refractive index, m , consists of two parts n and k . n is the real part of the complex refractive index and k is the imaginary part of the index. Hence $m = n + ik$. The real part of the index n is also called the refractive index. The refractive index, n , denotes how fast electromagnetic waves move inside the dielectric material [21]. The imaginary part of the index k denotes the attenuated part of the electromagnetic wave passing through the dielectric material [21]. Attenuation refers to the loss of intensity of the electromagnetic wave. This may be caused by scattering or absorption inside the medium, which is why the imaginary part of the complex refractive index k is also

sometimes referred to as the extinction [22]. The complex refractive index is also connected to the dielectric function ϵ by $m = \sqrt{\epsilon}$. Where the dielectric function refers to the behaviour of the material in an oscillating electric field [23]. DDSCAT, therefore, needs the complex refractive index of a dielectric material to calculate the synthetic extinction of a dust grain made from the material. Since the complex refractive index of the dielectric material tells how light is absorbed and scattered when it comes into contact with the dielectric material.

6.3 DDSCAT

Now that I have decided what materials and which size range to use in the fit, I have to figure out how to get the synthetic extinction of the individual grains. To get the individual synthetic extinction, I used the code DDSCAT version 7.3.3. DDSCAT is a Fortran code for calculating the scattering and absorption of light for irregular particles. It is developed by Bruce T. Draine and Piotr J. Flatau and uses the discrete-dipole approximation to do calculations [24]. The discrete-dipole approximation is used to solve Maxwell's equations for electromagnetic fields for any imaginable particle shape. The desired particle shape will in the discrete-dipole approximation be approximated by an array of polarisable points, the so-called dipoles. Once the grid of points have been defined Maxwell's equations can be used to find the absorption and scattering and hence the extinction of the target particle [24].

To get the synthetic extinction of the different grain sizes one first have to give the code the material file containing the complex refractive index of the material. After this one has to decide upon a grain size, the shape of the grain and the amount of dipoles one wants to use in the calculation of the effective extinction factor Q_{ext} . The effective extinction factor Q_{ext} will be explained in equation (6). Before running the code one also have to set the wavelength range and the amount of wavelengths to run the calculation at. The amount of wavelengths chooses how smooth the effective extinction calculation is going to be for the chosen wavelength range. Having a large amount of wavelengths in a short-range will give a smoother calculation than having a small amount of wavelengths in the same range. Once the wavelength range and the amount of points to calculate the synthetic extinction in has been set in the parameter file one can start running the calculation to get the effective extinction of the dust grain.

Like any other code DDSCAT has a set of limits that have to be upheld for the results to be accurate. The first limit is on the materials complex refractive index. This is set to make sure all structural features of the chosen material is accounted for in the generation of the synthetic dust grains. In order to get trustworthy results the complex refractive index, therefore, has to behave in the following way for the chosen wavelength range:

$$|m - 1| \lesssim 3. \quad (3)$$

Where m is the complex refractive index [25].

For this thesis I am using the complex refractive index for carbon from [26]. Here the complex refractive index is found by burning the carbon sample in air. The complex refractive index I am using for the silicates is calculated in [27, 28] using the materials dielectric function. If I use equation (3) on the data presented for the two materials from [26] and [27, 28], I then get the results shown in figure 11. Here it is clear that both materials are within the limit set by DDSCAT for the chosen wavelength range $0.1 - 1\mu m$. This particular wavelength range has been chosen so that it will cover the wavelength range of the different observed extinction curves I'm going to fit the synthetic dust grains to.

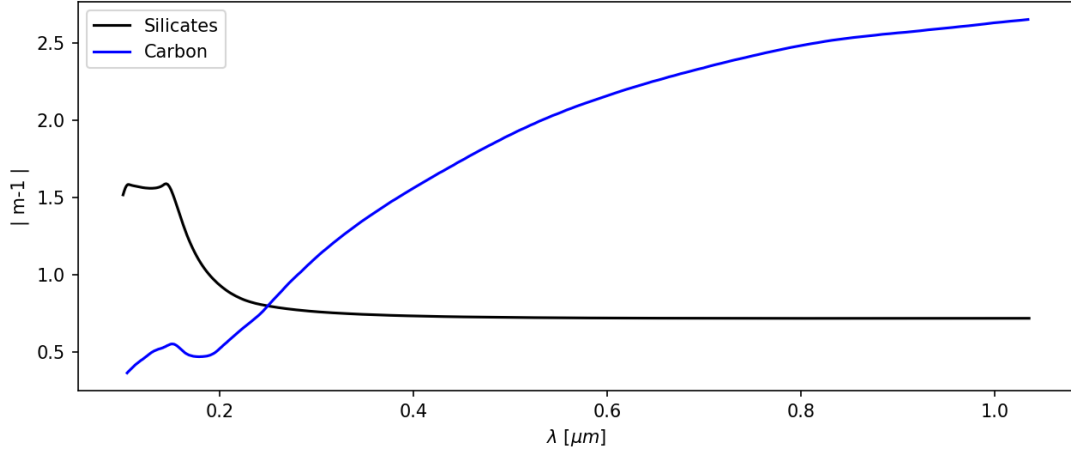


Figure 11: The DDSCAT limit for accurate results, based on the materials complex refractive index is that $|m - 1| \lesssim 3$ [25]. Here it is shown that the chosen silicate and carbon material are within the limit and therefore can be used to generate the synthetic dust grains.

Besides the limit on the materials complex refractive index, there is also a limit in regards to the grain size and the number of dipoles used in the calculation. In order for the calculation to be accurate and not overestimate the absorption generated by a grain size, the number of dipoles and the grain size have to uphold the following relation:

$$a_{eff} < 9.88 \frac{\lambda}{|m|} \left(\frac{N}{10^6} \right)^{1/3}. \quad (4)$$

Here m is the complex refractive index of the material, λ is the wavelength, N the number of dipoles and a_{eff} is the grain size [25].

If I take the same complex refractive indexes as before and use the same wavelength range and then use equation (4) I get the results presented in figure 12. Here I have calculated the limit on a_{eff} using 59728 dipoles. If I examine figure 12 I find that my largest grains namely

those that are $0.35\mu m$ and $0.4\mu m$ are not accurate in the wavelength range $0.1 - 0.2\mu m$, because I have used too few dipoles in their calculation. Figure 13 will show why this may be a problem.

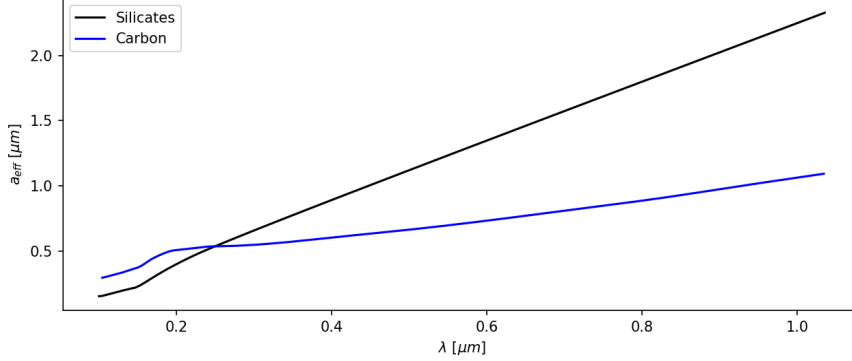


Figure 12: The DDSCAT limit for accurate results for the calculated grain size is $a_{eff} < 9.88 \frac{\lambda}{|m|} \left(\frac{N}{10^6} \right)^{1/3}$ [25]. Here presented using 59728 dipoles. Note that for from $0.1 - 0.3\mu m$ the larger grain sizes $0.30 - 0.40\mu m$ are not accurate.

In reality when examining extinction curves one generally looks at them in inverse wavelengths. Do I, therefore, invert the wavelengths in figure 12 the larger grain sizes $0.30 - 0.40\mu m$ are no longer accurate for most of the inverted wavelengths shown in figure 13. In figure 13 I have zoomed in on the y-axis containing the grain sizes, to get a better idea of where the different sizes stop being accurate. For carbon, all grain sizes up to $0.30\mu m$ are accurate in the entire range according to the criteria set by DDSCAT. The last sizes up to $0.40\mu m$, which is my max size, is only accurate to about $6\mu m^{-1}$. As I will show later, this is not likely a hindrance for the method I have chosen since I 1) hardly ever use the large carbon grains and 2) when I use them in a fit they only influence the fit at $\lambda^{-1} < 3\mu m^{-1}$, where the sizes are accurate. For the silicates, all sizes up to $0.15\mu m$ are accurate in the entire inverted wavelength range and the largest grains stops being accurate at $\lambda^{-1} > 6\mu m^{-1}$ depending on the exact size. This is again not a hindrance since as I will show later the largest silicate also only dominates the extinction when $\lambda^{-1} < 3\mu m^{-1}$, where they too are accurate. Should I need larger grains that were accurate in the entire inverted wavelength range I would need to use 159313 dipoles for the carbon grains and 1058292 dipoles for the silicates for $0.40\mu m$ to be an accurate size. I could have calculated the two largest carbon grains again using the required amount of dipoles for them to be accurate in the entire wavelength range, but I have not done so because I ended up not needing these carbon dust sizes for any of the dust compositions suggested as the best fit. For the largest silicate grains, I on the other hand would not recalculate the larger sizes with the required number of dipoles because it is recommended to keep the number of dipoles used under 10^6 for ones computer to have a fair chance of even finishing the computation [25]. I have therefore not recalculated any of the larger grain sizes with the suggested number of dipoles needed for them to be accurate in the entire inverse wavelength range that I am examining.

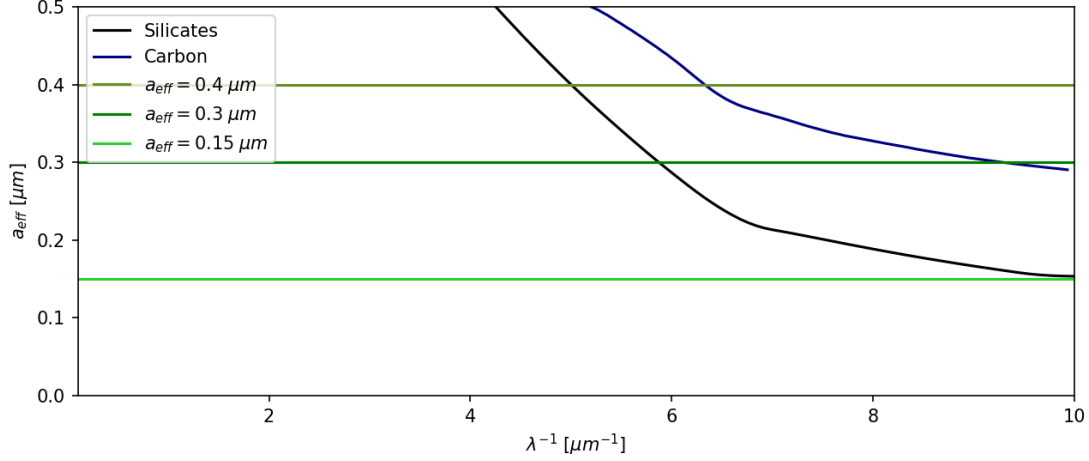


Figure 13: Zoom in on where different a_{eff} stops being accurate as a function of wavelength [25]. Note that when the vertical lines crosses the black and blue lines the respective grain size stops being accurate.

6.4 Grain shape

Before I generate all the synthetic grain sizes there is one final thing to consider. In space, much like here on Earth, grains aren't perfectly spherical [19]. It is therefore important to know what impact the grain shape has on the extinction. When looking at grains we assume they have an effective radius given as:

$$a_{eff} = \left(\frac{3V}{4\pi} \right)^{1/3}. \quad (5)$$

Here V is the volume of the grain [23].

This effective radius is also what normally is referred to as the grain size. Therefore when I have mentioned that I am going to use grains with sizes in the range $0.001\mu m$ to $0.4\mu m$, I have been referring to the size as defined above.

In DDSCAT it is possible to pick the shape of the synthetic dust grain as well as choosing the length of the x, y and z-axis. One can therefore make perfect cubes and spheres but also elongate or shorten boxes and ellipses, just to name a few of the possibilities. I have chosen four different shapes of one synthetic dust grain size to test how the shape affects the effective extinction factor Q_{ext} , which is what DDSCAT computes. The effective extinction factor is dependent on the size and is given as:

$$Q_{ext} = \frac{C_{abs} + C_{sca}}{\pi a_{eff}^2}. \quad (6)$$

Here C_{abs} is the absorption cross-section of the grain and C_{sca} is the scattering cross-section of the grain [23].

The shapes I have chosen, to test how the synthetic extinction behaves depending on the shape are a cube, a sphere, an oblate, which is an ellipse with one side smaller than the others and a prolate, which is an ellipse with one side larger than the others. I chose these shapes because of all the shape possibilities there is in DDSCAT these seemed like the most likely to actually be representative of interstellar dust. I have tested these four shapes on both the silicate and the carbon dust. I ended up running the test on the grain size $0.25\mu m$ because it was the default size set in the parameter file.

The first material I tested the shapes on was the astronomical silicates [27, 28]. Figure 14 show the effective extinction of each shape, as well as the effective absorption and scattering of the shapes. Depending on the inverse wavelength the cube has an effective extinction which displays both higher and lower values than the sphere. The oblate and the prolate also seemingly changes in having a smaller or larger effective extinction than the sphere. It is therefore hard to see if one of the shapes is considerably different from any of the other shapes.

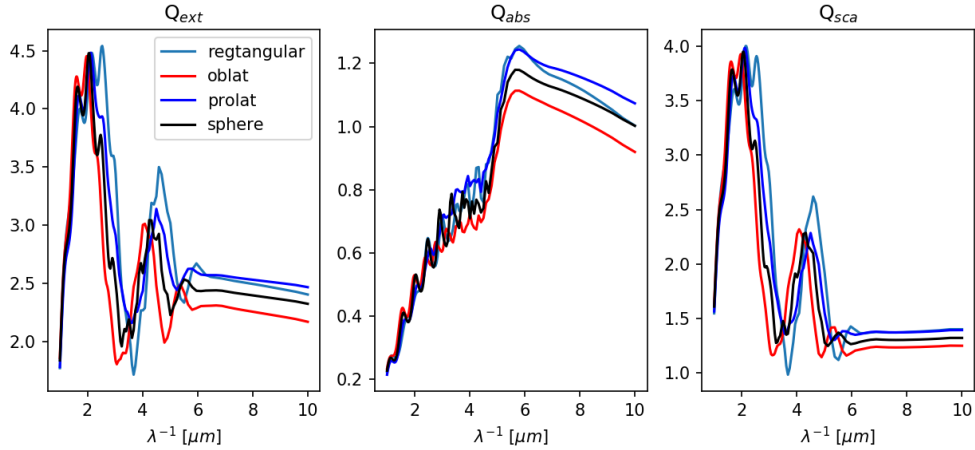


Figure 14: The frame on the left shows the synthetic extinction of four different shapes of silicates, to see how the synthetic extinction differs for different shapes with the same a_{eff} . Here is examined a cube, a sphere, an oblate with one side 1/4 shorter than the others and a prolate with a side that is 1/4 longer than the others. The middle frame shows the absorption from each shape and the last frame shows the scattering generated by the shapes.

Let's assume that the sphere is the actual grain shape. How do the other shapes differ from it? In figure 15 I have taken the sphere and subtracted it from all the shapes to see where and how the other shapes differ from it. Here one sees that there is some difference in the shapes but it is limited. For the cube the mean difference is $0.3 \pm 0.3Q_{ext}$, for the prolate it is $0.2 \pm 0.1Q_{ext}$ and for the oblate it is $0.2 \pm 0.2Q_{ext}$. This is not that big of a difference for the prolate and oblate, whereas the cube can result in a larger difference. I should therefore be able to use the sphere as the grain shape for the silicates without it having a large effect on the synthetic extinction, in case the grains aren't actually spherical. Are the grains indeed cubical this effect will of course be larger.

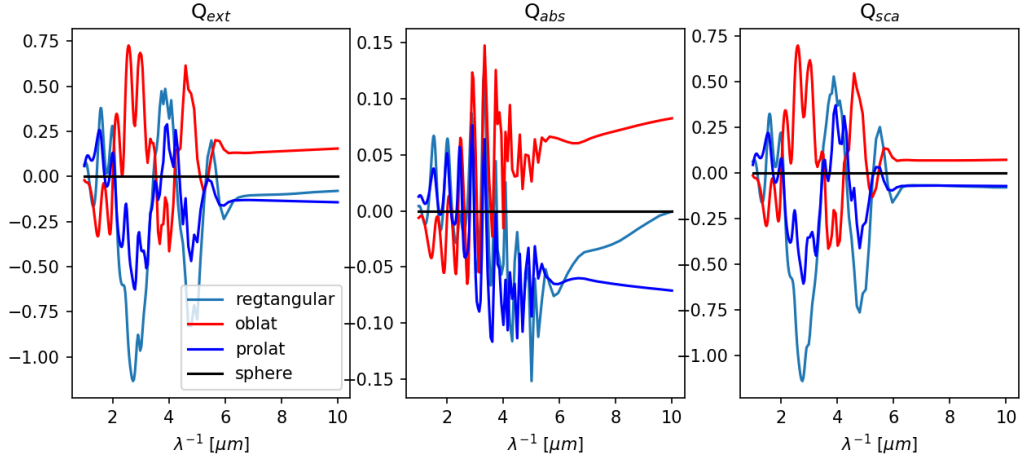


Figure 15: The frame on the left shows the difference in the synthetic extinction of four different shapes of silicates with the same a_{eff} . Here is examined how much the other shapes differs from a sphere, by simply subtracting the spheres synthetic extinction from the shapes. The middle frame shows what happens to the absorption of each shape and the last frame shows the scattering generated by the difference in shapes.

I also tested how the shape affects the effective extinction of the carbon grains. Here I used the same four shapes and the same size as for the silicates. Figure 16 shows the effective extinction, effective absorption and the effective scattering of the shapes. For the carbon grain, there is a visible difference between the different shapes. Here the oblate has a lower effective extinction than the sphere and the cube and prolate has a larger effective extinction.

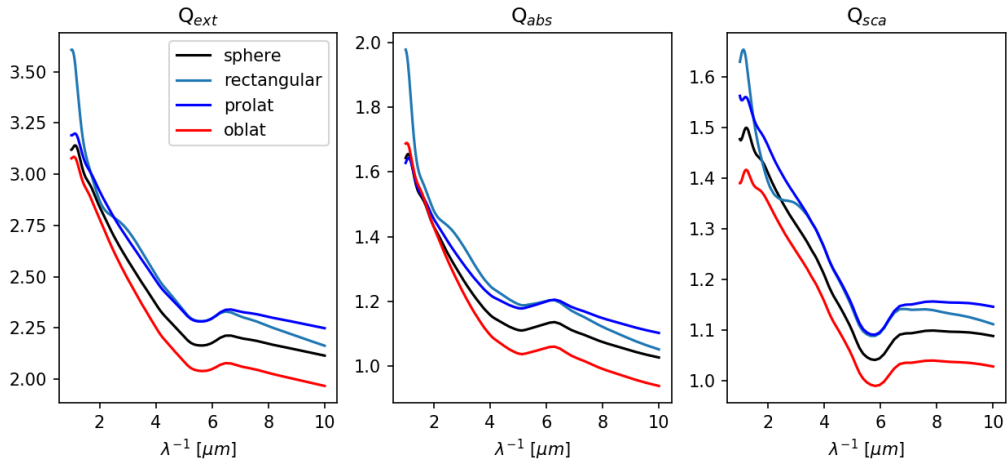


Figure 16: The frame on the left shows the synthetic extinction of four different shapes of carbon, to see how the synthetic extinction differs for different shapes with the same a_{eff} . Here is examined a cube, a sphere, an oblate with one side 1/4 shorter than the others and a prolate with a side that is 1/4 longer than the others. The middle frame shows the absorption from each shape and the last frame shows the scattering generated by the shapes.

If I again assume that the sphere is the actual grain shape, how do the other shapes differ from it this time? In figure 17 I have again subtracted the sphere from the other shapes. For carbon, the cube has a much higher effective extinction than the sphere in inverted wavelengths. The prolate and the oblate seem to have about the same amount more or less effective extinction than the sphere. The mean difference for the cube is $0.2 \pm 0.1 Q_{ext}$, the prolate has $0.08 \pm 0.02 Q_{ext}$ and the oblate has $0.08 \pm 0.03 Q_{ext}$. Again this is not that big a difference, it is in fact smaller than for the synthetic silicate grain. It should therefore also be good to just use the sphere for the synthetic carbon grains without it having a significant effect on the synthetic extinction of the individual grains.

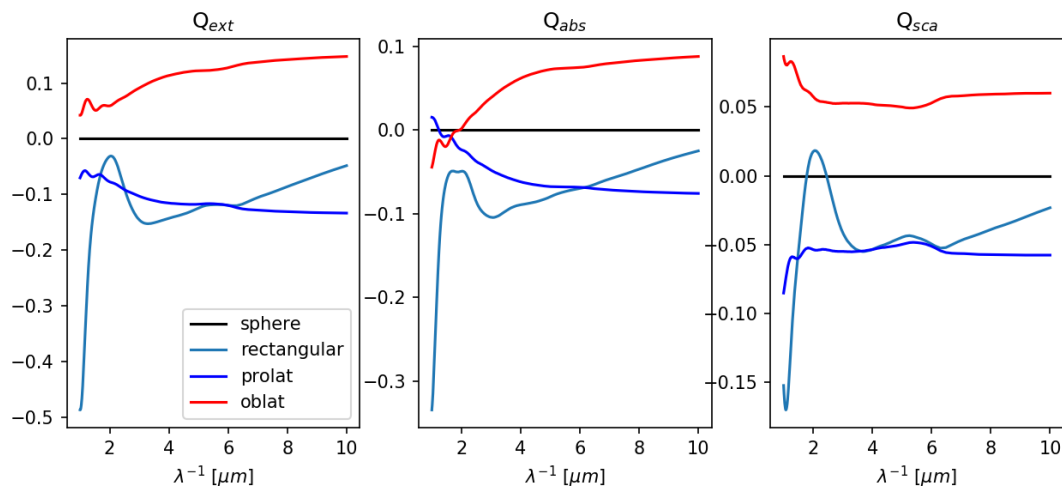


Figure 17: The frame on the left shows the difference in the synthetic extinction of four different shapes of carbon with the same a_{eff} . Here is examined how much the other shapes differs from a sphere, by simply subtracting the spheres synthetic extinction from the shapes. The middle frame shows what happens to the absorption of each shape and the last frame shows the scattering generated by the difference in shapes.

6.5 Carbon

Now that I have shown it is a good approximation to only use the spherical grains I can start generating the different synthetic grain sizes that I'm going to use in the fit of the observed extinction curves. For carbon, I am using the complex refractive index from [26]. This article contains the measurements from three different types of amorphous carbon. The one I am going to use contains structures made of benzene rings. This particular measurement is also called BE in the article [26]. One benzene ring is a ring made up of 6 carbon atoms on which there sit 6 hydrogen atoms. I have chosen the benzene measurement because it is sort of the average of the three amorphous carbons measured in [26]. This means that benzene's complex refractive index is in between the two other materials tested in [26].

Earlier in the thesis I augmented for why I picked the size range $0.001\mu m$ to $0.4\mu m$. When I generated the different sizes I found that the larger the grain got in size, the smaller the difference between the two sizes became in Q_{ext} . I, therefore, have more sizes for the small and ultra small grains than for the larger grain sizes. In the end, I chose the following sizes: $0.001\mu m, 0.002\mu m, 0.003\mu m, 0.004\mu m, 0.005\mu m, 0.006\mu m, 0.007\mu m, 0.008\mu m, 0.009\mu m, 0.01\mu m, 0.02\mu m, 0.03\mu m, 0.04\mu m, 0.05\mu m, 0.06\mu m, 0.07\mu m, 0.08\mu m, 0.09\mu m, 0.1\mu m, 0.15\mu m, 0.2\mu m, 0.25\mu m, 0.3\mu m, 0.35\mu m$ and $0.4\mu m$. The effective extinction of these sizes can be seen in figure 18, where I present the different carbon grains I going to use in the fit of the observed extinction curves.

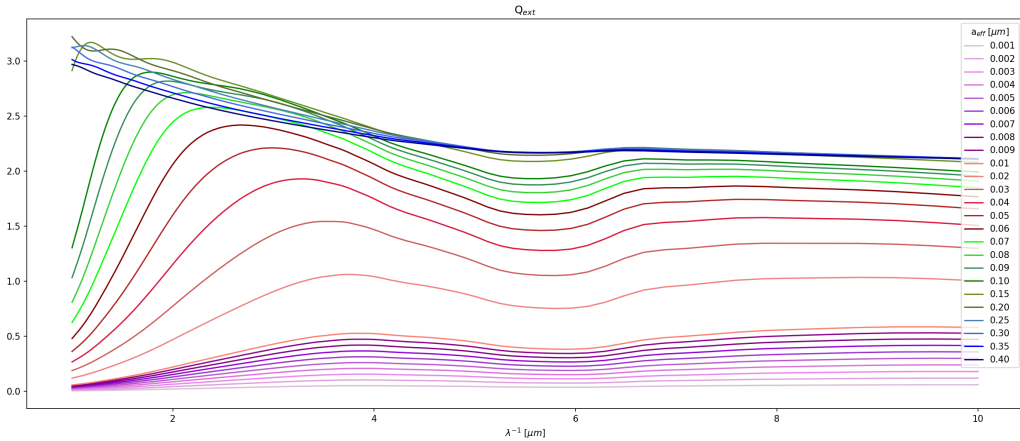


Figure 18: The different synthetic grains sizes picked for carbon. I have chosen more of the smaller sizes since there is a larger variation in their synthetic extinction than for the larger sizes. All the grains are in between $0.001\mu m$ and $0.4\mu m$ in a_{eff} .

6.6 Silicates

Besides the carbon grains, I am also going to use silicate grains to reproduce the observed extinction. The complex refractive index used to generate the synthetic silicate grains individual extinction can be found in [27, 28]. These articles calculate the complex refractive index of MgFeSiO_4 using a dielectric function that is adapted to fit the material properties of MgFeSiO_4 . MgFeSiO_4 belong to the olivine family of silicates. Olivine refers to silicates consisting of two metal atoms and a SiO_4 group [6]. Since MgFeSiO_4 is an olivine type of silicate it will be most relevant to compare my fit results with other mixes of carbon and olivine materials, such as the graphite and olivine mix used in MRN [3].

Like for the carbon grains I am going to generate the synthetic extinction of silicate grains with sizes between $0.001\mu\text{m}$ to $0.4\mu\text{m}$. When I generated the synthetic silicate grains I also found that the larger the grain got the smaller the difference between the two sizes became in Q_{ext} . I therefore also ended up having more of the small and ultra small silicate grains. For the silicates, I made the same grains sizes as for the carbon grains. The grains sizes and their respective effective extinction can be seen in figure 19.

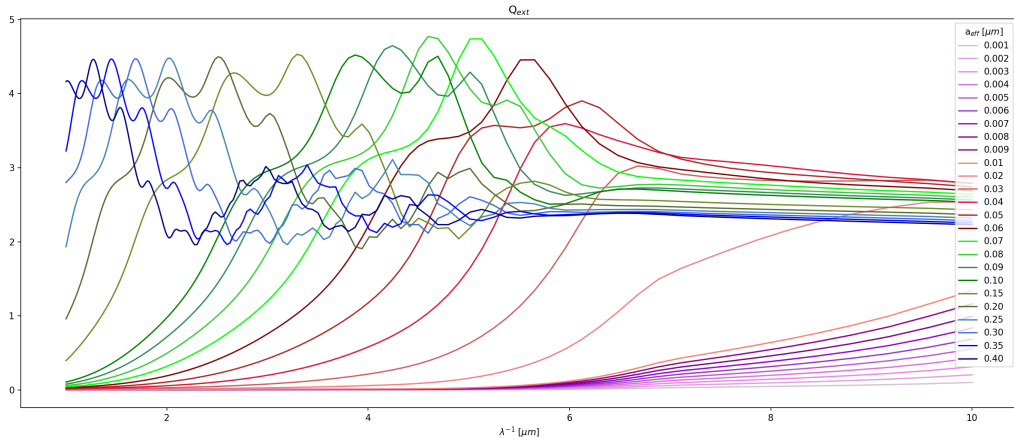


Figure 19: The different grains sizes used to represent the silicates. I have chosen more of the smaller sizes since there is a larger variation in their synthetic extinction, then for the larger sizes. All the grains are in between $0.001\mu\text{m}$ and $0.4\mu\text{m}$ in a_{eff} .

7 Fitting routine

Now that I have my observed GRB extinction curves and the synthetic dust grain sample from which I can reproduce the observed extinction curves, I can finally set up a fitting routine that fits the dust composition to the observed GRB extinction curves. In order to set up a fitting routine that can find suggestions for the best dust composition to the host galaxies, I first have to identify how to get the generated dust sizes to work with the observed data. The data comes in the units A_λ/A_V , which is the magnitude of the extinction normalised by the extinction of the V band filter, see the section about extinction on page 2 for the definition of A_λ/A_V . A_λ/A_V is also the unit that the observed MW, LMC and SMC curves, which I would like to fit are in. On the other hand, the synthetic grain sizes come in the unit of Q_{ext} which is the extinction effectiveness factor. Therefore I have to convert Q_{ext} to A_λ/A_V to find the dust composition of the observed extinction curves. Q_{ext} can be converted to A_λ the following way [29];

$$\frac{A_\lambda}{mag} = 1.086 \cdot \tau_\lambda . \quad (7)$$

Here τ is the optical depth which also can be written like this [30];

$$\tau_\lambda = \int_0^d d\tau = \int_0^d \bar{n} \cdot C_{ext} dl = n \cdot C_{ext} \cdot d . \quad (8)$$

Here d is the distance to the object, \bar{n} is the average particle density along the chosen path of observation and C_{ext} is the extinction cross section, which also can be written like this;

$$C_{ext} = \pi a_{eff}^2 Q_{ext} . \quad (9)$$

Here a_{eff} is the effective radius of the dust grain and Q_{ext} is extinction effectiveness factor. Meaning that the extinction magnitude A_λ becomes;

$$\frac{A_\lambda}{mag} = 1.086 \cdot \pi a_{eff}^2 Q_{ext} \cdot \bar{n} \cdot d . \quad (10)$$

Now that I know how to convert the dust grains to the right units, I am able to fit the best suggestion for the dust composition to the observed extinction curve.

In order to fit the best suggested dust composition to the observed extinction curves I have to make a routine that can combine 50 dust grain sizes into one synthetic extinction curve. Because I don't have one function that contains all the synthetic dust grain sizes I can't use the build-in fitting mechanism of python, since this fitting tool only can take one function as the input. I, therefore, have to make a fitting routine that can take multiple inputs and combine them to a fit. In a course on my bachelor, André E. Hartwigen and I solved this exact problem for an assignment. I, therefore, went back and looked at our old solution to see if it could be adapted to work on extinction curves. The adapted fitting routine takes a set number of input bins that it sums together to make the best dust combination. The best dust composition is then found by looking for the dust composition that deviates the least from the observed extinction curve.

7.1 Finding the average particle density

To get the fitting routine up and running, firstly I had to load in the observed GRB extinction curve I wanted to examine and the different synthetic generated grains. After this, I started to convert all the grains to the unit of A_λ using equation (10). During the conversion I ran into the first thing to consider; I know the radius of the grains and I also know the distance to the GRB host galaxy, but the average particle density in the line of sight is much harder to determine because it requires knowledge of the amount of material in the sightline. The grain models I'm looking at has a wavelength range from 0.1 to 1 μm , meaning that it covers the visible area plus a bit of UV and IR. I can therefore approximate \bar{n} to be :

$$\bar{n} = \pi a_{eff}^2 d , \quad (11)$$

as long as $a_{eff} \approx \lambda$ and the wavelength is in the visible area [29]. This approximation will be good for most of the wavelengths and most of the grain sizes. For the very small grains, $a_{eff}^2 < 0.009$, this may not be the best approximation, because the very small grains are not approximately equal in size to the largest of the wavelength in the range 0.1 – 1 μm . I'm still going to use the approximation for the very small grains so that Q_{ext} has been converted to A_λ with the same method for all grains. Using this approximation equation (10) reduces to;

$$\frac{A_\lambda}{mag} = 1.086 Q_{ext} . \quad (12)$$

I therefore just have to multiply my grain sizes with 1.086 to get them in A_λ .

7.2 Loop setup

Now that all input parameters are in the same units, the next step would be to set up the loop that suggests the best combination of synthetic grains. This loop first gets some initial conditions, such as use between 0.2 to 0.8 times of bin 1, 0.8 to 0.9 times of bin 2 and so forth, as a first guess of how many of the synthetic grains it have to use in order to fit the observed extinction curve. Then it takes a number within the initial condition and multiplies to the chosen synthetic grains. Here there is one nested for-loop per grain size, for the code to test combinations with different amounts of the different grains. After having multiplied the chosen amount of each grain to the specific grain bins, it adds the bins together to one final synthetic composition and then looks at the difference between the composition and the observed extinction curve. This is done by checking for the dust combination that has the smallest RMS value. The way I calculate the RMS is described in the section about picking the best fit. If the dust combination is the best match of those tested, meaning the combination with the smallest RMS value, it saves the numbers needed to make the synthetic composition. Finally, once the loop is done running and testing all the chosen possibilities it will print the numbers needed for the best match. The loop I ended up using to test the compositions, can be seen below.

```

def fitfunc4(Nt,runs):
    linit = a
    uinit = b

    for ir in range(runs):
        kul = np.linspace(linit[0],uinit[0],Nt)
        sil = np.linspace(linit[1],uinit[1],Nt)
        kul2 = np.linspace(linit[2],uinit[2],Nt)
        sil2 = np.linspace(linit[3],uinit[3],Nt)
        scoretabel = np.zeros([Nt**4,5])
        i = 0
        for a1 in range(Nt):
            for a2 in range(Nt):
                for a3 in range(Nt):
                    for a4 in range(Nt):
                        const = np.array([kul[a1],sil[a2],kul2[a3],sil2[a4]])
                        fixed = specs[0]*const[0]+specs[1]*const[1]+specs[2]*const[2]+specs[3]*const[3]
                        spe = np.interp(1/zub16[:,1],data[:,0],data[:,1]) #LMC SMC MW
                        spe = np.interp(data[:,0],1/zub1[:,1],fixed[:,1]) #GRB
                        score = np.sqrt(mean_squared_error(spe[:,1], data[:,1]/Av)) #GRB
                        score = np.sqrt(mean_squared_error(fixed[:,1], spe[:,1])) #LMC SMC MW
                        scoretabel[i,:] = [score,kul[a1],sil[a2],kul2[a3],sil2[a4]]
                        i = i+1

        bedstvalue = np.unravel_index(np.argmin(scoretabel[:,0]),scoretabel[:,0].shape)
        bv = bedstvalue[0]
        linit = scoretabel[bv,1:]*0.9
        uinit = scoretabel[bv,1:]*1.1
        const = scoretabel[bv,1:]
    return const

```

7.3 Bins vs computation time

Before I set up the loop, I have to consider how many different grains sizes and materials I have. As seen on figures 18 and 19, I have 25 different grain sizes per material. Making a loop that is nested 50 times to get all the sizes and material in one computation will give precise result, but may not be the smartest idea, since it would take longer than desired to run. So how do I get as many grain sizes as possible without the code running for several days? Here I tried binning some of the grain sizes together to see if I still could get satisfactory results while cutting the computation time down. I have tested what happens to the fit if I bin some of the

grains together in 2, 4 and 6 bins. For this specific test I used an extinction curve of GRB 121012A. For the 2 bin version I made a bin containing the synthetic grains from $0.001\mu m$ to $0.06\mu m$ plus again from $0.25\mu m$ to $0.40\mu m$. Here I did one in silicates and the other in carbon grains. I set the loop to pick 10 numbers within the initial condition (Nt) and asked it to run 50 times. The 2 and 6 bin version of the loop is setup in the same way as the 4 bin version shown above. For the 4 bin version I made two bins containing silicates and two containing carbon grains, by splitting the the bins used in the two bin version into two separate silicate bins and two separate carbon bins. The first set of bins had the sizes $0.001\mu m$ to $0.009\mu m$ and the other had $0.01\mu m$ to $0.06\mu m$ plus $0.25\mu m$ to $0.40\mu m$. This loop was set to run with the same initial conditions and the same amount of times as for the 2 bin version. Finally for the 6 bin version I again used the same initial conditions, but this time I had three bins of silicates and three bins of carbon grains. The bins for the 6 bin version contained synthetic grains in the sizes $0.001\mu m$ to $0.009\mu m$, $0.01\mu m$ to $0.06\mu m$ and $0.25\mu m$ to $0.40\mu m$. The result of the test runs can be seen in figure 20.

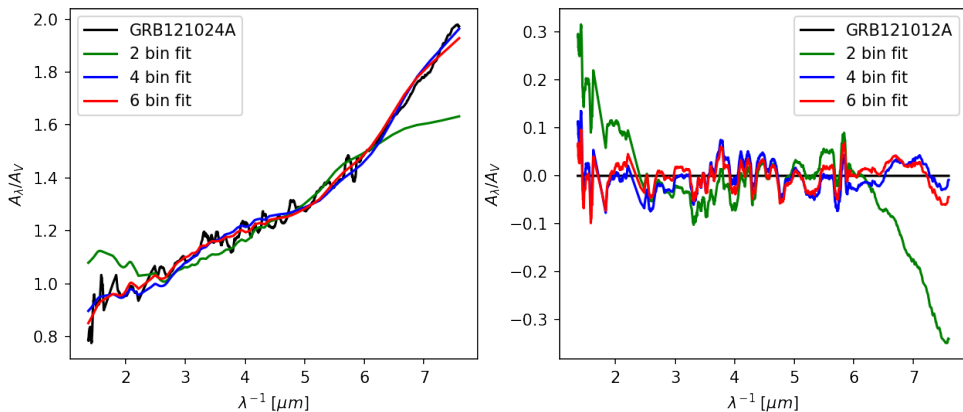


Figure 20: The left panel of the figure shows the fits made with two, four and six-grain size bins. To make the three fits there is used the same synthetic grains, they have just been spread out differently in the bins when making the different fits. This was done so that the 4 and 6 bin version contained the same synthetic grain size and materials as the 2 bin version, but also had the right number of bins. The bins used in the 2 bin version was therefore split into two new bins for the 4 bin version and into three new bins for the 6 bin version. The right panel shows how well the different binned fits fit the observed extinction curve.

The 2 bin version of the fit took 2 seconds to run and had an RMS of 0.1. Normally an RMS of 0.1 is really good but as can be seen on figure 20 it doesn't fit that well from 1 to $2.3 \mu m^{-1}$ and again from $6 \mu m^{-1}$ compared to the other fits. If I then look at the 4 bin version it took 3 minutes to run and had an RMS of 0.03. I can also see that it fit better in the before mentioned areas of the observed extinction curve. Now the 6 bin version took 5 hours to run and had an RMS of 0.03. It fits a bit better in the areas I mentioned, but you would have to look at the entire fit to see it because it is an improvement of less than 1% in A_λ/A_V . Was it worth

waiting 5 hours for the tiny improvement? Not if your just testing what synthetic grain size range will give a satisfactory result to your observed extinction curve, because the RMS value will be below 0.3 for most fits using the 4 bin version. If this is the case, the 4 bin version will give fine results where the observed extinction curve will have been reproduced. Later on, when you are running your final fit you can change to the 6 bin version, to get the best possible fit to the curve. For this reason, all the tests done on the code hereafter are done with the 4 bin version of the code presented above.

7.4 Interpolation

After figuring out that it was fine to go with the 4 bin version of the fitting routine, there was another thing to consider. The synthetic grain sizes and the observed GRB extinction curve or other data files did not have the same wavelength spacing. I, therefore, had to interpolate either the data file or the synthetic grain sizes, to be sure that the points I was comparing in the fit were the same. First I tried to get the observed GRB extinction curve to have the same wavelengths as the grain sizes. Here I could not understand why I got the same number for each of the interpolated points, till I looked at the help page for the interpolation function. When one uses the build-in interpolation function in Numpy the x-data has to be increasing in size, in order to get meaningful results [31]. It turned out that the GRB data I was using was decreasing in size. I, therefore, tried to reverse the order of the x-data points. When I then ran the interpolation again, I still got the same number for all the interpolated points. For the interpolation to work properly, one has to take the shortest data file and expand it. I, therefore, ended up getting the synthetic grain sizes to have the same wavelengths as the observed GRB extinction curve. Where I later to fit an observed extinction curve that has fewer data points than the synthetic grain sizes, I would have to expand the data wavelengths to fit those of the grain sizes. In both of these cases, I just have to choose the wavelength range from one of the synthetic grain sizes because all of them are evaluated at the same points. Therefore it won't matter which one of them I take the wavelength range from in this case.

7.5 Picking best fit

Now that the fit gets evaluated at the same points, it is time to look at how to identify the best fit. There are several ways one can use to determine the best fit. In figure 21 I have tested four ways to see how they differ from one another. First I tested how good the fit was if I took the smallest percentage difference between the fit and the data points. This method gave that the fit fitted either 98 or 94% of the observed data, depending on the dust combination. I determined the percentage difference in the following way:

$$\bar{\%} = \frac{|data - fit|}{data} \cdot 100 . \quad (13)$$

The next method I tested was the χ^2 . Depending on the grain combinations the χ^2 was either 3 or 18. This was not bad considering that the closer the χ^2 value is to 1, out of the number of data points examined, the better the fit is [32]. I have used the following definition of χ^2 [32]:

$$\chi^2 = \sum \frac{(fit - data)^2}{data} . \quad (14)$$

After this, I tested the combination of χ^2 and the percentage fit. This gave the same fit as just picking the percentage. The final method I tested was the root-mean-square (hereafter RMS) method. This gave an RMS of 0.03 or 0.09 (left, right panel of figure 21) depending on the grain combination. Generally speaking the lower the value of the RMS is, the better the fit is. I used the build-in RMS function `mean_squared_error` from the package `sklearn.metrics` to calculate the RMS values [33]. Typically the RMS is defined in the following way [34]:

$$RMS = \sqrt{\frac{\sum_{i=1}^n (data - fit)^2}{n}} . \quad (15)$$

Here n is the number of data points.

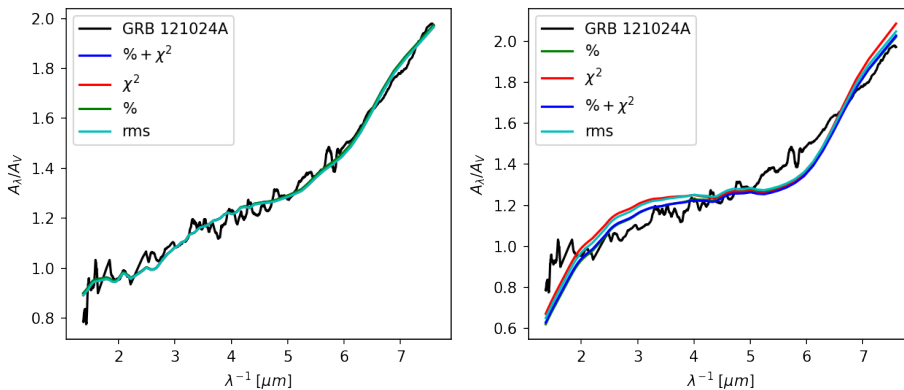


Figure 21: Fits to GRB 121024A, with different parameters set as the best-fit criteria. Tested is the smallest percentage difference from data, the χ^2 , a combination of χ^2 and percentage, and the root mean square method. The two figures are for two different grain combinations, that was tested to make sure it worked on more than one combination. The left panel lacks the sizes $0.25 - 0.40 \mu m$ in both materials and the right panel lacks the sizes $0.07 - 0.20 \mu m$ for both materials. The rest of the grain sizes not mentioned are used in both panels dust combinations.

In order to determine which one of the methods was the best I plotted them on top of the data for two different synthetic grain combinations. The results can be seen in figure 21. For the synthetic dust combination fitted in the left part of figure 21 it is hard to determine which of the fitting methods give the best fit because all the fits lie on top of each other. I, therefore, had to make another synthetic dust combination that would give a worse fit than the one in the left panel, while still using the different best fit methods so that I could see which of the methods would give the best fit to the observed extinction curve. Looking at the right part

of figure 21 therefore gives a better clue. Here at it is at least possible to see all the lines. Once again the four methods give relatively similar results, less than 2% difference in A_λ/A_V . I ended up picking the RMS method as the best fit method because it is the method that gives the average of the four fits in figure 21.

7.6 How to bin the grain sizes

The final thing to consider before I can start using the fitting routine to find the best synthetic dust composition for the different observed extinction curves is how I am going to bin the different grains. As mentioned earlier I can't use all the grain sizes simultaneously unless I bin them together, otherwise, the fitting routine would take much longer than desired to run. When I tested the number of bins vs the computation time I found that 4 bins would give a fit with an RMS less than 0.3 in a reasonable time frame, but that it is possible to go up to 6 bins if needed. I, therefore, have to find a way to get as many grains sizes as possible into four groups. I found that the best way to do this was to split the grains sizes into groups of three, containing three grains of similar sizes, and then add some of the groups together to make up a bin. This made it easier to adjust the grain bins depending on the extinction curve and to keep track of which grains were used in the fit. I chose not to mix the silicate and carbon grains in the bins so that it would be easier to find the percentage of the synthetic extinction coming from either the silicates or the carbon grains, once the fit was done.

8 Fitting routine tests

Now that I have the finished fitting routine that can suggest a dust composition of a certain size distribution and mineralogy, it is time to test the routine further. In this section, I will test if there is any bias in regards to how the code handles the bins and if there are parts of the observed extinction curves that are dominated by grains of certain sizes.

8.1 Position of bins

The first test I have run on the finished routine is to see if the input order of the bins has any effect on the result. If this is indeed the case it could make the results less accurate. I have tested this by picking four-grain bins and then rotated them around by moving the bins one place to the right after each run. I picked four bins containing only silicates grains. These bins were used to make a fit to the GRB 121014A extinction curve from [35]. The result of the test can be seen in figure 22. Here one can see that it indeed does give the same fit no matter where the different bins are poisoned in the fitting routine. There is therefore not a selection bias from the bins when the routine is figuring out how much to take of each bin in order to make the dust composition.

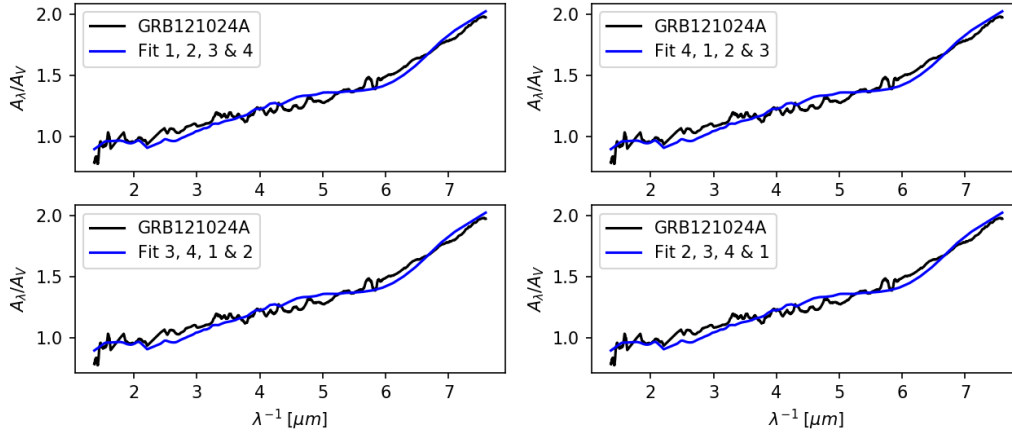


Figure 22: The four frames shows the different variations of the bin input. Here the numbers 1, 2, 3 & 4 denotes which bin was input first, second, third and fourth. All four frames look the same which shows that the input direction of the bins don't matter.

8.2 Which dust grains dominate the extinction curves

The next test I made was to see where the different synthetic dust grain sizes dominate the observed extinction curve. Earlier I showed that to get accurate results the dust grain sizes had to behave a certain way. Here I found that the largest grains weren't accurate (see figure 13) in the entire inverted wavelength range. I am therefore going to test where the different grain sizes dominate the observed extinction in order to show that the larger grains only dominate in an inverted wavelength range where they are accurate.

For the silicate grains I decided to test this on the SMC extinction curve since [1] says it is possible to fit the SMC extinction using only the silicate grains. I sorted the silicate grains into four bins after size. The ultra-small grains $0.001 - 0.009\mu m$ was put in one bin, the small grains $0.01 - 0.06\mu m$ was put in the next bin. Then the remaining small and medium-size grains $0.07 - 0.20\mu m$ were put in another bin and finally the large grains $0.25 - 0.40\mu m$ were put in the last bin. I then proceeded to leave out one of the bins when I ran the fitting routine to see where I would get a dip in the fitted extinction. In figure 23 the result of this test is shown.

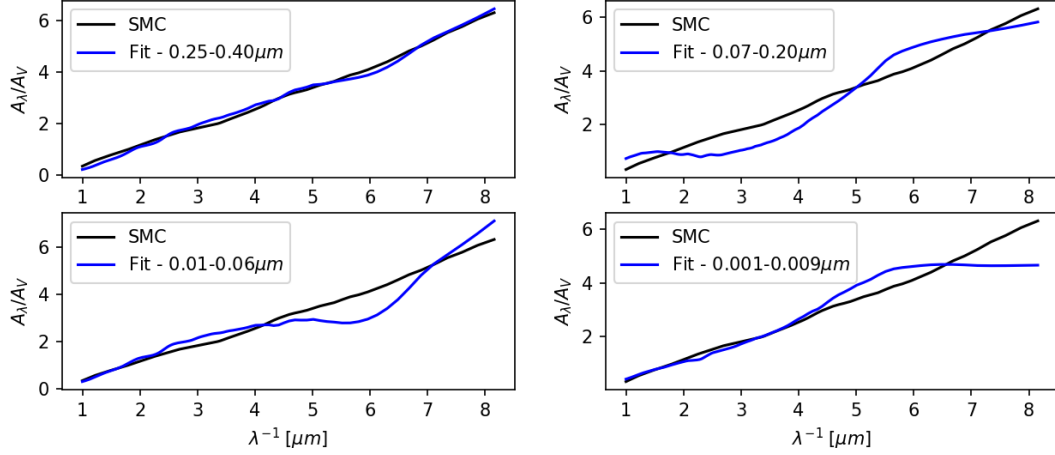


Figure 23: The four frames shows where different groups of silicate grains dominates the observed extinction.

Based on figure 23 the ultra small silicate grains dominates the extinction from $\gtrsim 6.5\mu m^{-1}$. The small grains dominated the extinction at $\sim 4.5 - 6.5\mu m^{-1}$. The small and medium grains dominate at $\sim 2 - 4.5\mu m^{-1}$ and finally the large silicate grains dominate the extinction at $\lesssim 2\mu m^{-1}$. The large silicate grains are therefore accurate in the part of the extinction curve where they dominate the extinction, according to figure 13 and figure 23. That the ultra-small and small grains dominate the larger inverse wavelengths makes sense because it is easier for the smaller grains to interact with shorter wavelengths since the wavelength and the grains size is approximately the same size. If one looks at the larger wavelengths the smallest grains become see-through because the wavelengths are much longer than the grain radius allowing the light to pass through without detecting the grain and therefore not partaking in the observed extinction at that wavelength.

Figuring out where the different carbon grains dominate is a bit more tricky since no extinction curve can be well fit with a combination made purely of carbon grains. My best suggestion for a curve that can be fitted with only carbon grains is the LMC supershell. The best fit made purely from carbon grains to this observed extinction curve can be seen in figure 24.

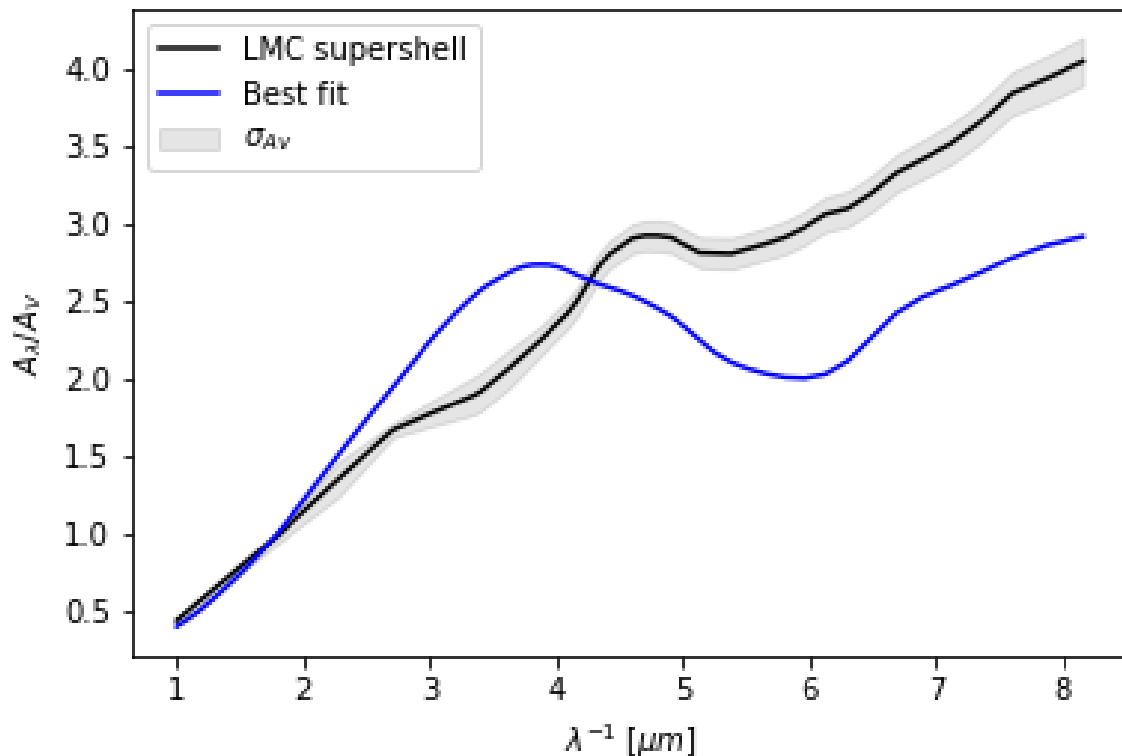


Figure 24: Best fit result of the LMC supershell extinction curve using only carbon grains.

This does obviously not give the nicest fit but shape wise the two are sort of similar. I, therefore, decided to continue with the test on this extinction curve. For the carbon grains, I have also made four bins containing the grains. I made the same size combinations as for the silicates. The result of the test can be seen in figure 25.

Unlike the silicate grains the ultra-small carbon grains dominate more than half of the inverted wavelengths. They dominate from $\gtrsim 4\mu m^{-1}$. To see which of the grains sizes dominates the observed extinction in the remaining inverted wavelength I have to go in and look at the different bin contributions to the different fits. Here the large carbon grains generally contributes the most along with the small and medium grains whereas the small carbon grains hardly appear in any of the combinations. It would therefore seem that the large and the small/medium bin dominates the remaining inverted wavelengths and that the small carbon grains don't dominate the observed extinction. The large carbon grains are therefore accurate in the part of the extinction curve they dominate according to figure 13 and figure 25.

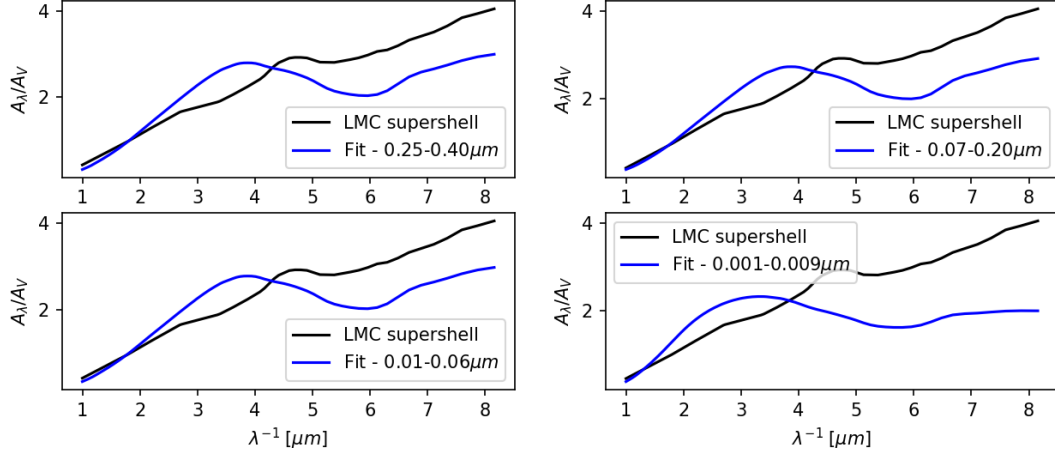


Figure 25: The four frames shows where different groups of carbon grains dominate the observed extinction.

Based on this test, the different grain sizes used to make the synthetic dust compositions are accurate since they only dominate the observed extinction in inverted wavelengths where the dust grain sizes are trustworthy according to the DDSCAT size limit.

9 Results

Now that I have finished testing the fitting routine I have made it is time to actually fit some of the extinction curves. In the following sections, I fit dust compositions to the MW, both the LMC curves, the SMC and ten different GRB host galaxies. In some of the figures, the original extinction curves may not have uncertainties plotted alongside the extinction, because the uncertainties weren't available in the data files I was kindly provided by Tayaba Zafar to run this routine on.

9.1 Milky Way extinction fit

The first extinction curve I have examined is the MW. The MW curve is characterised by its 2175Å bump and is therefore not as flat as the extinction curves I have run the fitting routine tests on so far. It will therefore be interesting to see if my routine actually can fit the 2175Å bump.

At first glance the fit in figure 26 looks like a descend fit to the MW extinction curve. The bump is sort of fitted and the rest of the extinction curve is also relatively well fitted. Looking at the RMS value of the fit, which is 0.1 doesn't give cause for concern either. The fit appears to be good when looking at the parameters we normally would use to evaluate the goodness of a fit. If I instead look at the dust composition needed to make the fit the story changes.

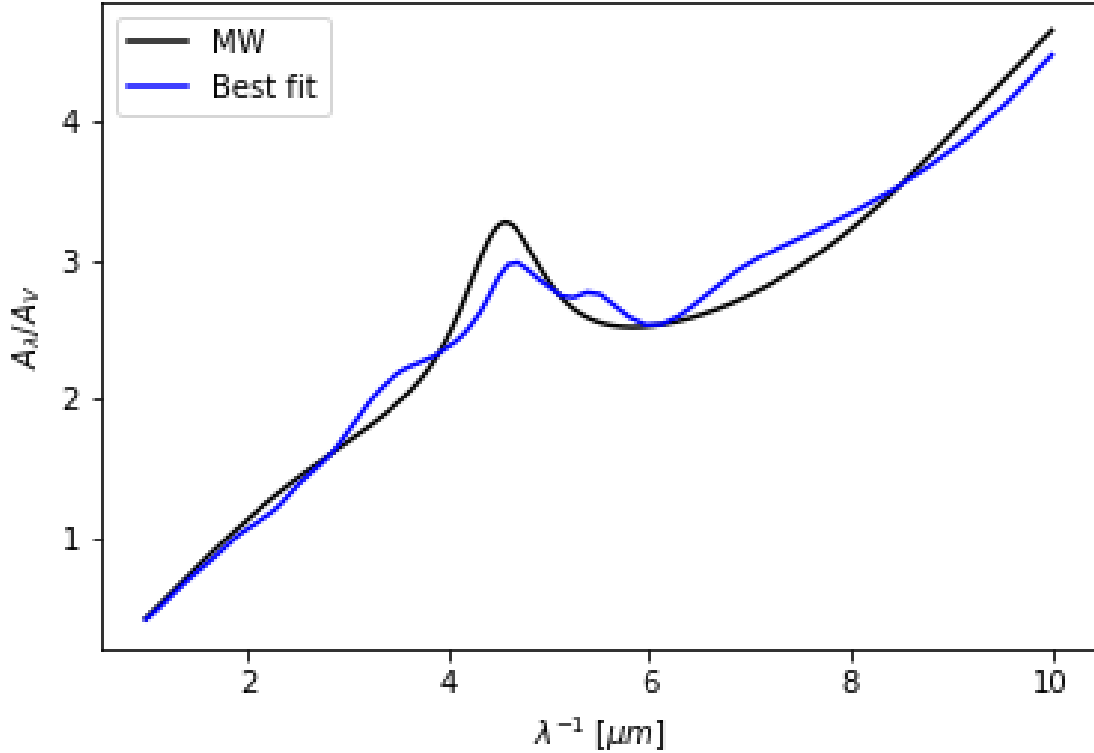


Figure 26: Best fit result of the MW extinction curve where the 2175\AA is partially fitted.

To produce the fit in figure 26 the following grain groups were used: the silicate grain with an effective radius of $0.08\mu m$, silicates in the sizes $0.01 - 0.20\mu m$ plus carbon grains in the sizes $0.07 - 0.20\mu m$, carbon grains in the sizes $0.001 - 0.009\mu m$ and finally silicate grains in the sizes $0.001 - 0.009\mu m$. Now, this in itself might not ring any alarm bells since I earlier wrote that the MW extinction should be able to be well fitted using a combination of silicates and carbon grains. The biggest problem for this dust combination arises when looking at the percentage distribution of each dust grain bin. To produce the fit in figure 26 40.1% of all the dust in the MW has to be silicate grains with the size $0.08\mu m$. That 40.1% of all the dust should have this one size sound too good to be true. In [1] they find that the MW extinction can be reproduced using roughly half silicate and half carbon dust. Should my result, therefore, be consistent with theirs, practically all the silicate grains in the MW should be one size, while the carbon grains could have any size possible. That one-grain material should be locked to one size while other grain materials are not sound really wired considering that all the grains are subjected to the same environments. One can therefore seemingly get a good fit to the extinction curve, with a dust composition that makes no sense at all. To determine which fit are the best to the extinction curve one therefore also have to look closely at the dust combination and not just at how well the fit fits the observed extinction curve.

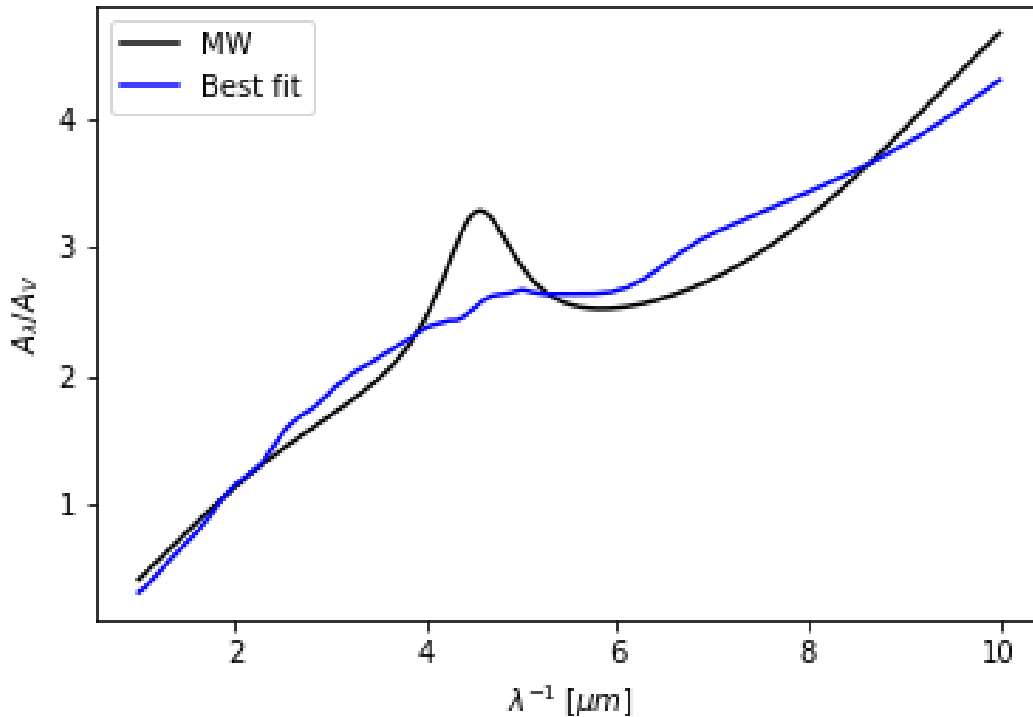


Figure 27: Best fit result of the MW extinction curve where the 2175\AA isn't fitted but the dust composition is realistic.

After concluding that the fit in figure 26 was no good I adjusted the grain bins. I changed them to contain 50:50 silicate and carbon grains, in the hopes that this would give a more realistic dust composition. This time around I used all the silicate and carbon grain up to the $0.20\mu\text{m}$ size. The best fit to the MW extinction curve can be seen in figure 27. This fit ended up containing 61% silicates and 39% carbon grains. For the exact distribution of each bin see table 1. This distribution is way more realistic since it doesn't assume that one particular grain size produces about half of the observed extinction. This fit is obviously not as perfect a fit to the extinction curve as the previous fit but it is still decent with an RMS of 0.2. Likewise, this fit is also consistent with the observation in [1], where the MW extinction was found to be about half silicate half carbon. In the article, they use graphite as their carbon grains whereas I use benzene. This could explain why I get a 60:40 relationship between the silicate and carbon grains and not a 50:50. Based on this I would conclude that even though the dust composition used to make the fit in figure 27 don't fit the 2175\AA bump, it is still a realistic dust composition for the MW. In order to improve the fit, it would require that there was developed complex refractive index for some PAHs materials which is thought to be responsible for the 2175\AA bump. As it is now it makes sense that a combination of silicate and benzene can't fit the bump since none of the individual grains has a bump of the right shape in their individual synthetic extinction. This can be seen on both figure 18 and figure 19. The fit in figure 27 is therefore as good as it can get using synthetic silicates and benzene dust grains.

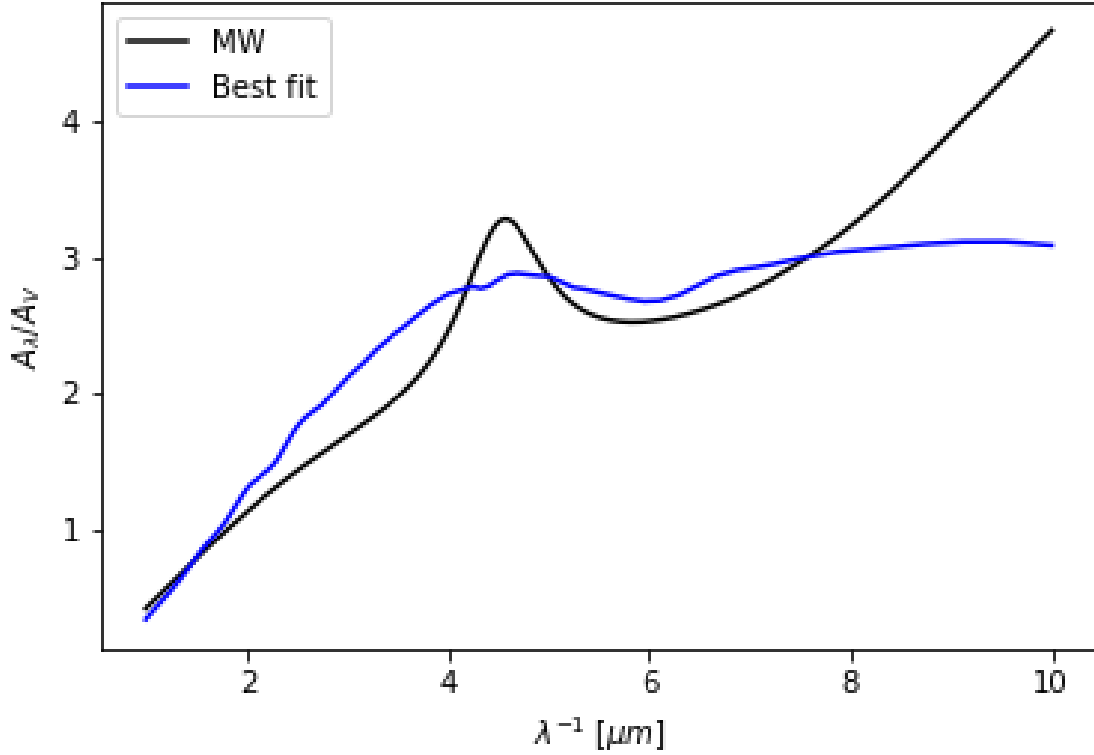


Figure 28: Best fit result of the MW extinction curve using the grain sizes from the MRN dust grain size distribution.

Even though I have found a satisfactory fit to the MW extinction I have tried one last dust combination. The MRN dust grain sizes distribution is one of the most widely used to constrain the dust grain sizes in a dust composition. I have therefore tried fitting the MW extinction curve only using the sizes in the MRN distribution, namely the carbon grains with the sizes $0.005 - 0.40 \mu m$ and the silicate grains with the sizes $0.02 - 0.25 \mu m$. The result of this fit can be seen in figure 28. This fit has an RMS value of 0.4 and it doesn't fit the extinction at $\gtrsim 8 \mu m^{-1}$. Likewise, the extinction from the fit should come from 92.9% ultra-small carbon grains, leaving room for practically no other carbon grain sizes or silicate grains. This does again seem odd since both [1] and the MRN article itself [3] find that the best fit is a combination of graphite and silicates. It could therefore look like the MRN dust grains size distribution is not well suited to fit the MW extinction, since it lacks a large part of the observed extinction curve. I don't blame the MRN distribution for not fitting the bump since none of the material used in the fit has the right shape to reproduce the 2175 \AA bump. Based on my earlier examination of where the different dust grain sizes dominate, the lack of fitting the inverted wavelengths larger than 8 can be contributed to the MRN dust grain sizes distributions, lack of ultra-small silicate grains. The ultra-small silicate grains dominate the silicate extinction from about $6.5 \mu m^{-1}$ onwards. This could therefore be a reasonable explanation of why the MRN size distribution can't fit the entire observed extinction curve.

	MW Bump		MW		MW MRN	
Bin 1	s: $0.08\mu m$	40.1%	c: $0.01 - 0.20\mu m$	2.2%	c: $0.01 - 0.06\mu m$	0.02%
Bin 2	s: $0.01 - 0.20\mu m$ c: $0.07 - 0.20\mu m$	4.1%	s: $0.01 - 0.20\mu m$	10.6%	s: $0.02 - 0.25\mu m$	7.05%
Bin 3	c: $0.001 - 0.009\mu m$	3.0%	c: $0.001 - 0.009\mu m$	37.0%	c: $0.005 - 0.009\mu m$	92.90%
Bin 4	s: $0.001 - 0.009\mu m$	52.8%	s: $0.001 - 0.009\mu m$	50.2%	c: $0.07 - 0.40\mu m$	0.02%
RMS		0.1		0.2		0.4
χ^2		7.2		19.4		47.3

Table 1: The dust grain bins used to produce the three different fits to the MW extinction curve. s and c denotes if the sizes used in the fit are either silicate or carbon. The percentage after the sizes is the amount needed to reproduce the observed extinction

Based on the three different fits I have made to the MW extinction curve, the dust composition that gives the most accurate result in is the one that overall gives a 60:40 relationship between the silicate and carbon grains. Table 1 shows the exact distribution of the different sizes. At the beginning of the thesis, I wrote that the larger the grain gets the fewer of the grains are found. It, therefore, fits well that there is needed less of both the larger silicate and carbon grains to make the best fit of the MW extinction curve. The best dust composition for the MW, therefore, consists of; 2.2% carbon grains in the sizes $0.01 - 0.20\mu m$, 10.6% silicate grains in the sizes $0.01 - 0.20\mu m$, 37.0% carbon grains in the sizes $0.001 - 0.009\mu m$ and 50.2% silicate grains in the sizes $0.001 - 0.009\mu m$.

9.2 Large Magellanic Cloud average extinction fit

After having fitted the MW extinction curve I went on fit the LMC curves. I started with the average LMC extinction curve since this one is very similar to that of the standard MW extinction curve. The biggest difference is that the 2175\AA bump is a bit smaller in the average LMC extinction curve.

Like the MW extinction curve the average LMC curve also has the characteristic 2175\AA bump. Looking at figure 29 one could be tempted to believe that the fitting routine has found the perfect dust composition to the average LMC extinction curve. It even has an extremely good RMS value of 0.07 and most of the fit is well within the observed extinction curves uncertainties. If one on the other hand look closer at the composition one will find that not everything is as it seem.

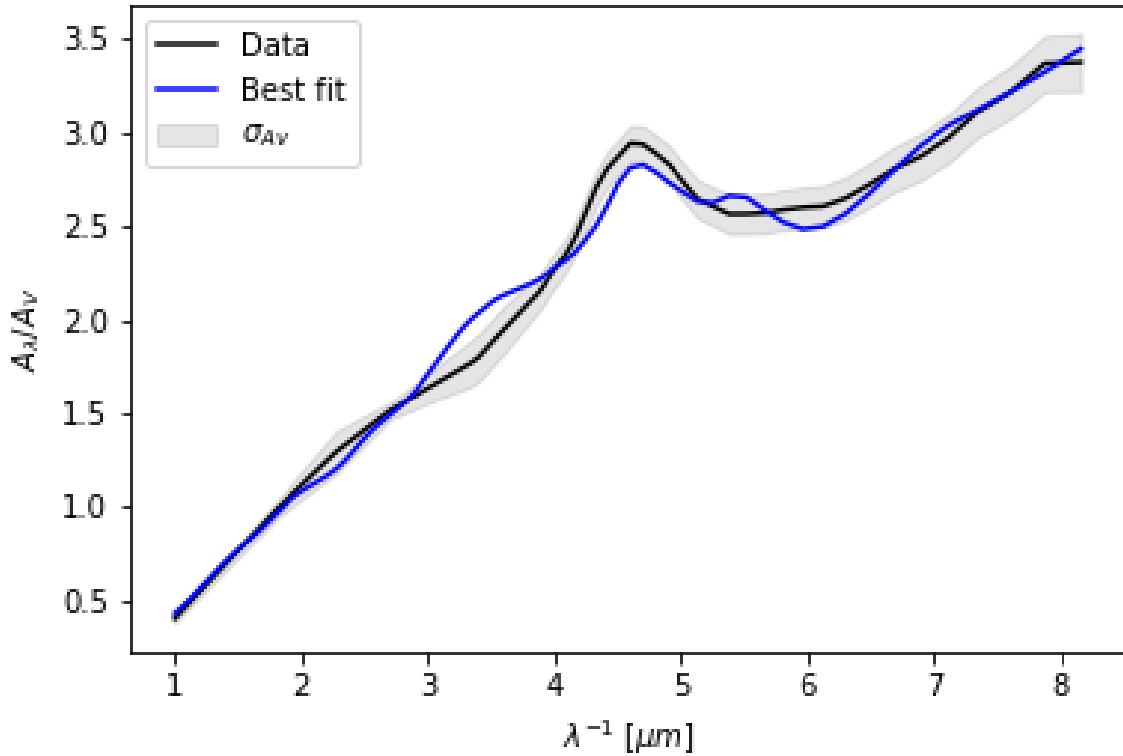


Figure 29: Best fit result of the LMC average extinction curve where the 2175Å bump is fitted.

What again cheats the eye and the goodness of fit measurement is the dust composition. To make the fit in figure 29 there has to be 35.5% silicate dust with the size $0.08\mu m$. That is a lot of dust that has to have one particular size. For the LMC this is not as bad as for the MW since the LMC generally is found to contain more silicates than carbon dust [1, 6]. But still, the fact that more than 1/3 of all the dust grains in the LMC have to be of one particular material in one particular size is hard to believe. Again one would assume that when all the dust grain is in the same environment they would develop in the same way because they in theory should be subjected to the same changes. This would mean that there either had to be another third of the dust grains that were reserved to carbon grains of the size $0.08\mu m$ or that there is no way that about 70% of all the grains are locked in one size distributed among the two materials. As for the MW, the fit that actually fit the 2175Å bump is therefore not realistic when looking at the dust composition. Had the fit on the other hand given let's say 1-3% of the dust had to be this one size, the suggested dust composition would have been more believable. This would have made the fit a fantastic fit to the LMC average extinction curve. But as the fit in figure 29 is now there is very little chance this is the actual dust grain composition of the average LMC extinction curve.

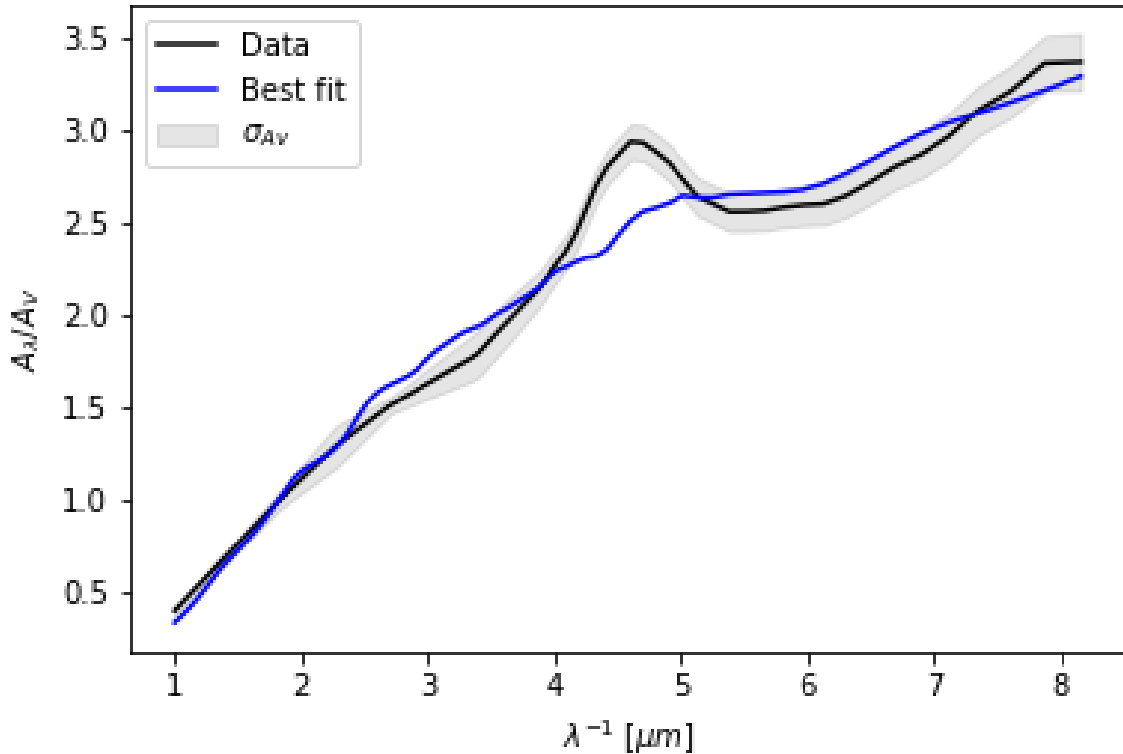


Figure 30: Best fit result of the LMC average extinction curve where the dust composition is made of 50:50 silicate and carbon grain sizes.

Next I tried a combination of bins that contained 50:50 silicate and carbon dust grains. Since the average LMC extinction curve is similar to that of the MW I chose the same bins as when I fitted the MW extinction curve. The result of this fit can be seen in figure 30. Here the fitting routine has fitted everything but the 2175Å bump. That the bump hasn't been fitted is again contributed to the fact that none of the individual synthetic dust grains has the right shape in their individual extinction. The dust distribution used to make figure 30 has 95% silicate dust and 5% carbon dust. The exact combination can be seen in table 2. That there are 95% silicates does seem like a very large change from the MW which had a similar curve, but as mentioned earlier the LMC does have a larger part of silicates in it. It is therefore not impossible that there should be 95% silicates in the average LMC extinction curve. In reality, there are properly fewer silicates than 95% since the 2175Å bump generally is attributed to PAHs which is a type of carbon. Should I have a chance to fit the entire average LMC extinction curve I would need the complex refractive index of the PAHs to generate the dust grains. These are sadly very tricky to obtain and it is therefore currently not possible to test if they indeed would be able to fit the 2175Å bump. The fit in figure 30 is, therefore, the best that can be generated with the chosen synthetic dust data. If I were to examine the LMC extinction curve further I would try using other dust materials since changing the sizes won't change the current best fit. I can't pick smaller sizes than the smallest size currently used because the dust grains

then become molecules and are no longer considered dust grains [4]. If I were to pick larger sizes than $0.40\mu m$ there would be so few of them that they hardly are observed in interstellar dust [5]. The larger dust grains should therefore not affect the total observed extinction that much. Including the larger sizes in the size range is therefore not necessary in order to fit the extinction curve. Having excluded the sizes as a parameter leaves the dust materials as the only changeable parameter in order to gain a better fit to the average LMC extinction curve in the future.

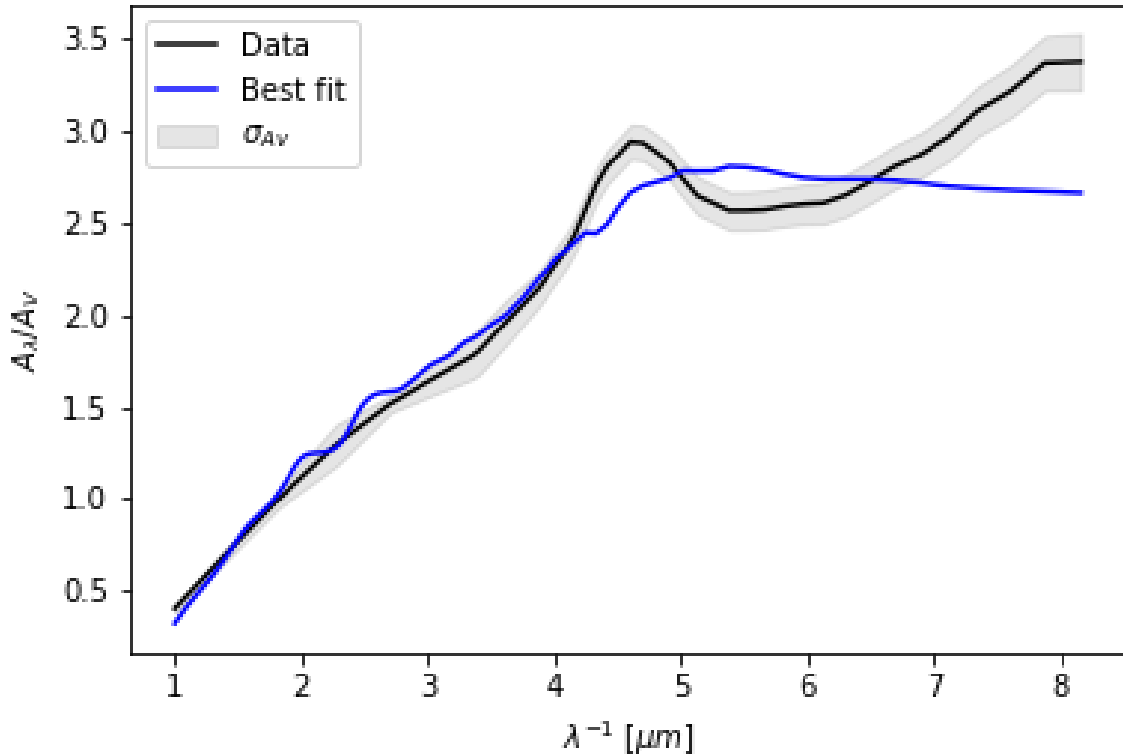


Figure 31: Best fit result of the LMC average extinction curve using the MRN dust grain size distribution.

The last combination I tested was the MRN dust grain size distribution. In figure 31 the result of the fit is shown. Compared to figure 30 the fit in figure 31 don't fit the extinction from $\sim 6.5\mu m^{-1}$ on-wards. This could be due to the lack of ultra-small silicate grains in the MRN dust grain size distribution. If I look at the different components of the fit there is again clearly more silicate dust than carbon dust. In the fit 89.5% of the dust is from silicates and the reaming 10.5% is from the carbon dust. This time around the bump in the curve is sort of fitted it is therefore doubtful there would be added more carbon dust in the fit to improve it. Adding the ultra-small silicate grains could on the other hand take care of the part of the extinction curve that is not fitted using the MRN distribution since they dominate the silicate extinction from about $6.5\mu m^{-1}$ onwards. Judging the fit in figure 30 and figure 31 solely on the RMS value would tell you that both fits are equally good. One, therefore, has to look at

the dust composition to see which of the fits actually gives the most realistic fit. Here my assessment is that the fit in figure 30 is better than the fit in figure 31. I have come to this conclusion since everything but the bump is fitted, which I knew would be hard to fit with the available synthetic grain sizes. The fit in figure 31 on the other hand has the possibility to be good if the MRN model had allowed the ultra-small silicate grains. But since they are not part of the model and a reasonable chunk of the observed extinction curve, therefore, isn't fitted, my assessment is that the fit is worse than the one in figure 30. Others have successfully used the MRN grain size distribution and managed to fit the entire extinction curve in figure 31 [1]. The difference between their fit and mine is that they use graphite as their carbon dust giving them an advantage in fitting the 2175Å bump because graphite dust can reproduce the bump [36]. The different choice of carbon dust type could therefore explain why I can't get the MRN size distribution to work well for my fits.

	LMC average Bump		LMC average		LMC average MRN	
Bin 1	s: $0.08\mu m$	35.3%	c: $0.01 - 0.20\mu m$	4.9%	c: $0.01 - 0.06\mu m$	0.1%
Bin 2	s: $0.01 - 0.20\mu m$ c: $0.07 - 0.20\mu m$	4.5%	s: $0.01 - 0.20\mu m$	19.6%	s: $0.02 - 0.25\mu m$	89.5%
Bin 3	c: $0.001 - 0.009\mu m$	0.5%	c: $0.001 - 0.009\mu m$	0.1%	c: $0.005 - 0.009\mu m$	9.6%
Bin 4	s: $0.001 - 0.009\mu m$	59.8%	s: $0.001 - 0.009\mu m$	75.4%	c: $0.07 - 0.40\mu m$	0.8%
RMS		0.07		0.1		0.1
χ^2		0.5		1.3		1.4

Table 2: The three different fit results for the average LMC extinction curve. s and c denotes if the dust grain sizes are silicate or carbon dust grains.

The best fit to the average LMC extinction curve is therefore the one in figure 30. The precise dust composition is presented in table 2.

9.3 Large Magellanic Cloud supershell extinction fit

Moving on from the average LMC extinction curve it is time to examine the LMC supershell extinction curve. This curve has a very small 2175Å bump compared to the MW and the average LMC extinction curve. Since the LMC supershell is part of the LMC galaxy I would expect the majority of the dust composition to be the same as for the average LMC extinction. There is of course some variations in the dust compositions since the extinction curves are different.

As for the two previous curves the 2175Å bump is again tricky to fit. Looking at figure 32 one would again assume that the fit is very good. After all, it has an RMS value of 0.07 and most of the fit is well within the uncertainties. There is therefore nothing measured in the goodness of fit that indicates the fit to be unlikely. One more time it is the dust composition that ends up ruining the otherwise perfect fit to the observed extinction curve.

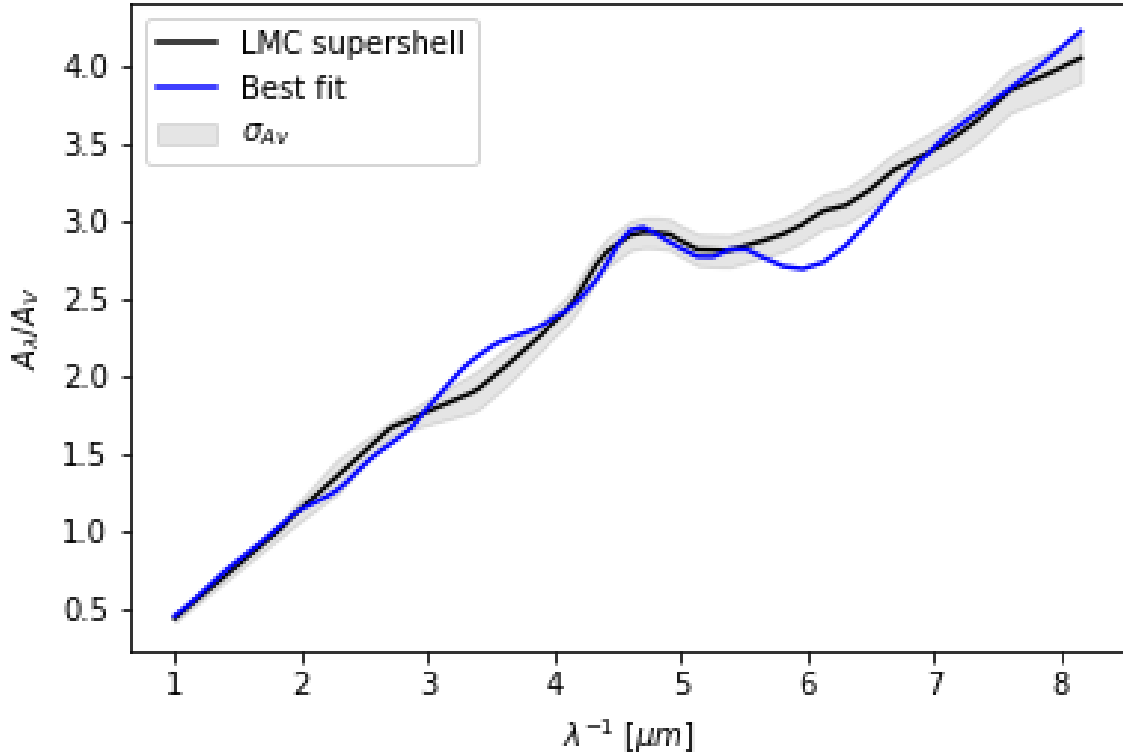


Figure 32: Best fit result of the LMC supershell extinction curve where the 2175Å bump is fitted.

Like before the problem arises from the need to have a large amount of one grain size. Since the 2175Å bump is smaller in the supershell extinction curve it makes sense that there is needed less of this grain size to fit this extinction curve. The problem is that even though there is needed a smaller percentage of the grain size, 27.1% is still a lot of dust to have with one size of one material compared to the total amount of dust in the galaxy. Since the extinction curve is from the supershell sightline which is close to the star-forming area 30 Dor [12] the dust in the sightline is affected by the star formation. This means that dust in the sightline may not be as homogene as for the LMC sightline. This leaves a tiny possibility that 27.1% of the dust actually is silicate dust with the size $0.08\mu m$. To me, it still seems unlikely that 27.1% of the dust should have one size. If $0.08\mu m$ is the preferred size for the dust to have in this sightline I would think that there should be a relatively large group of grains with similar sizes such as 0.07 or $0.09\mu m$ because there should be a natural spread of the dust grains around the size $0.08\mu m$ if it had a physical advantage. If I look at the dust composition found to be the best

fit this group of grains don't show up as unnaturally large. Getting a realistic fit of the 2175Å bump is therefore seemingly impossible with the current input variables. If this is indeed the case I will know once I tried fitting the LMC supershell extinction curve with a 50:50 mix of silicate and carbon dust. The 50:50 silicate and carbon fit is shown in figure 33.

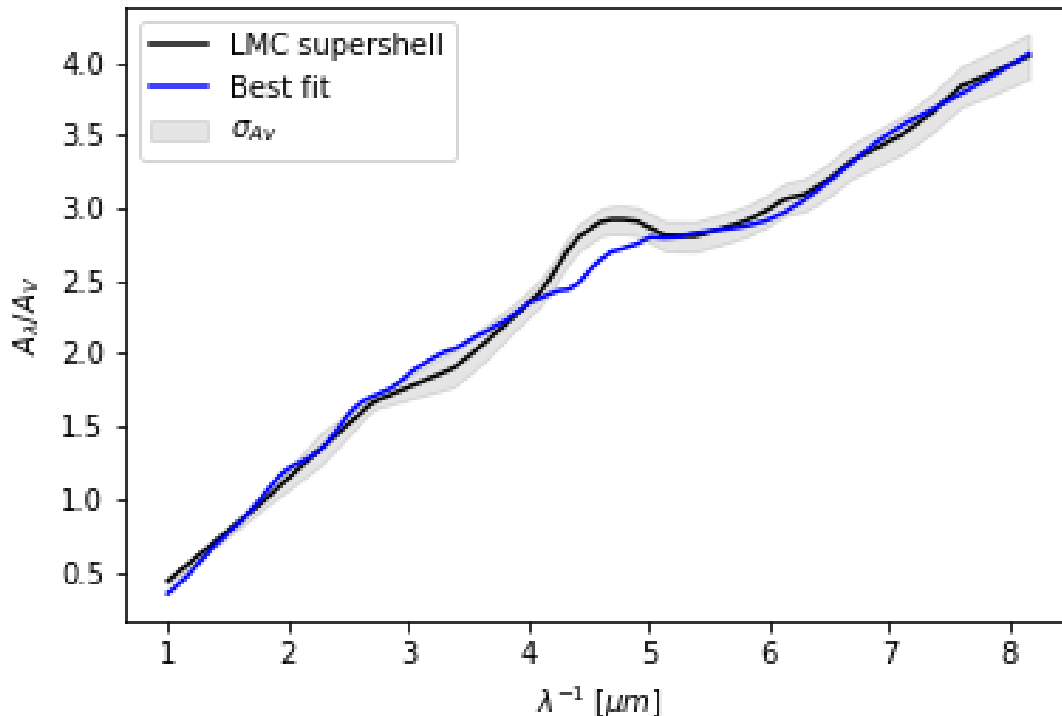


Figure 33: Best fit result of the LMC supershell extinction curve using 50:50 silicate and carbon dust.

The next combination I tried fitting to the LMC supershell extinction curve was a 50:50 silicate and carbon dust combination. I used the same bins for the average LMC extinction curve since it is the same galaxy, just different sightlines. Once more the 50:50 combination cannot fit the 2175Å bump as seen in figure 33. For the supershell extinction curve, the lack of fitting the bump is less severe than for the MW and the average LMC because the bump is much smaller. This means that the fit in figure 33 is closer to the actual extinction than that of the MW and average LMC. The fit in figure 33 has an RMS of 0.02 which is better than the fit that actually fit the bump for the supershell extinction. The dust composition used to make the fit in figure 33 contains 97% silicates and 3% carbon dust. This is consistent with the average LMC fit that contained 95% silicate and 5% carbon dust. I would expect to find more silicate dust in the supershell extinction curve since it is steeper than the average LMC extinction curve. This usually indicates that there are more of the ultra small grains, typically the silicates. Having 2% more silicates in the supershell extinction, therefore, sound reasonable considering it is the same galaxy just different sightlines. This especially makes sense because there are more of the ultra small grains in the supershell dust composition than in the average LMC composition.

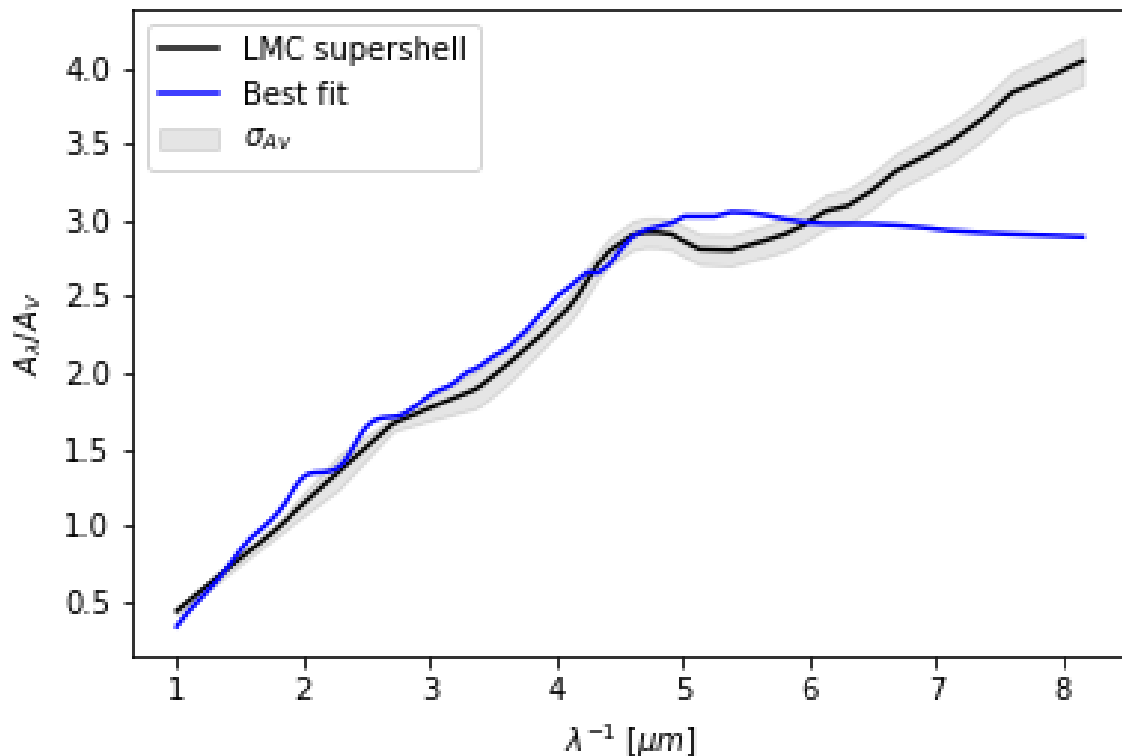


Figure 34: Best fit result of the LMC supershell extinction curve using the MRN dust grain size distribution.

The final dust combination I tried fitting to the LMC supershell extinction curve was the MRN dust grain size distribution. Once again the final part of the extinction curve is not well fitted when using the MRN size distribution. This can once more be attributed to the lack of ultra-small silicate grains in the MRN size distribution. If I look at the distribution of the different materials in the MRN fit in figure 34 it agrees with the previous fit in that the majority of the extinction is caused by the silicate grains. This time it needs 99.6% silicate dust grains. The lack of fitting the entire curve, therefore, has an interesting impact on the suggested dust composition. By not fitting the last part of the curve the carbon grains have been practically eliminated from the synthetic extinction fit. Based on the three different curves I have fitted with the MRN size distribution so far, the MRN size distribution is only capable of fitting the extinction well up to $\sim 6\mu m^{-1}$. The MRN size distribution consistently lacks some grains that are capable of fitting the remaining observed extinction. It, therefore, seems like the MRN are not the ideal dust grain distribution to use in either the MW or LMC. If it works well for extinction curves that lack the 2175Å bump is still to be determined. To answer this question I will have to fit the SMC using the MRN size distributions as well.

	LMC supershell Bump		LMC supershell		LMC supershell MRN	
Bin 1	s: $0.08\mu m$	27.1%	c: $0.01 - 0.20\mu m$	3.0%	c: $0.01 - 0.06\mu m$	0.1%
Bin 2	s: $0.01 - 0.20\mu m$ c: $0.07 - 0.20\mu m$	3.5%	s: $0.01 - 0.20\mu m$	12.3%	s: $0.02 - 0.25\mu m$	99.6%
Bin 3	c: $0.001 - 0.009\mu m$	0.3%	c: $0.001 - 0.009\mu m$	0.02%	c: $0.005 - 0.009\mu m$	0.1%
Bin 4	s: $0.001 - 0.009\mu m$	69.2%	s: $0.001 - 0.009\mu m$	84.7%	c: $0.07 - 0.40\mu m$	0.1%
RMS		0.07		0.02		0.2
χ^2		0.5		1		2.6

Table 3: The different results from fitting the LMC supershell extinction. s and c denotes if the dust grains are either silicate or carbon.

After examining the three different fits to the LMC supershell extinction curve, I find that the best fit to the LMC supershell is the one in figure 33, which have an RMS value of 0.02. This fit contains 97% silicate and 3% carbon dust. For the exact amount of each dust grain size see table 3.

9.4 Small Magellanic Cloud extinction fit

The last of the galactic extinction curves I have examined is the SMC extinction curve. Unlike the MW and both the LMC curves, the SMC doesn't have a bump at 2175\AA . I have therefore not made a specific plot where I tried to fit the bump in this curve, since there is none. According to [1], it should be possible to fit the SMC curve using purely silicate grains. I would therefore expect the dust compositions to lean very strongly in the direction of the silicate grains. I have tested the two statements that the SMC could be fitted with purely silicates [1] and that it is possible to get a satisfactory fit without using carbon grains smaller than $\sim 0.02\mu m$ [6]. Besides these, I will also test the MRN dust composition and the 50:50 silicate and carbon combination I used to fit the other extinction curves with, to see if any of these give better results than the before mentioned methods. It will be interesting to see how well the SMC curve can be fitted since most of the GRB host galaxy extinction curves are found to be variations of the SMC curve. If the routine therefore can fit the SMC satisfactory it becomes promising in regards to fitting the observed extinction of the GRB host galaxy extinction curves and thereby finding their dust composition.

The first dust combination I tested was the MRN dust grain size distribution to see if it behaved better when there was no 2175\AA bump in the observed extinction. As we shall see in a moment this is sadly not the case.

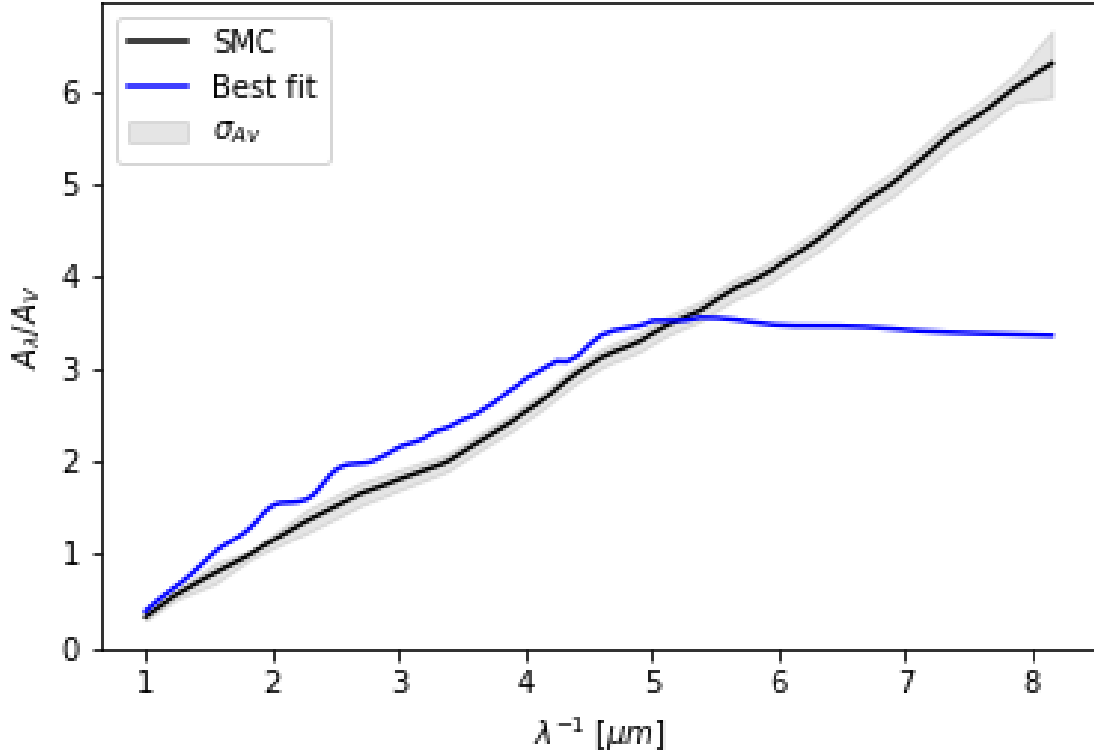


Figure 35: Best fit result of the SMC extinction curve using the MRN dust grain size distribution.

In figure 35 the MRN dust grain size distribution has been used to fit the SMC extinction curve. Once again the last part of the observed extinction curve isn't fitted. The MRN dust composition can therefore neither fit the SMC extinction curve or any of the other galactic extinction curves. Once more I attributed the lack of fitting the entire extinction curve to the lack of ultra-small silicate grains in the MRN size distribution. In figure 19 and figure 23 one can see that the ultra-small silicate grains dominate the extinction in the part of the curve there is not fitted. The other possibility would have been the ultra-small carbon grains because they too dominate the extinction in the missing area. Since most of the ultra-small carbon grains already are part of the MRN size distribution these can't be used to explain why it consequently won't fit $\gtrsim 6\mu m^{-1}$. This leaves me to conclude that the MRN size distribution needs to be expanded in the silicates to fit the entire extinction curve, meaning that the silicate grains $0.001 - 0.01\mu m$ would have to be included in the existing size range of $0.02 - 0.25\mu m$ for the MRN size distribution. Based on all the plots with the MRN distribution, I would therefore not recommend using this distribution of dust grain sizes since there is another dust combination that would give better results when fitting the entire observed extinction curve.

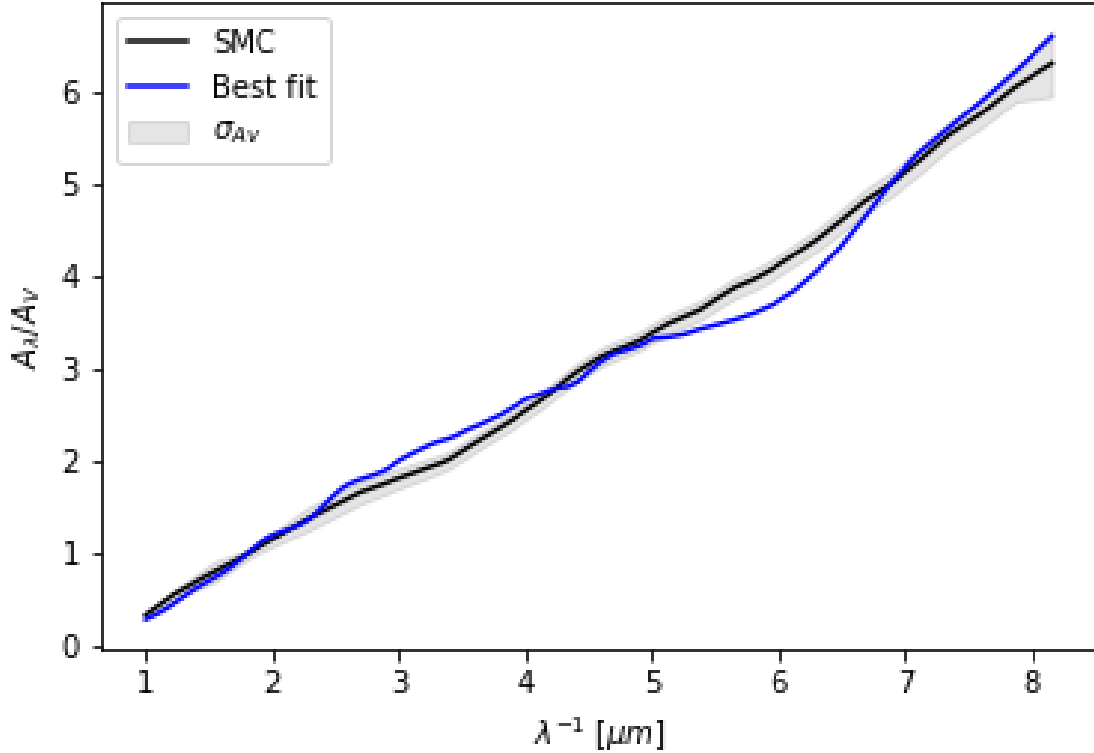


Figure 36: Best fit result of the SMC extinction curve using the same dust composition as the best fit MW and LMC curves.

The next dust combination I tried fitting to the SMC curve was the combination that contained 50:50 silicate and carbon dust grain sizes. I chose this combination because I was interested in seeing how well it would fit an extinction curve without the 2175Å bump. The combination gives a much more reasonable fit than the MRN dust combination. First of all the fit in figure 36 fits the entire extinction curve because it contains the ultra-small silicate grains, whereas the fit in figure 35 did not. Secondly, the 50:50 silicate and carbon dust combination also lean strongly in the direction of the silicate grains. This combination contains 99.4% silicates. This is consistent with both the MRN fit but also the finding from [1] where they find that the SMC extinction curve can be fitted using purely silicate grains. It will therefore be interesting to see if a pure silicate fit can improve the already good RMS value of 0.1 for the fit in figure 36. Besides the pure silicate dust combination, it should also be possible to reproduce the SMC extinction without using carbon grains smaller than $\sim 0.02\mu m$ [6]. Which one of these methods will give the best fit to the SMC extinction curve I will know once I've fitted the remaining combinations.

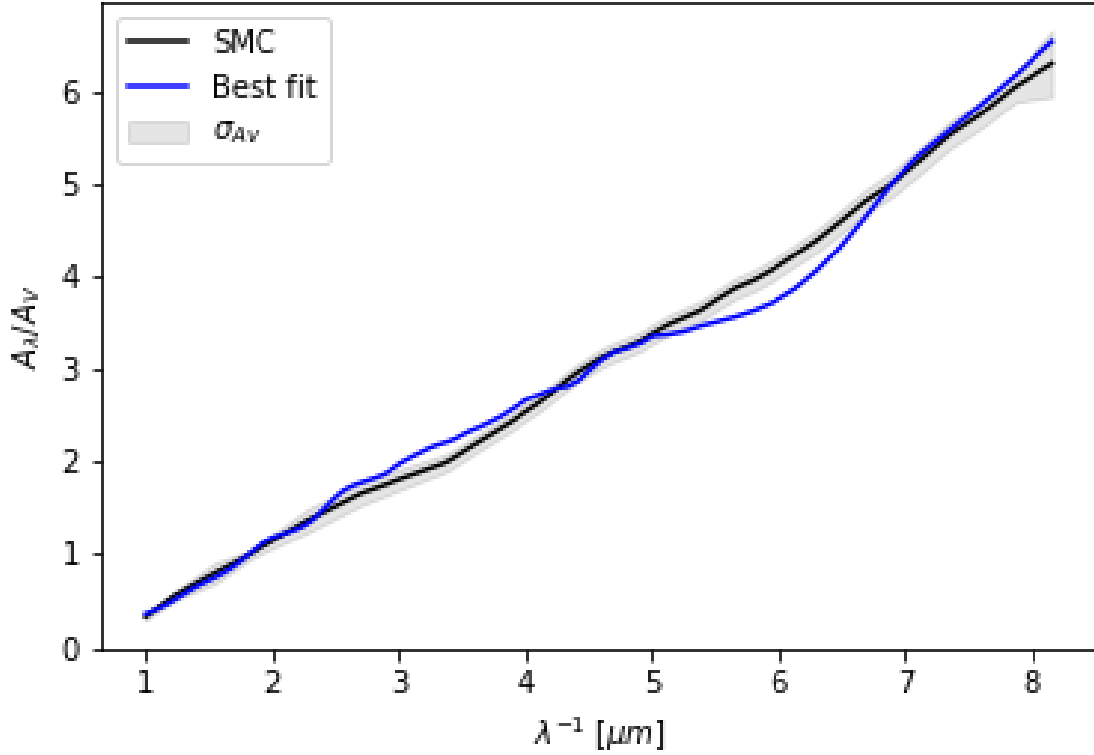


Figure 37: Best fit result of the SMC extinction curve without using carbon grains smaller than $0.01\mu m$.

Next I tested the statement from [6], that the SMC extinction can be reproduced without using carbon grains smaller than $\sim 0.02\mu m$. Because of the way I had set up my bins the fit in figure 37 contains the size $0.02\mu m$ and $0.01\mu m$ but any of the ultra-small carbon grains have been left out of the dust combination. The fit in figure 37 looks very similar to that of figure 36 where I had used the ultra-small carbon grains. The two fits in fact have the same RMS value and are therefore equally good. The fit without the ultra-small carbon grains contains 99.4% silicates as well. There is therefore no difference in the percentage of silicates used in the fits. One can therefore fit the SMC extinction curve well without using any of the ultra-small carbon grains as stated in [6]. This method is just as good as picking the 50:50 silicate and carbon dust grain size combination since the result is practically the same. This can also be seen in table 4 where the distribution of the different dust grain sizes for the fits to the SMC extinction curve is shown. Now that I tested the finding from [6] I only have to test the finding from [1] where they only use silicates to reproduce the SMC extinction curve, to know which of the different methods will give the best fit to the SMC extinction curve.

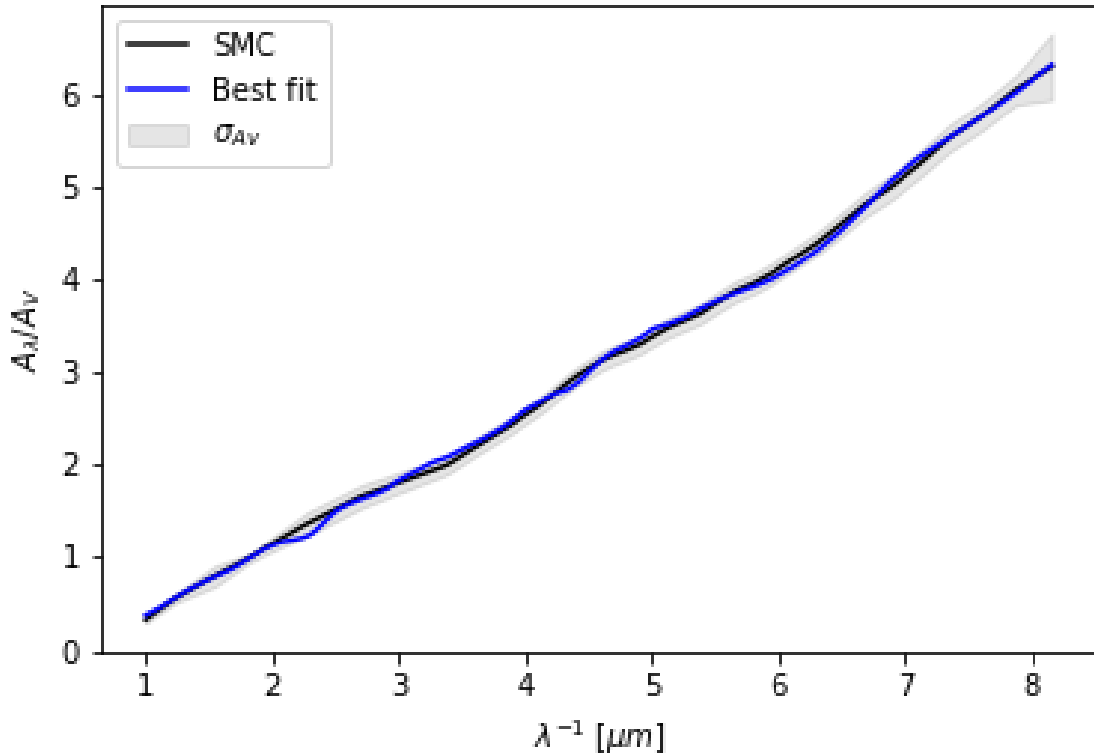


Figure 38: Best fit result of the SMC extinction curve using only silicate grains.

The final dust combination I used to fit the SMC extinction curve was the one made up of only silicate dust. As seen in figure 38 this dust combination fits the SMC extinction curve extremely well. This can also be seen on the fits RMS value which is 0.04 and the fact that the fit lies within the SMC extinction curves uncertainties. The pure silicate dust combination obviously only contains silicates dust. If I look closely at the distribution of the different grains sizes used to make the fit in figure 38 I see that the larger the grains get, the less of them is needed in order to fit the observed extinction. This is consistent with what I wrote in the beginning of the thesis. There I wrote that there was found very few of the large grains and the larger they got the less of them was found when examining the interstellar medium. That there therefore are needed less of the different grain sizes as they become larger in the fit in figure 38 therefore fits with this statement. To see how much of the different grain sizes are needed in order to fit the SMC extinction curve see table 4. Having fitted the SMC extinction curve with only silicate dust I agree with [1]. One can indeed fit the SMC extinction curve only using silicate dust. In fact it gives the best fit out of the four methods I have tested on this particular extinction curve.

	SMC MRN		SMC	
Bin 1	c: 0.01 – 0.06 μm	0.1%	c: 0.01 – 0.20 μm	0.6%
Bin 2	s: 0.02 – 0.25 μm	99.6%	s: 0.01 – 0.20 μm	6.7%
Bin 3	c: 0.005 – 0.009 μm	0.1%	c: 0.001 – 0.009 μm	0.03%
Bin 4	c: 0.07 – 0.40 μm	0.1%	s: 0.001 – 0.009 μm	92.7%
RMS		0.5		0.1
χ^2		15.1		1.9

	SMC Minimal carbon		SMC Pure silicate	
Bin 1	c: 0.01 – 0.20 μm	0.6%	s: 0.01 – 0.06 μm	10.8%
Bin 2	s: 0.01 – 0.20 μm	6.7%	s: 0.07 – 0.20 μm	6.5%
Bin 3	c: 0.25 – 0.40 μm	0.03%	s: 0.25 – 0.40 μm	1.3%
Bin 4	s: 0.001 – 0.009 μm	92.7%	s: 0.001 – 0.009 μm	81.3%
RMS		0.1		0.04
χ^2		0.9		0.3

Table 4: The four different dust compositions used to fit the SMC extinction curve. s and c denotes if the dust grain are silicate or carbon.

Having examined the four different fits to the SMC extinction curve it is once more clear the MRN dust grain size distribution is not well suited to fit the entire observed extinction curve. Both the 50:50 silicate and carbon dust combination and the combination without the ultra-small silicate grains gives a good fit to the SMC extinction curve. Had I not tested the pure silicate combination I would have found both of these fits to have been satisfactory fits to the SMC extinction curve. The best fit to the SMC extinction curve is by far the pure silicate fit. This fit has a really good RMS value and if comes with a realistic dust composition since it gradually needs less and less of the sizes as they increase in sizes. This fits with the statement at the beginning of the thesis where I said that the larger the grain becomes the less of them was found in the interstellar medium.

9.5 GRB host galaxy extinction fits

Before I present the best fits to the different GRB host galaxy extinction curves there are a few things worth noticing. The ten featureless GRB host galaxy extinction curves presented below all come from [18]. In this article all the GRB host galaxy extinction curves I am using in this thesis, are found to be SMC like in their extinction. When I examined the SMC extinction curve I found that the best fit was obtained using only silicate dust. I have therefore chosen to

only present the GRB host galaxy extinction curve fits, that are made purely of silicate dust below. These should give the best fits to the different GRB host galaxy extinction curves, since they are SMC like in their extinction. For the best dust combination using a mix of silicate and carbon dust to fit the GRB host galaxy extinction curves please see figure 49 - 58 and table 7 in appendix B.

		GRB 090313A	GRB 100219A	GRB 100418A	GRB 100901A
Bin 1	s: $0.07 - 0.20\mu m$	4.69%	3.55%	4.51%	9.29%
Bin 2	s: $0.25 - 0.40\mu m$	2.72%	1.26%	1.80%	5.07%
Bin 3	s: $0.001 - 0.009\mu m$	85.60%	92.19%	87.62%	73.19%
Bin 4	s: $0.01 - 0.06\mu m$	6.99%	2.99%	6.07%	12.45%
RMS		0.13	0.27	0.11	0.11
χ^2		7.77	9.83	8.30	7.42
		GRB 111008A	GRB 111209A	GRB 120119A	GRB 120815A
Bin 1	s: $0.07 - 0.20\mu m$	5.57%	4.39%	7.02%	3.86%
Bin 2	s: $0.25 - 0.40\mu m$	2.17%	1.97%	3.86%	1.75%
Bin 3	s: $0.001 - 0.009\mu m$	84.56%	87.92%	79.43%	89.67%
Bin 4	s: $0.01 - 0.06\mu m$	7.70%	5.72%	9.69%	4.73%
RMS		0.14	0.17	0.11	0.20
χ^2		7.97	8.44	6.73	9.79
		GRB 121024A	GRB 130427A		GRB 121024A
Bin 1	s: $0.07 - 0.20\mu m$	5.34%	5.24%	c: $0.01 - 0.06,$ $0.25 - 0.40\mu m$	4.76%
Bin 2	s: $0.25 - 0.40\mu m$	2.43%	3.09%	s: $0.01 - 0.06,$ $0.25 - 0.40\mu m$	7.83%
Bin 3	s: $0.001 - 0.009\mu m$	85.84%	83.85%	c: $0.001 - 0.009\mu m$	35.39%
Bin 4	s: $0.01 - 0.06\mu m$	6.38%	7.83%	s: $0.001 - 0.009\mu m$	52.02%
RMS		0.14	0.12		0.04
χ^2		7.41	7.09		3.08

Table 5: Overview over the different grain sizes used to make the fits to the different GRB host galaxy extinction curves. S denotes that the grain sizes are silicate dust and c is carbon dust. For GRB 121024A the last entry corresponds to the right panel in figure 47 and entry number 9 is the left panel of figure 47.

Besides the ten featureless GRB host galaxy extinction curves, I also have one very flat GRB host galaxy extinction curve from [35]. This specific flat extinction curve comes from GRB 121024A, of which I also have a featureless extinction curve from [18]. I, therefore, have two very different extinction curves of the same GRB host galaxy. I will not attempt to say which of the extinction curves are the correct extinction curve, but I will fit both curves since the differences can be used to show some of the different characteristics of very steep and very flat extinction curves in general.

For all the dust combinations presented above I have found the percentage needed of each dust bin to reproduce the observed GRB host galaxy extinction, as well as the RMS and χ^2 of each fit. These are presented in table 5. Based on the RMS and χ^2 values presented in table 5 and table 7 in appendix B, the pure silicate dust fit does indeed give the best fit to all of the featureless GRB host galaxy extinction curves presented below. The GRB host galaxy extinction curves that are SMC like in their extinction, can therefore like the SMC extinction curve best be reproduced using a pure silicate dust model.

9.6 GRB 090313A extinction fit

The first GRB host galaxy extinction curve I have fitted is from the GRB 090313A. The featureless extinction curve in figure 39 is very similar to the ones we will see from all the other GRB host galaxy extinction curves I will work on within this thesis. Since the GRB 090313A extinction curve is supposed to be similar to the SMC extinction curve [18], I would expect it to be a flat relatively steep extinction curve. Looking at figure 39 there is no 2175Å bump and the curve is indeed flat and rising fast in A_λ/A_V when the inverse wavelength gets higher, just like the SMC extinction curve. The best fit to the GRB host galaxy extinction curve is obtained when using only silicate grains in the sizes $0.001 - 0.40\mu m$, just like the SMC extinction curve. Because the GRB 090313A extinction curve is similar to the SMC extinction curve, it makes sense that both curves best dust combination is made of the same grain sizes and materials. Of course, there is some variation in the percentages needed of the different grain sizes since the two curves aren't exact copy's of one another, but just very similar in shape and steepness. Once more the dominating grain sizes are the silicate grains $0.001 - 0.009\mu m$ with 85.60% of the dust belonging to this group of grains in the best fit of the GRB 090313A extinction curve. This is typical for a steep extinction curve, since the steeper the curve, the more of the ultra small grains are needed to get a good fit. This will also be illustrated by some of the even steeper GRB host galaxy extinction curves that have yet to be fitted in the coming sections. The dust combination used to fit the GRB 090313A extinction curve is therefore typical for a fast-rising extinction curve without the 2175Å bump. In table 5 all the dust combinations used to fit the different GRB host galaxies can be seen. Looking at this table one can see that the best fit to GRB 090313A is indeed a typical fit for an SMC like extinction curve, since the rest of the SMC like GRB host galaxy extinction curve best fits are very similar to it.

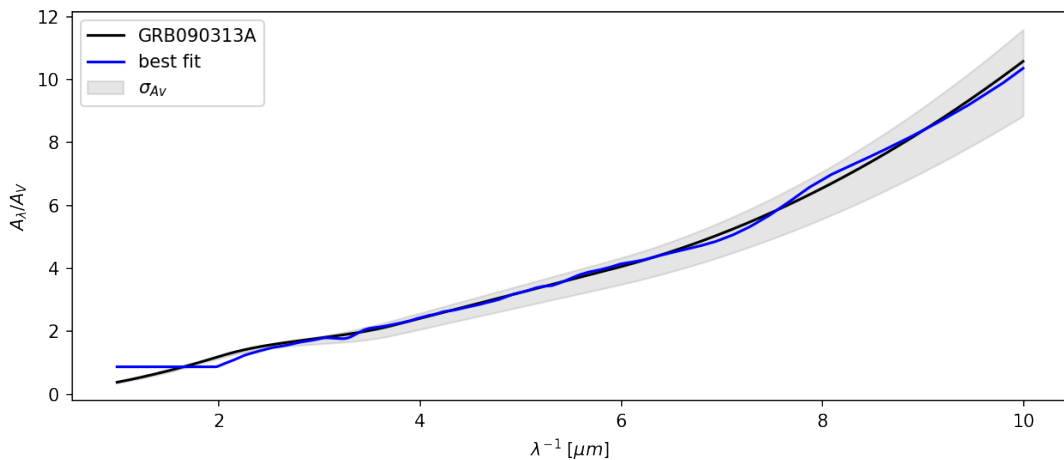


Figure 39: Best fit result of GRB 090313A, using only silicate dust in the size range $0.001 - 0.40\mu m$.

9.7 GRB 100219A extinction fit

The next GRB I worked with is the GRB 100219A. This GRB host galaxy extinction curve is also similar to that of the SMC extinction curve since it lacks the 2175\AA bump and is otherwise a featureless rising curve. What set the GRB 100219A extinction curve apart from the rest of the GRB host galaxy extinction curves presented in result section 9.6-9.15, is that it has a rise in the larger inverse wavelengths that are considerably steeper than the other extinction curves, see figure 40. Examples of other steep rising GRB host galaxy extinction curves are GRB 100418A, GRB 111209A and GRB 120815A. These extinction curves "only" rise to an A_λ/A_V of 14-16, whereas GRB 100219A goes all the way up to 17.5. That GRB 100219A is the steepest of the extinction curves can also be seen in the dust combination used to fit the extinction curve. As mentioned earlier, the steeper a curve is, the more of the ultra small grains are needed to get a good fit to the curve. For GRB 100219A there is needed 92.19% of the grain sizes $0.001 - 0.009\mu m$. This is the largest percentage needed for any of the GRB host galaxies, as can be seen in table 5. Once again the best dust combination is made purely of silicate dust. This makes sense since the GRB 100219A extinction curve is similar to the SMC extinction curve, which best fit contained only silicate dust. That the two curves, therefore, have a similar type of dust model as the best fit is expected. For the rest of the dust grain sizes used in the fit of the GRB 100219A extinction curve, as well as the goodness of fit, please see table 5.

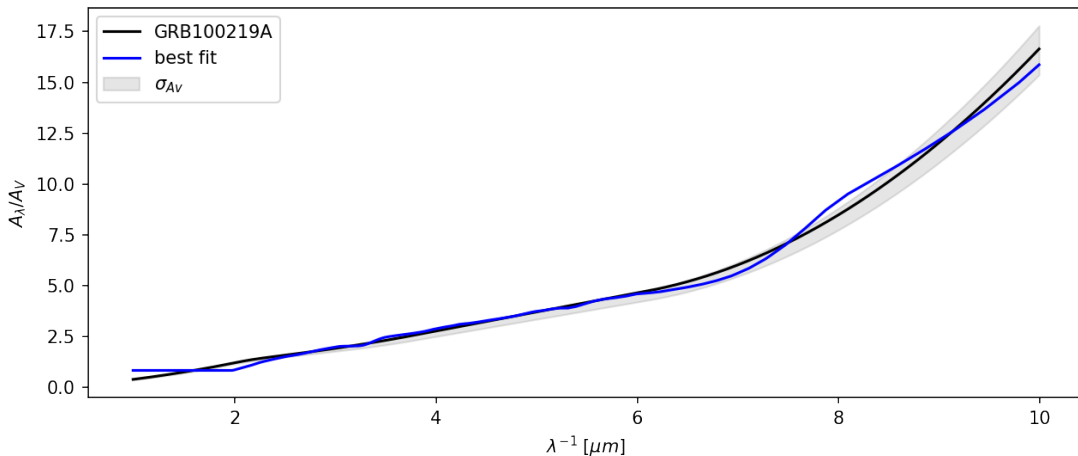


Figure 40: Best fit result of GRB 100219A, using only silicate dust in the size range $0.001 - 0.40\mu m$.

9.8 GRB 100418A extinction fit

After working with GRB 100219A I started working on fitting the extinction curve of GRB 100418A. Like the GRB host galaxy extinction curves presented above, the GRB 100418A extinction curve is SMC like in its extinction. This once again means that there is no 2175Å bump and that the extinction curve is a steep featureless curve. Because the GRB host galaxy extinction curve is SMC like in its extinction I would expect the two to have a similar dust composition. When fitting the SMC extinction curve I found that the best fit was obtained using only silicate dust. It was therefore no surprise that the best fit of the GRB 100418A extinction curve was found to only use silicates as well. Because the GRB 100418A extinction curve is a steep extinction curve, one has to include a large percentage of very small dust grains to get a good fit for the extinction curve. For the specific fit shown in figure 41, 87.62% of the dust is silicate grains with the sizes 0.001 – 0.009 μm . The GRB 100418A extinction curve and dust combination are therefore similar to not only that of the SMC extinction but also the two GRB extinction curves presented above. For the exact amount of each dust group needed to reproduce the extinction in figure 41 see table 5.

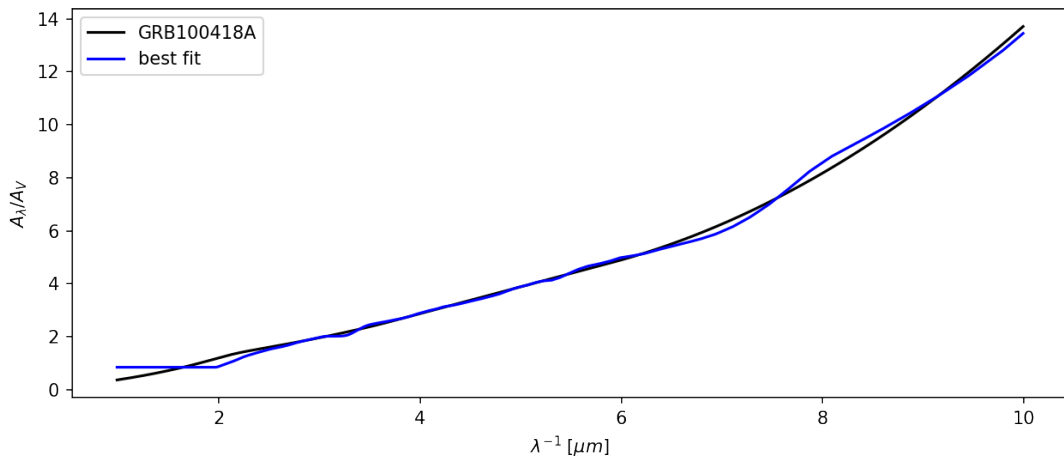


Figure 41: Best fit result of GRB 100418A, using only silicate dust in the size range 0.001 – 0.40 μm .

9.9 GRB 100901A extinction fit

Next, I examined the extinction curve of GRB 100901A. This extinction curve is also an SMC like extinction curve because this one also lacks the 2175\AA bump and is a step featureless curve. The GRB 100901A curve varies from the other GRB host galaxy extinction curves by being the least steep of all the GRB curves. Because the GRB 100901A extinction curve isn't as steep as the other GRB host galaxy extinction curves it should not require as large a percentage of the ultra small silicate grains when fitting the extinction curve. As predicted the GRB 100901A extinction curve only needs 73.19% silicate dust with the grain sizes $0.001 - 0.009\mu m$, compared to the over 80% needed for the curves presented above. Once again it makes sense that the best fit to the observed extinction curve is achieved when using only silicate dust in the synthetic dust composition. Since the GRB 100901A extinction curve is classified as an SMC like extinction curve in [18], I would expect the two to have similar dust compositions. Therefore when I found that the SMC extinction curve best could be fitted using only silicate dust, it would make sense that the best fit to the GRB 100901A extinction curve would also consist of pure silicate dust, because the two extinction curves are very similar. It is therefore not surprising that the fit in figure 42 is consisting only of silicate dust in the sizes $0.001 - 0.40\mu m$. For the exact combination of dust used to reproduce fit the extinction see table 5.

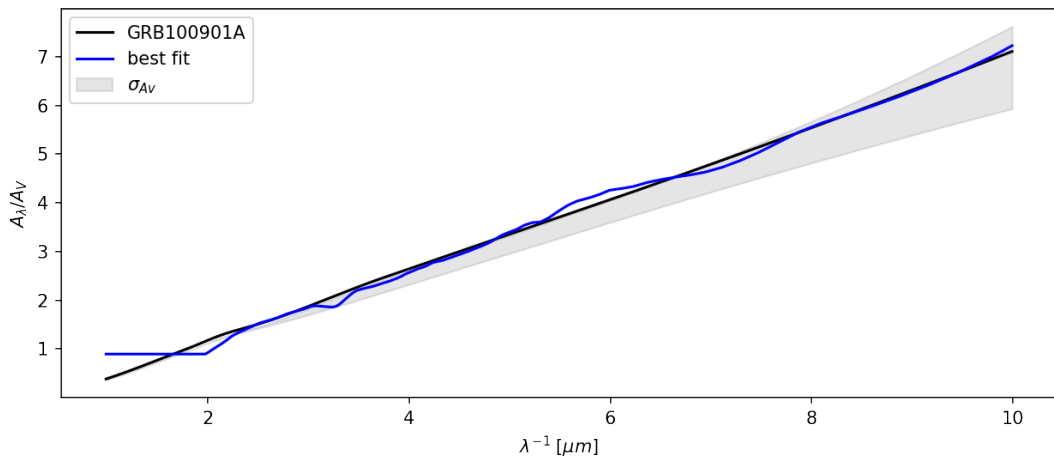


Figure 42: Best fit result of GRB 100901A, using only silicate dust in the size range $0.001 - 0.40\mu m$.

9.10 GRB 111008A extinction fit

The next GRB host galaxy I looked at was GRB 111008A. Like the other GRB host galaxies, the GRB 111008A extinction curve is also SMC like in the extinction. This can be seen in the lack of the 2175Å bump and the steep featureless curve. When I examined the SMC extinction curve I found that the best fit to the SMC extinction was obtained when using only silicate dust. Therefore when trying to reproduce the observed extinction of GRB 111008A, it was no surprise that the best fit to this curve also was obtained when only using silicate dust, because it is so similar to the SMC extinction curve. Like all the other GRB host galaxy extinction curves presented so far, the GRB 111008A extinction curve is steep meaning that the fit would need a large percentage of ultra small dust grains to reproduce the observed extinction well. For the fit presented in figure 43 there is 84.65% silicate dust with the sizes 0.001 – 0.009 μm . The behaviour of the GRB 111008A extinction curve is therefore as expected since it has a similar dust composition to the SMC and it needs a large percentage of ultra small grains to reproduce the steep rise in A_λ/A_V .

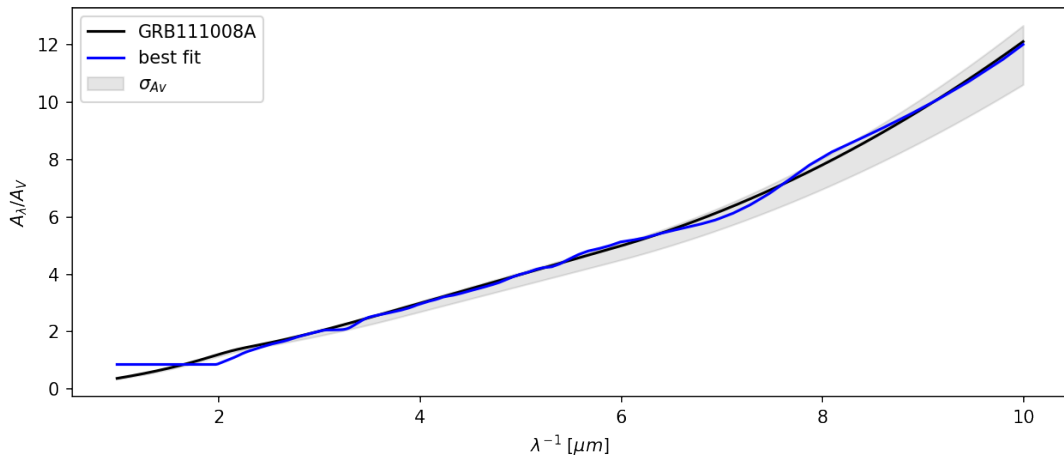


Figure 43: Best fit result of GRB 111008A, using only silicate dust in the size range 0.001 – 0.40 μm .

9.11 GRB 111209A extinction fit

Continuing to the next GRB host galaxy which is GRB 111209A, I once more have an SMC like extinction curve. This is again due to the steep rise in A_λ/A_V over the inverse wavelengths and the lack of the 2175Å bump in the extinction curve. Like all the GRB host galaxy extinction curves presented above, the GRB 111209A extinction curve can best be reproduced using only silicate dust grains of the sizes $0.001 - 0.40\mu m$. At this point, it comes as no surprise, since both the SMC and all the other GRB SMC like extinction curves have had the same dust combinations as the best fit. Because the GRB 112009A extinction curve is one of the steeper GRB host galaxy extinction curves I am examining, I would expect it to have one of the larger percentages of the $0.001 - 0.009\mu m$ silicate dust grains compared to the other GRB host galaxy dust combinations. The GRB 111209A extinction curve contains 87.92% of the ultra small grains. This is indeed one of the larger percentages compared to the other GRB host galaxy extinction curves, see table 5. The behaviour of the dust combination used to reproduce the GRB 111209A extinction in figure 44 is therefore as expected based on the shape of the extinction curve and the previously examined GRB host galaxy extinction curves.

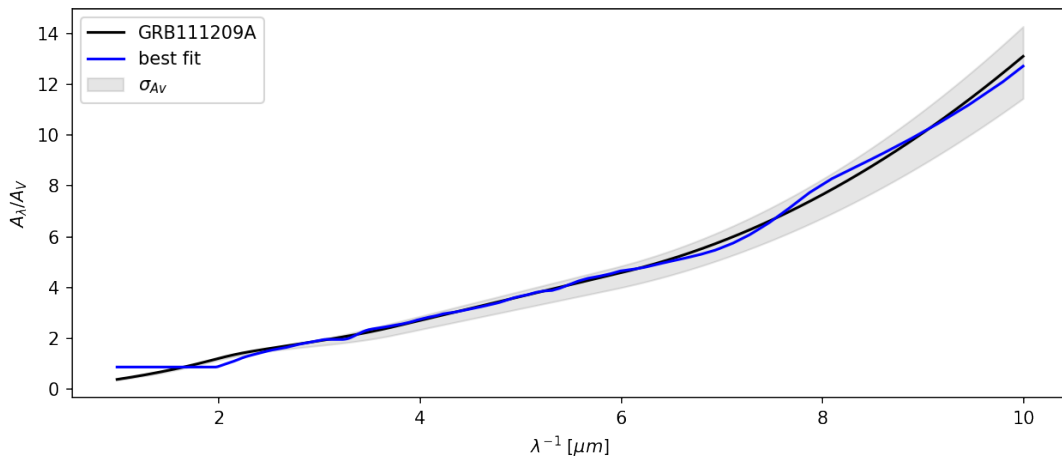


Figure 44: Best fit result of GRB 111209A, using only silicate dust in the size range $0.001 - 0.40\mu m$.

9.12 GRB 120119A extinction fit

After having examined GRB 111209A I started looking at GRB 120119A. Like all the other GRB host galaxy extinction curves presented so far the GRB 120119A extinction curve is SMC like in its extinction. This means that the GRB 120119A extinction curve lacks the 2175Å bump and is otherwise a steep featureless curve. When examining the extinction curve I found that the dust combination that best could reproduce the observed extinction was made purely of silicate dust. This dust combination is size-wise the same as the dust combination giving the best fit to the SMC extinction curve. The GRB 120119A extinction curve is very similar to the SMC extinction curve. It does therefore make sense that the two curves would have similar dust compositions. The GRB 120119A extinction curve is one of the least steep GRB host galaxy extinction curves I have examined so far. I would therefore expect it to contain a smaller percentage of the ultra small dust grains, namely the sizes $0.001 - 0.009\mu m$ because the steeper an extinction curve is the more of the ultra small dust grains are needed to get a good fit to the observed extinction. The GRB 120119A extinction fit contains 79.43% of the ultra small silicate grains. This is indeed less than most of the other GRB host galaxy extinction curves I have examined so far. The GRB 120119A extinction curve, therefore, behaves as I would expect it to since it has a lesser amount of small silicate dust due to not being as steep as the other GRB host galaxy extinction curves and because it contains only silicate dust like all the other SMC like GRB extinction curves.

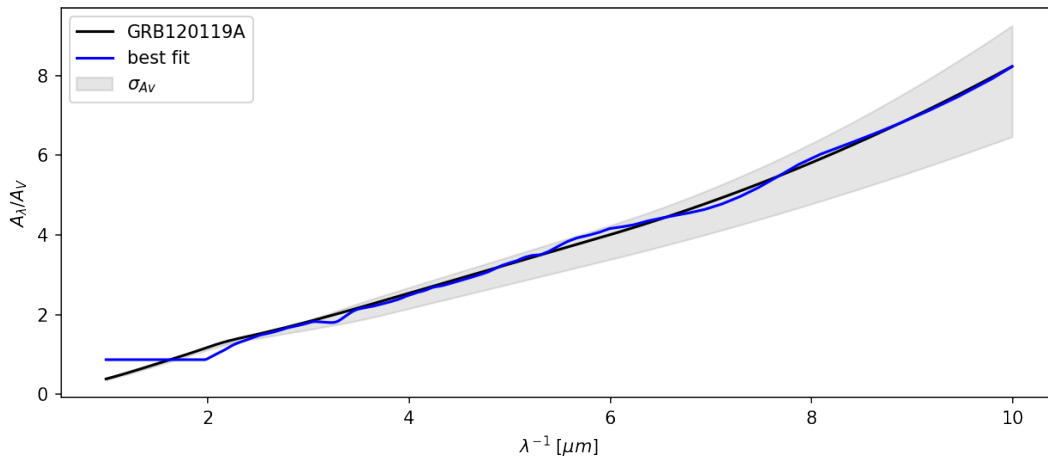


Figure 45: Best fit result of GRB 120119A, using only silicate dust in the size range $0.001 - 0.40\mu m$.

9.13 GRB 120815A extinction fit

Next, I examined the GRB 120815A extinction curve. Like all the other GRB host galaxy extinction curves presented so far, this GRB extinction curve is also classified as an SMC like extinction curve in [18]. This means that the GRB 120815A extinction curve lacks the 2175Å bump and is a steep featureless extinction curve. Because the GRB 120815A extinction curve is SMC like in its extinction I would expect the two extinction curves to have similar dust compositions. For the SMC extinction curve, I found that the best dust combination contained only silicate dust. When I examined the GRB 120815A extinction curve I would therefore expect it to have a similar type of dust combination. Therefore finding that the dust combination that best reproduces the GRB 120815A extinction was only made of silicate dust was no surprise. Besides the dust combination, it is worth noticing that the GRB 120815A extinction curve is one of the steeper GRB host galaxy extinction curves I have worked with so far. I would therefore expect this extinction curve to have one of the largest percentages of the ultra small silicate dust grains in its dust combination. Looking in table 5 shows that the dust combination used to reproduce the GRB 120815A extinction in figure 46 is made of 89.67% silicate dust with the sizes $0.001 - 0.009\mu m$. This is the second-largest percentage needed for any of the GRB host galaxies presented in the table. This fits with the data since GRB 120815A has the second steepest extinction curve of all the GRB host galaxies and therefore should contain the second largest percentage of the ultra small silicate grains. The dust combination of GRB 120815A, therefore, behaves as expected.

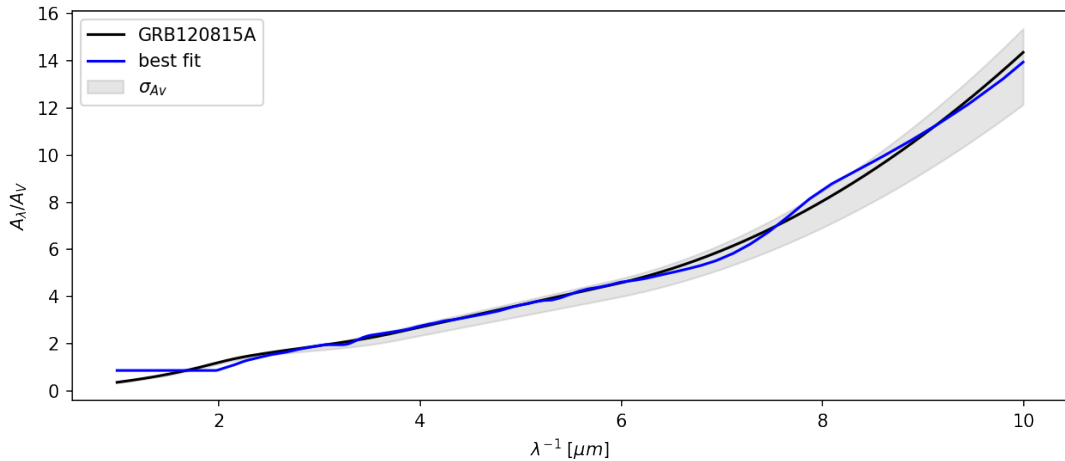


Figure 46: Best fit result of GRB 120815A, using only silicate dust in the size range $0.001 - 0.40\mu m$.

9.14 GRB 121024A extinction fit

Next, it was time to examine the two extinction curves of GRB 121024A. One of the extinction curves is very similar to the other GRB host galaxy extinction curves I have presented so far. This is the extinction curve in the left panel of figure 47. This GRB 121024A extinction curve is also SMC like in its extinction. The best dust combination to this extinction curve is therefore also a pure silicate dust fit like for the SMC extinction curve. Once again because the curve is steep, it is expected that there are needed a large percentage of the ultra small dust grains to get a good fit to the extinction curve. For the extinction curve in the left panel of figure 47, there is needed 85.84% of the ultra small dust grains. This is indeed a large percentage of the total dust grains needed to reproduce the observed extinction.

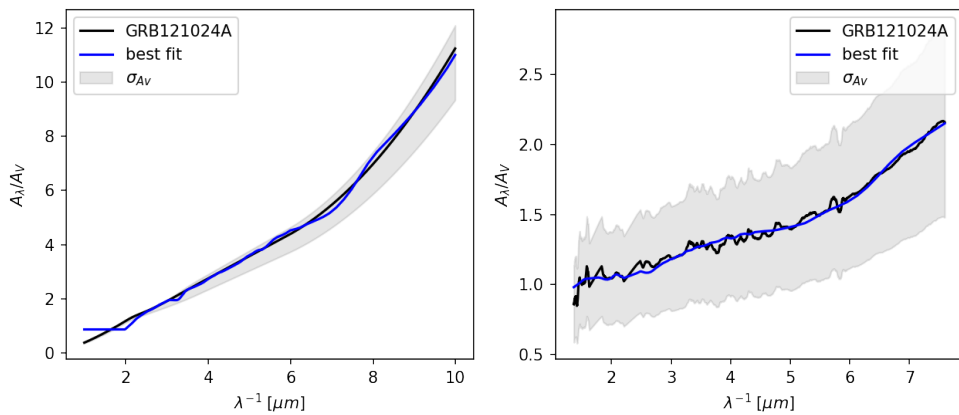


Figure 47: Best fit result of GRB 121024A. For the left panel of the figure, the best fit is obtained using silicate grains of the sizes $0.001 - 0.40\mu m$, using the GRB 121024A extinction curve from [18]. Whereas the right panels best fit to the GRB 121014A extinction curve from [35] is obtained using a mix of silicate and carbon dust.

The extinction curve in the right panel of figure 47 is not like any of the extinction curves presented so far. First of all, it is a very flat curve that only rises to 2 in A_λ/A_V at $8\mu m^{-1}$. Secondly, the curve itself can not be classified as either an MW, LMC or SMC like extinction curve. The MW and LMC type is excluded due to the lack of the 2175\AA bump and the SMC type is excluded because the curve isn't steep enough. Finding the best dust combination to this curve, can therefore not be based on what previously have fitted curves of the same type best. The extinction curve does give one clue to what dust grain sizes need to be in the dust combination. As I have shown with the best-fit dust combinations to the other GRB host galaxy extinction curves, the steeper an extinction curve gets the more of the ultra small dust grain are needed to get a good fit. Likewise the flatter an extinction curve is it is supposed to contain more of the large dust grains, than the steep curves. The flat extinction curve in the right panel of figure 47 should therefore contain a considerable portion of the largest grain sizes. To reproduce the extinction I need both silicate and carbon grains. It is therefore hard to make

a direct comparison with the other GRB 121024A extinction curve's dust combinations since that was pure silicate dust. By having a mix of the two dust types I had to exclude some sizes from the dust composition for it to give a good fit to the observed extinction. This also makes it harder to compare the two fits directly to one another. Looking at the ultra small silicate grains there is needed 52.02% to reproduce the in fit in the right panel of figure 47. This is considerably less than for the fit in the left panel. It would therefore seem like there are indeed needed more of the large grains to fit the flatter of the two extinction curves. One though has to keep in mind that the dust combination used is very different and therefore can't be directly compared. Looking at the dust composition as a whole it does seem reasonable because it contains a good amount of the large grains compared to the curves steepness and the ultra small dust grains are not nearly as dominant in the dust combination as for the very steep curve.

After having examined the two very different extinction curves of the same GRB host galaxy, the best dust combinations to the two curves have shown that by looking at the steepness of the curve one can indeed say something about the need for either large or ultra small dust grains in the dust composition. Very steep curves do need a large percentage of the ultra small grains and flat curves don't.

9.15 GRB 130427A extinction fit

The last GRB host galaxy extinction curve I worked with came from GRB 130427A. This extinction curve was also an SMC like extinction curve, meaning that there is no 2175Å bump and that the extinction curve is steep and featureless. Once more the best dust combination was found to only contain silicate dust. This makes sense since the SMC and the GRB 130427A extinction curve are very similar in shape. Therefore when the best fit dust combination to the SMC extinction curve was pure silicate dust, it would make sense that the best fit dust combination to the GRB 130427A extinction curve also was silicate dust. As mentioned when examining the other GRB host galaxy extinction curves, the steeper an extinction curve is the more of the ultra small dust grains are needed to get a good fit for the observed extinction. Therefore needing 83.85% silicate dust of the sizes $0.001 - 0.009\mu m$ to reproduce the GRB 130427A extinction is reasonable. Especially so when comparing with the other GRB host galaxies I have examined. In table 5 all the dust combinations used to fit the different GRB host galaxies are presented. Here some of the GRB host galaxies have a lower percentage of the ultra small grains than the GRB 130427A. This is in accordance with the data because some of the other GRB host galaxy extinction curves namely those of GRB 100119A and GRB 120119A are less steep than GRB 130427A. Likewise, some of the GRB host galaxies in table 5 need larger percentages of the ultra small dust grains, but these curves are also steeper than GRB 130427A. Therefore having a pure silicate dust combination with 83.85% ultra small silicate grains is a reasonable dust combination for the observed extinction curve.

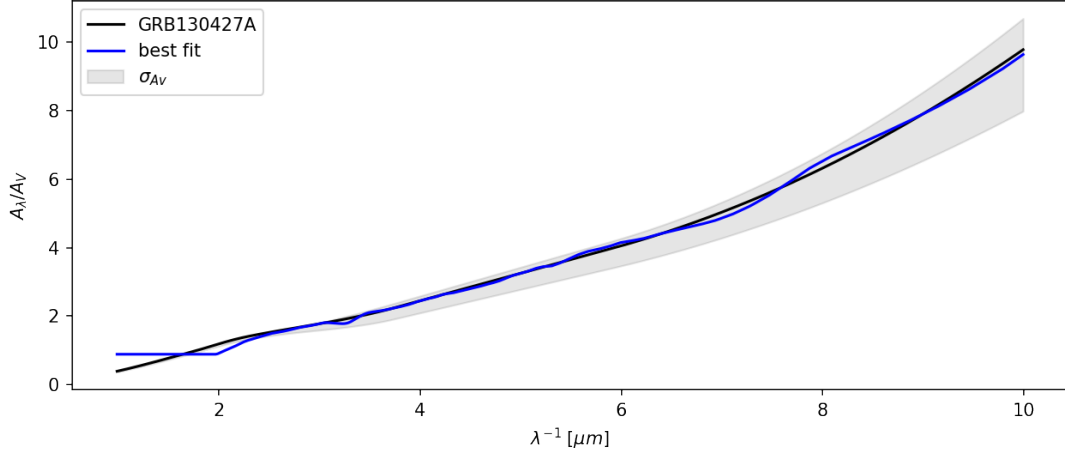


Figure 48: Best fit result of GRB 130427A, using only silicate dust in the size range $0.001 - 0.40\mu m$.

10 Discussion

Having examined all the extinction curves, some tendencies have emerged. Specifically that all the SMC like GRB extinction curves best fits contain only silicate dust and the lack of good fits to the 2175\AA bump for the MW and LMC extinction curves. This naturally gives rise to some questions about the results, like why can't the 2175\AA bump be fitted, with the used dust grains? Why is it silicate dust that gives the best dust combination? Just to name a few. In the next sections, I will try to answer these questions.

10.1 Why can't the 2175\AA bump fitted?

When I was examining the extinction curves of the MW, the LMC and the LMC supershell, I found that the 2175\AA bump in all three cases could be fitted using the silicate grain of the size $0.08\mu m$. The fits had really good RMS and χ^2 values, but the dust compositions were not that realistic since up to 40% of the dust had to have this specific size and be made of silicate. Having nearly half of all the dust in an area of the interstellar medium be of one size and material, is not really realistic, because why would it be this one size and not a similar size that took up 40% of the dust? And secondly, why are there so few of the surrounding dust sizes, should there not be more of these if the dust tended to clump around a specific size? Had it for instance been the sizes $0.05\mu m$ or $0.10\mu m$ that had been the dominant size the bump would not be fitted. Neither would it have been fitted had there been a larger percentage of the dust grain size between $0.05\mu m$ and $0.10\mu m$. All this strongly suggest that the dust combination cannot be right. So why is it that the realistic dust combinations without the 40% of one dust grain size can not fit the 2175\AA bump as I have shown for the three extinction curves?

The first suggestion would be that I lack dust grain sizes of the right material. It has been suggested that to get a good fit for the 2175Å bump one have to either use PAHs [19] or graphite grains. Currently, there are no available complex refractive index of a good PAH mix, leaving me unable to test if PAH could be reasonable for the bump. On the other hand, there are measurements of graphite, meaning that I could in principle test if graphite gives a good fit. The problem with graphite is that it can not explain the behaviour of the 2175Å bump [6]. By behaviour is meant that depending on the sightline in the MW, the 2175Å bump has slightly different FWHM [6]. Using graphite to fit the bump would not be able to give a good fit to all the sightlines leaving it unlikely to be the true material reasonable for the 2175Å bump [6]. My suggestion would therefore be that I can not fit the 2175Å bump because I lack the right material to do so.

10.2 Why is it silicate dust that gives the best dust combination?

The other major question left by the results is why does there only need to be silicate dust in the dust composition for the SMC and the GRB host galaxies? Before I try to answer that question, lest take a closer look at the GRB host galaxies themselves. Since all the GRB host galaxy extinction curves behave like the SMC extinction curve it would be natural to think that they had some similar properties that favoured an SMC like extinction curve and hence silicate dust. This could for example be that all the GRB host galaxies had SMC like metallicity, which would grant the possibility of having the same dust composition and extinction curve. In table 6 all the GRB host galaxy metallicities are listed. Looking at these there is not a clear pattern of SMC like metallicities. About half of the GRB host galaxies have metallicities that are larger than the SMC. The metallicity alone can therefore not explain why all the GRB host galaxy extinction curves are SMC like and favour silicate dust. Examining table 6 further does not indicate that there is a clear pattern all these GRB host galaxies follow that could explain why all the extinction curves are SMC like or why they favour silicate dust. Granted all the GRB host galaxy extinction curves have an R_V value between 2 and 3, but so does the MW, LMC and SMC extinction curves. R_V can therefore not be used as an indicator for extinction curve type. There is therefore no obvious reason as to why all the GRB host galaxy extinction curves are SMC like. This also still leaves my original question unanswered and possibly even more interesting. Because why do 10 somewhat different GRB host galaxies and the SMC only need silicate dust in order to reproduce the observed extinction?

	z [18]	Metallicity		R_V [18]	A_V [18]
GRB 090313A	3.373	[Fe/H]=-1.4±0.3 [37]	< SMC	2.67 ± 0.17	0.34 ± 0.06
GRB 100219A	4.667	[S/H]=-1.1±0.2 [37]	< SMC	2.65 ± 0.09	0.14 ± 0.03
GRB 100418A	0.624	12+log(O/H)=8.52±0.10 [38]	LMC like	2.42 ± 0.10	0.12 ± 0.03
GRB 100901A	1.408	-		3.01 ± 0.11	0.25 ± 0.08
GRB 111008A	4.990	[S/H]=-1.70±0.10 [37]	< SMC	2.47 ± 0.09	0.12 ± 0.04
GRB 111209A	0.677	12+log(O/H)=7.95±0.30 [38]	SMC like	2.53 ± 0.15	0.18 ± 0.08
GRB 120119A	1.728	12+log(O/H)=8.60±0.14 [38]	MW like	2.99 ± 0.24	1.02 ± 0.11
GRB 120815A	2.358	[Zn/H]=-1.15±0.12 [39]	< SMC	2.38 ± 0.09	0.19 ± 0.04
GRB 121024A	2.300	12+log(O/H)=8.41±0.12 [38]	LMC like	2.81 ± 0.20	0.26 ± 0.07
GRB 130427A	0.340	12+log(O/H)=8.57±0.13 [38]	MW like	2.92 ± 0.19	0.11 ± 0.04

Table 6: Overview over some general properties of the GRB host galaxy extinction curves and GRB host galaxies. It has not been possible to find the metallicity of GRB 100901A. The column next to the metallicities shows if the metallicity is closer to the SMC [40], LMC [41], MW [42] or lower than the SMC metallicity [43, 44, 45].

In the beginning of this thesis I wrote that the most common types of dust were the silicate and carbon based dust as well as the smaller group of possible iron based dust. Looking closer at the individual dust groups can therefore give an idea of why the dust aren't present in the extinction curves. Iron has long been suspected to play an important role in the dust composition as it is one of the most abundant elements [46]. It is thought to either be present as metallic iron dust, iron oxides or part of the silicate dust such as the pyroxenes family. If all the iron is locked up in the silicate dust it will not show up as its own group of dust, since it would be an essential part of the silicate dust. If this was the case it would therefore make sense that iron is not part of the dust composition. Looking at observations there is evidence that suggests a large part of the iron is indeed locked in the silicate dust and therefore don't show up in the dust composition [46]. This leaves whatever iron there is left to either be metallic iron dust or iron oxide. Both metallic iron and iron oxide are constant in their extinction across all wavelengths in the examined extinction curves [36], in this case meaning the wavelength range $0.1 - 1\mu m$. Since the iron and iron oxide extinction are constant it leaves the remaining iron dust harder to detect in the total extinction, because adding the remaining iron dust is equal to adding a scalar to the extinction. This means that adding iron dust will not change the shape of the extinction curve but only change the max/minimum A_λ/A_V of the total extinction. Therefore not having iron dust in the dust composition can be explained by the iron's constant extinction, which leaves it harder to detect.

Since the lack of iron-based dust in the dust composition can be explained, it leaves the question of why the carbon doesn't show up in the dust composition when the silicate dust clearly does. When examining different dust models many different version of carbon dust is suggested as the major carbon dust type. Most of the models use graphite as their preferred dust type. In this thesis, I have used benzene as the carbon dust and not graphite. This could explain why I don't need carbon dust in the SMC dust composition when others who are using graphite as the dust type do need it [19]. Graphite is also suggested to play a major part in fitting the 2175Å bump [19, 36]. In most cases, graphite dust is introduced to fit the 2175Å bump, but since the extinction curves whose dust composition only contained silicate dust lacks the 2175Å bump, does graphite or carbon dust then need to be part of the dust composition? If carbon dust truly is responsible for the 2175Å bump, then not having a bump could be a sign of not needing a large amount of carbon dust. Examining the MW and LMC extinction curves showed that when the bump became less dominant in the LMC supershell extinction curve the carbon percentages went down. Therefore not having the 2175Å bump could explain why there is no carbon dust in the dust composition for these curves. Also looking at figure 18 one sees the individual extinction of the carbon grains used in the fit are more or less constant in Q_{ext} across the wavelengths. This would mean that the carbon grains would have the same effect as the iron grains, where they act as a constant that changes the max/minimum A_λ/A_V , but don't affect the shape of the extinction curve.

Lastly there is some evidence for the silicate dust being more dominant in determining the extinction curve shape than originally thought. In [46] they find that when carbon is not the dominant dust type, based on measured Si and Fe abundances for the host galaxies, the extinction curve is much more likely to be featureless like the SMC extinction curve, because of the presence of silicate dust. If this is indeed the case it would explain why all the GRB host galaxy extinction curves are featureless even though it is only one of them that have SMC metallicity. Furthermore, it would explain why the dust composition only need silicate dust, since the silicate dust dominates the dust content and hence the extinction. Looking at the dust compositions I have found for all the GRB host galaxy extinction curves and the SMC curve, they would suggest that this is indeed the case. The lack of other dust types in the dust composition can therefore be attributed to the lack of carbon and iron dust in the actual dust, making a dust composition containing mainly silicates the natural outcome. Having only silicates in the dust composition is therefore not as strange as it initially sounds when looking closer at what dust dominates the extinction curve shape.

11 Conclusion and outlook

Interstellar dust is an important part of every galaxy but it has long been a mystery what it is made of. At the end of the 20th century the first dust models trying to describe the dust composition in the MW, LMC and SMC emerged. The silicate and carbon dust model quickly became the most popular model. Since then the dust in the three galaxies have been examined thoroughly and the preferred dust composition is still silicate and carbon dust, though the type of carbon preferred has changed over the years. In this thesis, I find that the best dust composition for the MW and the LMC is consistent with the silicate and carbon model being the best. I also find that the MW indeed needs a larger percentage of carbon dust than the LMC extinction curves. This is consistent with other studies of the MW and LMC extinction curve [1]. I have not been able to fit the 2175Å bump for the MW and LMC extinction curves. This is mostly due to the type of carbon dust used as it is suspected the bump originates from either graphite or PAHs. Further examination of the extinction curves is therefore needed in order to confirm what carbon type is responsible for the bump. The SMC extinction curve differs from both the MW and LMC extinction curves since it lacks the 2175Å bump. The lack of the bump in the extinction curves leads to a different dust profile for the galaxy. I find that the best dust composition from the SMC is obtained only using silicate dust. This is in agreement with the study in [1]. For a while, these were the only galaxies in which we could study the extinction curves in detail. Within the last ~ 10 years it has become possible to find the extinction curves of GRB host galaxies opening up for the study of dust compositions in faraway galaxies. In this thesis, I have examined extinction curves from 10 different GRB host galaxies, all of which were featureless. For all the extinction curves I find that the best dust composition is made of silicate dust only. This makes sense since silicate dust dominates the extinction curve shape if carbon is not the dominant dust component [46]. The study in [46] includes 7 out of the 10 GRBs I have examined and find this to be the case for all the GRB extinction curves include in their sample. That I, therefore, find the dust composition of all the GRB host galaxy extinction curves to contain only silicate dust is justifiable.

In the future it would be interesting to examine a larger sample of GRB extinction curves once they become available, to see if the silicate dust tendency is universal. Likewise, it would also be interesting to fit some of the GRB extinction curves that behave more like the LMC and the MW to see if the dust compositions in these cases also would be similar to their extinction curve type. Staying with the MW and the LMC extinction curves adding PAH dust grains to the best dust composition, once a refractive index becomes available, would be interesting to see if the 2175Å bump finally can be fitted with a realistic dust composition. Likewise trying other forms of carbon or silicates grains would be interesting to see how the dust composites would behave and what effect other materials would have on the reproduced extinction. There are therefore several topics that could be explored more in-depth in the future.

12 Litterateur

- [1] Y. C. Pei, “Interstellar Dust from the Milky Way to the Magellanic Clouds,” *apj*, vol. 395, p. 130, Aug. 1992.
- [2] K. D. Gordon, G. C. Clayton, K. A. Misselt, A. U. Landolt, and M. J. Wolff, “A Quantitative Comparison of the Small Magellanic Cloud, Large Magellanic Cloud, and Milky Way Ultraviolet to Near-Infrared Extinction Curves,” *apj*, vol. 594, no. 1, pp. 279–293, Sep. 2003.
- [3] J. S. Mathis, W. Ruml, and K. H. Nordsieck, “The size distribution of interstellar grains.” *apj*, vol. 217, pp. 425–433, Oct. 1977.
- [4] B. Draine, *Physics of the Interstellar and Intergalactic Medium*, ser. Princeton Series in Astrophysics. Princeton University Press, 2011, Chapter 21.
- [5] B. S. Hensley and B. T. Draine, “Observational Constraints on the Physical Properties of Interstellar Dust in the Post-Planck Era,” *apj*, vol. 906, no. 2, p. 73, Jan. 2021.
- [6] B. T. Draine, “Interstellar Dust Grains,” *araa*, vol. 41, pp. 241–289, Jan. 2003.
- [7] B. Draine, *Physics of the Interstellar and Intergalactic Medium*, ser. Princeton Series in Astrophysics. Princeton University Press, 2011, Chapter 23.
- [8] J. Bland-Hawthorn and O. Gerhard, “The Galaxy in Context: Structural, Kinematic, and Integrated Properties,” *araa*, vol. 54, pp. 529–596, Sep. 2016.
- [9] A. Mann, “Hidden history of the milky way revealed by extensive star maps,” [accessed 08-March-2021]. [Online]. Available: <https://www.nature.com/articles/d41586-019-00123-y>
- [10] E. Brunier, “Magellanic clouds — irregular dwarf galaxies,” [accessed 08-March-2021]. [Online]. Available: <https://www.eso.org/public/images/b01/>
- [11] R. P. van der Marel, D. R. Alves, E. Hardy, and N. B. Suntzeff, “New Understanding of Large Magellanic Cloud Structure, Dynamics, and Orbit from Carbon Star Kinematics,” *aj*, vol. 124, no. 5, pp. 2639–2663, Nov. 2002.
- [12] F. Galliano, M. Galametz, and A. P. Jones, “The Interstellar Dust Properties of Nearby Galaxies,” *araa*, vol. 56, pp. 673–713, Sep. 2018.
- [13] D. Graczyk, G. Pietrzyński, I. B. Thompson, W. Gieren, B. Pilecki, P. Konorski, A. Udalski, I. Soszyński, S. Villanova, M. Górski, K. Suchomska, P. Karczmarek, R.-P. Kudritzki, F. Bresolin, and A. Gallenne, “The Araucaria Project. The Distance to the Small Magellanic Cloud from Late-type Eclipsing Binaries,” *apj*, vol. 780, no. 1, p. 59, Jan. 2014.

- [14] S. C. Russell and M. A. Dopita, “Abundances of the Heavy Elements in the Magellanic Clouds. III. Interpretation of Results,” *apj*, vol. 384, p. 508, Jan. 1992.
- [15] A. MacFadyen, “Long gamma-ray bursts,” *Science*, vol. 303, no. 5654, pp. 45–46, 2004.
- [16] J. Bolmer, J. Greiner, T. Krühler, P. Schady, C. Ledoux, N. R. Tanvir, and A. J. Levan, “Dust reddening and extinction curves toward gamma-ray bursts at $z \lesssim 4$,” *aap*, vol. 609, p. A62, Jan. 2018.
- [17] J. Selsing, D. Malesani, P. Goldoni, J. P. U. Fynbo, T. Krühler, L. A. Antonelli, M. Arab-salmani, J. Bolmer, Z. Cano, L. Christensen, S. Covino, P. D’Avanzo, V. D’Elia, A. De Cia, A. de Ugarte Postigo, H. Flores, M. Friis, A. Gomboc, J. Greiner, P. Groot, F. Hammer, O. E. Hartoog, K. E. Heintz, J. Hjorth, P. Jakobsson, J. Japelj, D. A. Kann, L. Kaper, C. Ledoux, G. Leloudas, A. J. Levan, E. Maiorano, A. Melandri, B. Milvang-Jensen, E. Palazzi, J. T. Palmerio, D. A. Perley, E. Pian, S. Piranomonte, G. Pugliese, R. Sánchez-Ramírez, S. Savaglio, P. Schady, S. Schulze, J. Sollerman, M. Sparre, G. Tagliaferri, N. R. Tanvir, C. C. Thöne, S. D. Vergani, P. Vreeswijk, D. Watson, K. Wiersema, R. Wijers, D. Xu, and T. Zafar, “The X-shooter GRB afterglow legacy sample (XS-GRB),” *aap*, vol. 623, p. A92, Mar. 2019.
- [18] T. Zafar, D. Watson, P. Møller, J. Selsing, J. P. U. Fynbo, P. Schady, K. Wiersema, A. J. Levan, K. E. Heintz, A. de Ugarte Postigo, V. D’Elia, P. Jakobsson, J. Bolmer, J. Japelj, S. Covino, A. Gomboc, and Z. Cano, “VLT/X-shooter GRBs: Individual extinction curves of star-forming regions,” *mnras*, vol. 479, no. 2, pp. 1542–1554, Sep. 2018.
- [19] J. C. Weingartner and B. T. Draine, “Dust Grain-Size Distributions and Extinction in the Milky Way, Large Magellanic Cloud, and Small Magellanic Cloud,” *apj*, vol. 548, no. 1, pp. 296–309, Feb. 2001.
- [20] R. Maiolino, R. Schneider, E. Oliva, S. Bianchi, A. Ferrara, F. Mannucci, M. Pedani, and M. Roca Sogorb, “A supernova origin for dust in a high-redshift quasar,” *nat*, vol. 431, no. 7008, pp. 533–535, Sep. 2004.
- [21] D. Griffiths, *Introduction to electrodynamics*. Pearson, 2013, Chapter 9.
- [22] R. e. a. Rennie, *Dictionary of physics*. Oxford university press, 2015.
- [23] B. Draine, *Physics of the Interstellar and Intergalactic Medium*, ser. Princeton Series in Astrophysics. Princeton University Press, 2011, Chapter 22.
- [24] B. T. Draine and P. J. Flatau, “Discrete-dipole approximation for scattering calculations,” *J. Opt. Soc. Am. A*, vol. 11, no. 4, pp. 1491–1499, Apr 1994. [Online]. Available: <http://josaa.osa.org/abstract.cfm?URI=josaa-11-4-1491>

- [25] —, “User guide for the discrete dipole approximation code *ddscat* 7.3,” 2013.
- [26] V. G. Zubko, V. Mennella, L. Colangeli, and E. Bussoletti, “Optical constants of cosmic carbon analogue grains - I. Simulation of clustering by a modified continuous distribution of ellipsoids,” *mnras*, vol. 282, no. 4, pp. 1321–1329, Oct. 1996.
- [27] B. T. Draine, “Scattering by Interstellar Dust Grains. I. Optical and Ultraviolet,” *apj*, vol. 598, no. 2, pp. 1017–1025, Dec. 2003.
- [28] —, “Scattering by Interstellar Dust Grains. II. X-Rays,” *apj*, vol. 598, no. 2, pp. 1026–1037, Dec. 2003.
- [29] H. Scheffler, A. Armstrong, and H. Elsässer, *Physics of the Galaxy and Interstellar Matter*, ser. Astronomy and Astrophysics Library. Springer Berlin Heidelberg, 2012. Page 158, [accessed 11-January-2021]. [Online]. Available: <https://books.google.dk/books?id=HjLzCAAQBAJ>
- [30] H. Karttunen, P. Kröger, H. Oja, M. Poutanen, and K. Donner, *Fundamental Astronomy*. Springer Berlin Heidelberg, 2007. Page 309, [accessed 16-April-2021]. [Online]. Available: <https://books.google.dk/books?id=DjeVdb0sLEAC>
- [31] [numpy.org](https://numpy.org/doc/stable/reference/generated/numpy.interp.html), “*numpy.interp*,” [accessed 20-November-2020]. [Online]. Available: <https://numpy.org/doc/stable/reference/generated/numpy.interp.html>
- [32] [math.hws.edu](https://math.hws.edu/javamath/ryan/ChiSquare.html), “The chi square statisitc,” [accessed 16-April-2021]. [Online]. Available: <https://math.hws.edu/javamath/ryan/ChiSquare.html>
- [33] [scikit learn.org](https://scikit-learn.org/stable/modules/generated/sklearn.metrics.mean_squared_error.html), “*sklearn.metrics.squared_mean_error*,” [accessed 16-April-2021]. [Online]. Available: https://scikit-learn.org/stable/modules/generated/sklearn.metrics.mean_squared_error.html
- [34] [statweb.stanford.edu](http://statweb.stanford.edu/~susan/courses/s60/split/node60.html), “Rms error,” [accessed 16-April-2021]. [Online]. Available: <http://statweb.stanford.edu/~susan/courses/s60/split/node60.html>
- [35] M. Friis, A. De Cia, T. Krühler, J. P. U. Fynbo, C. Ledoux, P. M. Vreeswijk, D. J. Watson, D. Malesani, J. Gorosabel, R. L. C. Starling, P. Jakobsson, K. Varela, K. Wiersema, A. P. Drachmann, A. Trotter, C. C. Thöne, A. de Ugarte Postigo, V. D’Elia, J. Elliott, M. Maturi, P. Goldoni, J. Greiner, J. Haislip, L. Kaper, F. Knust, A. LaCluyze, B. Milvang-Jensen, D. Reichart, S. Schulze, V. Sudilovsky, N. Tanvir, and S. D. Vergani, “The warm, the excited, and the molecular gas: GRB 121024A shining through its star-forming galaxy,” *mnras*, vol. 451, no. 1, pp. 167–183, Jul. 2015.
- [36] N. V. Voshchinnikov, V. B. Il’in, T. Henning, and D. N. Dubkova, “Dust extinction and absorption: the challenge of porous grains,” *aap*, vol. 445, no. 1, pp. 167–177, Jan. 2006.

- [37] M. Arabsalmani, P. Møller, J. P. U. Fynbo, L. Christensen, W. Freudling, S. Savaglio, and T. Zafar, “On the mass-metallicity relation, velocity dispersion, and gravitational well depth of GRB host galaxies,” *mnras*, vol. 446, no. 1, pp. 990–999, Jan. 2015.
- [38] T. Krühler, D. Malesani, J. P. U. Fynbo, O. E. Hartoog, J. Hjorth, P. Jakobsson, D. A. Perley, A. Rossi, P. Schady, S. Schulze, N. R. Tanvir, S. D. Vergani, K. Wiersema, P. M. J. Afonso, J. Bolmer, Z. Cano, S. Covino, V. D’Elia, A. de Ugarte Postigo, R. Filgas, M. Friis, J. F. Graham, J. Greiner, P. Goldoni, A. Gomboc, F. Hammer, J. Japelj, D. A. Kann, L. Kaper, S. Klose, A. J. Levan, G. Leloudas, B. Milvang-Jensen, A. Nicuesa Guelbenzu, E. Palazzi, E. Pian, S. Piranomonte, R. Sánchez-Ramírez, S. Savaglio, J. Selsing, G. Tagliferri, P. M. Vreeswijk, D. J. Watson, and D. Xu, “GRB hosts through cosmic time. VLT/X-Shooter emission-line spectroscopy of 96 γ -ray-burst-selected galaxies at $0.1 < z < 3.6$,” *aap*, vol. 581, p. A125, Sep. 2015.
- [39] T. Krühler, C. Ledoux, J. P. U. Fynbo, P. M. Vreeswijk, S. Schmidl, D. Malesani, L. Christensen, A. De Cia, J. Hjorth, P. Jakobsson, and et al., “Molecular hydrogen in the damped Lyman- α system towards grb 120815a at $z = 2.36$,” *Astronomy & Astrophysics*, vol. 557, p. A18, Aug 2013. [Online]. Available: <http://dx.doi.org/10.1051/0004-6361/201321772>
- [40] K. M. Sandstrom, A. D. Bolatto, B. T. Draine, C. Bot, and S. Stanimirovic, “The Spitzer Surveys of the Small Magellanic Cloud: Insights into the Life-Cycle of Polycyclic Aromatic Hydrocarbons,” in *EAS Publications Series*, ser. EAS Publications Series, C. Joblin and A. G. G. M. Tielens, Eds., vol. 46, Mar. 2011, pp. 215–221.
- [41] C. Kobulnicky and D. Zaritsky, “Chemical Properties of Star-Forming Emission Line Galaxies at $z=0.1 - 0.5$,” in *American Astronomical Society Meeting Abstracts*, ser. American Astronomical Society Meeting Abstracts, vol. 193, Dec. 1998, p. 03.07.
- [42] H.-W. Chen, S. D. Johnson, L. A. Straka, F. S. Zahedy, J. Schaye, S. Muzahid, N. Bouché, S. Cantalupo, R. A. Marino, and M. Wendt, “Characterizing circumgalactic gas around massive ellipticals at $z \approx 0.4$ - III. The galactic environment of a chemically pristine Lyman limit absorber,” *mnras*, vol. 484, no. 1, pp. 431–441, Mar. 2019.
- [43] S. Choudhury, A. Subramaniam, A. A. Cole, and Y. J. Sohn, “Photometric metallicity map of the Small Magellanic Cloud,” *mnras*, vol. 475, no. 4, pp. 4279–4297, Apr. 2018.
- [44] A. J. Fox, P. Richter, B. P. Wakker, N. Lehner, J. C. Howk, N. Ben Bekhti, J. Bland-Hawthorn, and S. Lucas, “The COS/UVES Absorption Survey of the Magellanic Stream. I. One-tenth Solar Abundances along the Body of the Stream,” *apj*, vol. 772, no. 2, p. 110, Aug. 2013.

- [45] D. E. Welty, J. T. Lauroesch, J. C. Blades, L. M. Hobbs, and D. G. York, “Interstellar Abundances in the Magellanic Clouds. I. GHRS Observations of the Small Magellanic Cloud Star Sk 108,” *apj*, vol. 489, no. 2, pp. 672–692, Nov. 1997.
- [46] T. Zafar, K. E. Heintz, A. Karakas, J. Lattanzio, and A. Ahmad, “Silicon and iron dust in gamma-ray burst host galaxy absorbers,” *Monthly Notices of the Royal Astronomical Society*, vol. 490, no. 2, p. 2599–2605, Oct 2019. [Online]. Available: <http://dx.doi.org/10.1093/mnras/stz2827>

A Fitting routine raw code

In the next pages is included the entire fitting routine used to make the fits of the GRB host galaxy, the MW, LMC and SMC extinction curves. This includes the fitting function for the six and two bin versions as well as the four bin version shown in the section about setting up the fitting routine. Besides the loop, the most used bins are also included in the code section.

Fitting routine GRB

June 7, 2021

```
[2]: import numpy as np
import matplotlib.pyplot as plt
from scipy.optimize import curve_fit
```

```
[3]: # load data file
data = np.loadtxt('MW_pei.dat')
```

```
[4]: # silicate and carbon grains of different sizes
sil1 = np.loadtxt('astrosil_a0_01',skiprows=14)
sil2 = np.loadtxt('astrosil_a0_02',skiprows=14)
sil3 = np.loadtxt('astrosil_a0_03',skiprows=14)
sil4 = np.loadtxt('astrosil_a0_04',skiprows=14)
sil5 = np.loadtxt('astrosil_a0_05',skiprows=14)
sil6 = np.loadtxt('astrosil_a0_06',skiprows=14)
sil7 = np.loadtxt('astrosil_a0_07',skiprows=14)
sil8 = np.loadtxt('astrosil_a0_08',skiprows=14)
sil9 = np.loadtxt('astrosil_a0_09',skiprows=14)
sil10 = np.loadtxt('astrosil_a0_10',skiprows=14)
sil11 = np.loadtxt('astrosil_a0_15',skiprows=14)
sil12 = np.loadtxt('astrosil_a0_20',skiprows=14)
sil13 = np.loadtxt('astrosil_a0_25',skiprows=14)
sil14 = np.loadtxt('astrosil_a0_30',skiprows=14)
sil15 = np.loadtxt('astrosil_a0_35',skiprows=14)
sil16 = np.loadtxt('astrosil_a0_40',skiprows=14)
sil17 = np.loadtxt('astrosil_a0_001',skiprows=14)
sil18 = np.loadtxt('astrosil_a0_002',skiprows=14)
sil19 = np.loadtxt('astrosil_a0_003',skiprows=14)
sil20 = np.loadtxt('astrosil_a0_004',skiprows=14)
sil21 = np.loadtxt('astrosil_a0_005',skiprows=14)
sil22 = np.loadtxt('astrosil_a0_006',skiprows=14)
sil23 = np.loadtxt('astrosil_a0_007',skiprows=14)
sil24 = np.loadtxt('astrosil_a0_008',skiprows=14)
sil25 = np.loadtxt('astrosil_a0_009',skiprows=14)
zub1 = np.loadtxt('zubko_a0_01',skiprows=14)
zub2 = np.loadtxt('zubko_a0_02',skiprows=14)
zub3 = np.loadtxt('zubko_a0_03',skiprows=14)
zub4 = np.loadtxt('zubko_a0_04',skiprows=14)
zub5 = np.loadtxt('zubko_a0_05',skiprows=14)
```

```

zub6 = np.loadtxt('zubko_a0_06',skiprows=14)
zub7 = np.loadtxt('zubko_a0_07',skiprows=14)
zub8 = np.loadtxt('zubko_a0_08',skiprows=14)
zub9 = np.loadtxt('zubko_a0_09',skiprows=14)
zub10 = np.loadtxt('zubko_a0_10',skiprows=14)
zub11 = np.loadtxt('zubko_a0_15',skiprows=14)
zub12 = np.loadtxt('zubko_a0_20',skiprows=14)
zub13 = np.loadtxt('zubko_a0_25',skiprows=14)
zub14 = np.loadtxt('zubko_a0_30',skiprows=14)
zub15 = np.loadtxt('zubko_a0_35',skiprows=14)
zub16 = np.loadtxt('zubko_a0_40',skiprows=14)
zub17 = np.loadtxt('zubko_a0_001',skiprows=14)
zub18 = np.loadtxt('zubko_a0_002',skiprows=14)
zub19 = np.loadtxt('zubko_a0_003',skiprows=14)
zub20 = np.loadtxt('zubko_a0_004',skiprows=14)
zub21 = np.loadtxt('zubko_a0_005',skiprows=14)
zub22 = np.loadtxt('zubko_a0_006',skiprows=14)
zub23 = np.loadtxt('zubko_a0_007',skiprows=14)
zub24 = np.loadtxt('zubko_a0_008',skiprows=14)
zub25 = np.loadtxt('zubko_a0_009',skiprows=14)
zubo = np.loadtxt('zubko_p_o200',skiprows=14)
zubp = np.loadtxt('zubko_p_p200',skiprows=14)
zubr = np.loadtxt('zubko_p_r200',skiprows=14)

```

```
[5]: av = 1.086 # converting factor form Qext to A_lambda
```

```
[6]: AV = data[:,0]
print(np.where((AV > 1.78) & (AV < 1.82)) )# finding inverse wavwlength 1.8 mu m
↳ beacuse that => Av = 1
```

```
(array([2143]),)
```

```
[7]: Av = data[2143,1] # setting the value to make Av = 1 at inverse wavwlength 1.8
↳ mu m
print(Av)
```

```
1.0437833986581184
```

```
[8]: # Bining of grain sizes in A_lambda/Av
msi = (av*sil1[:,2]/Av)+(av*sil2[:,2]/Av)+(av*sil3[:,2]/Av)+(av*sil4[:,2]/
↳ Av)+(av*sil5[:,2]/Av)+(av*sil6[:,2]/Av)
mku = (av*zub1[:,2]/Av)+(av*zub2[:,2]/Av)+(av*zub3[:,2]/Av)+(av*zub4[:,2]/
↳ Av)+(av*zub5[:,2]/Av)+(av*zub6[:,2]/Av)
msi2 = (av*sil7[:,2]/Av)+(av*sil8[:,2]/Av)+(av*sil9[:,2]/Av)+(av*sil10[:,2]/
↳ Av)+(av*sil11[:,2]/Av)+(av*sil12[:,2]/Av)
mku2 = (av*zub7[:,2]/Av)+(av*zub8[:,2]/Av)+(av*zub9[:,2]/Av)+(av*zub10[:,2]/
↳ Av)+(av*zub11[:,2]/Av)+(av*zub12[:,2]/Av)
```

```

msi3 = (av*sil13[:,2]/Av)+(av*sil14[:,2]/Av)+(av*sil15[:,2]/Av)+(av*sil16[:,2]/
↪Av)
mku3 = (av*zub13[:,2]/Av)+(av*zub14[:,2]/Av)+(av*zub15[:,2]/Av)+(av*zub16[:,2]/
↪Av)
msi4 = (av*sil17[:,2]/Av)+(av*sil18[:,2]/Av)+(av*sil19[:,2]/Av)+(av*sil20[:,2]/
↪Av)+(av*sil21[:,2]/Av)+(av*sil22[:,2]/Av)+(av*sil23[:,2]/Av)+(av*sil24[:,2]/
↪Av)+(av*sil25[:,2]/Av)
mku4 = (av*zub17[:,2]/Av)+(av*zub18[:,2]/Av)+(av*zub19[:,2]/Av)+(av*zub20[:,2]/
↪Av)+(av*zub21[:,2]/Av)+(av*zub22[:,2]/Av)+(av*zub23[:,2]/Av)+(av*zub24[:,2]/
↪Av)+(av*zub25[:,2]/Av)
mrns= (av*sil12[:,2]/Av)+(av*sil13[:,2]/Av)+(av*sil14[:,2]/Av)+(av*sil15[:,2]/
↪Av)+(av*sil16[:,2]/Av)+(av*sil17[:,2]/Av)
mrns2= (av*sil18[:,2]/Av)+(av*sil19[:,2]/Av)+(av*sil110[:,2]/Av)+(av*sil111[:,2]/
↪Av)+(av*sil112[:,2]/Av)+(av*sil113[:,2]/Av)
mrnk= (av*zub21[:,2]/Av)+(av*zub22[:,2]/Av)+(av*zub23[:,2]/Av)+(av*zub24[:,2]/
↪Av)+(av*zub25[:,2]/Av)

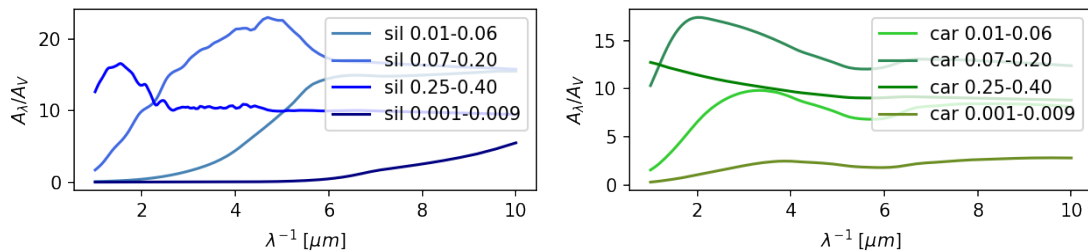
```

```

[9]: # plot of the different bins
plt.figure(figsize=(10,4),dpi=150)
plt.subplot(221)
plt.plot(1/sil1[:,1],msi,'steelblue',label='sil 0.01-0.06')
plt.plot(1/sil6[:,1],msi2,'royalblue',label='sil 0.07-0.20')
plt.plot(1/sil13[:,1],msi3,'b',label='sil 0.25-0.40')
plt.plot(1/sil17[:,1],msi4,'navy',label='sil 0.001-0.009')
plt.legend()
plt.xlabel(r'\$\lambda^{-1} \; [\mu m]\$')
plt.ylabel(r'\$A_{\lambda}/A_V\$')
#plt.ticklabel_format(style='sci', axis='y', scilimits=(0,0))
plt.subplot(222)
plt.plot(1/zub1[:,1],mku,'limegreen',label='car 0.01-0.06')
plt.plot(1/zub6[:,1],mku2,'seagreen',label='car 0.07-0.20')
plt.plot(1/zub13[:,1],mku3,'green',label='car 0.25-0.40')
plt.plot(1/zub17[:,1],mku4,'olivedrab',label='car 0.001-0.009')
plt.legend()
plt.xlabel(r'\$\lambda^{-1} \; [\mu m]\$')
plt.ylabel(r'\$A_{\lambda}/A_V\$')

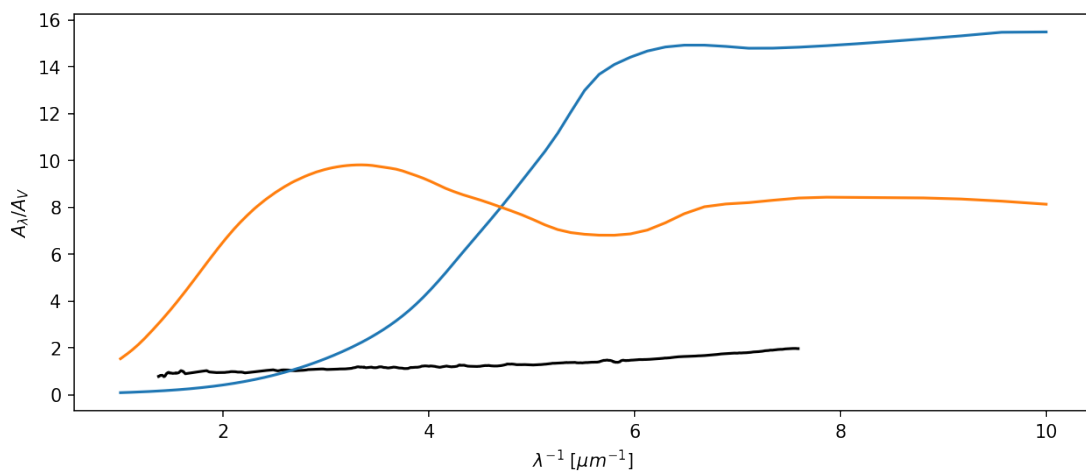
```

[9]: Text(0, 0.5, '\$A_{\lambda}/A_V\$')



```
[10]: # comparing bins to data
plt.figure(figsize=(10,4),dpi=150)
plt.plot(data[:,0],data[:,1]/Av,'k',label='LMC average')
plt.plot(1/sil1[:,1],msi)
plt.plot(1/zub1[:,1],mku)
plt.xlabel(r'$\lambda^{-1}$ \; [\mu m^{-1}]$')
plt.ylabel(r'$A_{\lambda}/A_V$')
```

```
[10]: Text(0, 0.5, '$A_{\lambda}/A_V$')
```



```
[37]: #setting the combination of dust to fit
specs = np.array([msi2,msi3,msi4,msi])

# setting initial conditions
a = [0.02,0.02,0.02,0.02,0.02,0.02]
b = [0.08,0.08,0.08,0.08,0.08,0.08]
```

```
[38]: from sklearn.metrics import mean_squared_error
```

```
[39]: def fitfunc6(Nt,runs): #very slow version 6 bin version
    linit = a
    uinit = b

    for ir in range(runs):
        kul = np.linspace(linit[0],uinit[0],Nt)
        sil = np.linspace(linit[1],uinit[1],Nt)
        kul2 = np.linspace(linit[2],uinit[2],Nt)
        sil2 = np.linspace(linit[3],uinit[3],Nt)
```

```

    kul3 = np.linspace(linit[4],uinit[4],Nt)
    sil3 = np.linspace(linit[5],uinit[5],Nt)
    scoretabel = np.zeros([Nt**6,7])
    i = 0
    for a1 in range(Nt):
        for a2 in range(Nt):
            for a3 in range(Nt):
                for a4 in range (Nt):
                    for a5 in range (Nt):
                        for a6 in range (Nt):
                            const = np.
↪array([kul[a1],sil[a2],kul2[a3],sil2[a4],kul3[a5],sil3[a6]])
                            fixed =
↪specs[0]*const[0]+specs[1]*const[1]+specs[2]*const[2]+specs[3]*const[3]
↪+specs[4]*const[4]+specs[5]*const[5]
                            spe=np.interp(data[:,:-1,0],1/zub1[:,
↪-1,1],fixed[:,:-1])
                            score = np.sqrt(mean_squared_error(spe[:,:-1],
↪data[:,1]/Av))
                            scoretabel[i,:]
↪=[score,kul[a1],sil[a2],kul2[a3],sil2[a4],kul3[a5],sil3[a6]]
                            i = i+1
        bedstvalue = np.unravel_index(np.argmin(scoretabel[:,0]),scoretabel[:,
↪,0].shape)
        bv = bedstvalue[0]
        linit = scoretabel[bv,1:]*0.9
        uinit = scoretabel[bv,1:]*1.1
        const = scoretabel[bv,1:]
    return const

```

```

[40]: def fitfunc4(Nt,runs): #okay time 4 bin version
    linit = a
    uinit = b

    for ir in range(runs):
        kul = np.linspace(linit[0],uinit[0],Nt)
        sil = np.linspace(linit[1],uinit[1],Nt)
        kul2 = np.linspace(linit[2],uinit[2],Nt)
        sil2 = np.linspace(linit[3],uinit[3],Nt)
        scoretabel = np.zeros([Nt**4,5])
        i = 0
        for a1 in range(Nt):
            for a2 in range(Nt):
                for a3 in range(Nt):
                    for a4 in range (Nt):
                        const = np.array([kul[a1],sil[a2],kul2[a3],sil2[a4]])

```

```

        fixed =  $\square$ 
         $\rightarrow$ specs[0]*const[0]+specs[1]*const[1]+specs[2]*const[2]+specs[3]*const[3]
            #spe = np.interp(1/zub16[5:,1],data[:,0],data[:,1]) $\square$ 
         $\rightarrow$ #LMC SMC
            spe=np.interp(data[:,:-1,0],1/zub1[:,:-1,1],fixed[:,:-1]) $\square$ 
         $\rightarrow$ #GRB
            #spe=np.interp(1/data[:,:-1,0],1/zub1[:,:-1,1],fixed[:,:-1])
         $\rightarrow$ -1]) #MW pei
            #spe=np.interp(data[450:,-1,0],1/zub1[:,:-1,1],fixed[:,:-1])
         $\rightarrow$ -1]) #GRB tayaba
            score = np.sqrt(mean_squared_error(spe[:,:-1], data[:,1]/
         $\rightarrow$ Av)) #GRB MW pei
            #score = np.sqrt(mean_squared_error(spe[:,:-1], data[49:
         $\rightarrow$ ,1]/Av)) #GRB tayaba
            #score = np.sqrt(mean_squared_error(fixed[5:], spe[:,])) $\square$ 
         $\rightarrow$ #LMC SMC
            scoretabel[i,:] $\square$ 
         $\rightarrow$ =[score,kul[a1],sil[a2],kul2[a3],sil2[a4]]
            i = i+1
            bedstvalue = np.unravel_index(np.argmin(scoretabel[:,0]),scoretabel[:,
         $\rightarrow$ ,0].shape)
            bv = bedstvalue[0]
            linit = scoretabel[bv,1:]*0.9
            uunit = scoretabel[bv,1:]*1.1
            const = scoretabel[bv,1:]
        return const

```

```

[41]: def fitfunc2(Nt,runs): #fast version 2 bin version
        linit = a
        uunit = b

        for ir in range(runs):
            kul = np.linspace(linit[0],uunit[0],Nt)
            sil = np.linspace(linit[1],uunit[1],Nt)
            scoretabel = np.zeros([Nt**2,3])
            i = 0
            for a1 in range(Nt):
                for a2 in range(Nt):
                    const = np.array([kul[a1],sil[a2]])
                    fixed = specs[0]*const[0]+specs[1]*const[1]
                    spe=np.interp(data[:,:-1,0],1/zub1[:,:-1,1],fixed[:,:-1])
                    score = np.sqrt(mean_squared_error(spe[:,:-1], data[:,1]/Av))
                    scoretabel[i,:] =[score,kul[a1],sil[a2]]
                    i = i+1
                bedstvalue = np.unravel_index(np.argmin(scoretabel[:,0]),scoretabel[:,
         $\rightarrow$ ,0].shape)

```

```

    bv = bedstvalue[0]
    linit = scoresetabel[bv,1:]*0.9
    uinit = scoresetabel[bv,1:]*1.1
    const = scoresetabel[bv,1:]
    return const

```

```

[42]: consti = fitfunc4(10,50)
      print(consti)

```

```

[0.02989101 0.04691319 0.37144286 0.01802974]

```

```

[27]: fix =  $\underline{\quad}$ 
      ↪ specs[0]*consti[0]+specs[1]*consti[1]+specs[2]*consti[2]+specs[3]*consti[3]  $\underline{\quad}$ 
      ↪ #+specs[4,:]*consti[4]+specs[5,:]*consti[5]
      spe=np.interp(data[:,0],1/zub1[:,1],fix[:,1]) #GRB MW

```

```

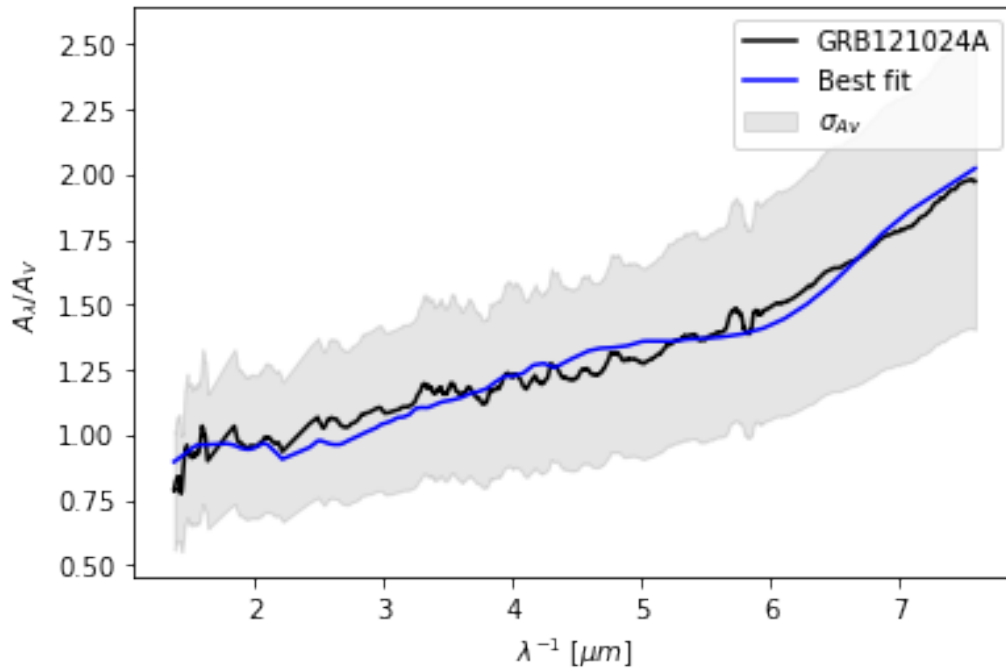
[28]: plt.plot(data[:,0],data[:,1]/Av,'k',label='GRB121024A') #GRB MW
      plt.plot(data[:,0],spe[:,1],'b',label='Best fit')#GRB MW
      #plt.plot(1/zub16[5:,1],np.interp(1/zub16[5:,1],data[:,0],data[:,1]/
      ↪ Av),'k',label='Data') # LMC SMC
      #plt.plot(1/zub16[5:,1],fix[5:], 'b',label='Best fit') # LMC SMC
      #plt.fill_between(data[49:,0],data[49:,2],data[49:,3],color="k",alpha=0.
      ↪ 1,label=r'\sigma_{Av}') #GRB Tayaba
      plt.fill_between(data[:,0],data[:,1]/Av-np.sqrt((((-data[:,1]/(Av**2))*0.
      ↪ 3)**2)),data[:,1]/Av+np.sqrt((((-data[:,1]/Av**2))*0.
      ↪ 3)**2),color="k",alpha=0.1,label=r'\sigma_{Av}') #GRB MW
      plt.xlabel(r'\lambda^{-1} \; [\mu m]')
      plt.ylabel(r'$A_{\lambda}/A_V$')
      plt.legend()
      rms = np.sqrt(mean_squared_error(spe[:,1], data[:,1]/Av)) #GRB MW
      chi2 = np.sum((spe[:,1]-data[:,1]/Av)**2/(data[:,1]/Av)) #GRB MW
      #rms = np.sqrt(mean_squared_error(fix[5:], np.interp(1/zub16[5:,1],data[
      ↪ :,0],data[:,1]))) #LMC SMC
      #chi2 = np.sum((fix[5:]-np.interp(1/zub16[5:,1],data[:,0],data[:,1])/Av)**2/(np.
      ↪ interp(1/zub16[5:,1],data[:,0],data[:,1])/Av))
      print(r'rms',rms,'chi^2',chi2,'std',np.std(spe[:,1])) #GRB MW
      #print(r'rms',rms,'chi^2',chi2,'std',np.std(np.interp(1/zub16[5:,1],data[
      ↪ :,0],data[:,1]))) #LMC SMC

```

```

rms 0.0521878602825071 chi^2 5.763431849095555 std 0.24158804836311196

```



```
[18]: prokul = (consti[0]*100)/np.sum(consti)
prosil = (consti[1]*100)/np.sum(consti)
prokul2 = (consti[2]*100)/np.sum(consti)
prosil2 = (consti[3]*100)/np.sum(consti)
#prokul3 = (consti[4]*100)/np.sum(consti)
#prosil3 = (consti[5]*100)/np.sum(consti)
#print('percentage model dust', prokul, '%', prosil, '%')
print('percentage model dust', prokul, '%', prosil, '%', prokul2, '%', prosil2,
      ↪, '%')
#print('percentage model dust', prokul, '%', prosil, '%', prokul2, '%', prosil2,
      ↪, '%', prokul3, '%', prosil3, '%')
```

```
percentage model dust 8.080952985008384 % 7.333356517919454 %
0.00867625481715823 % 84.577014242255 %
```

```
[ ]:
```

B Mixed dust combination fits of GRB's

Below are included the best fits obtained for the ten GRB host galaxies using a mix of silicate and carbon dust. These are included to show the difference between a pure silicate fit, as shown in the results section, and a fit combining the two dust types.

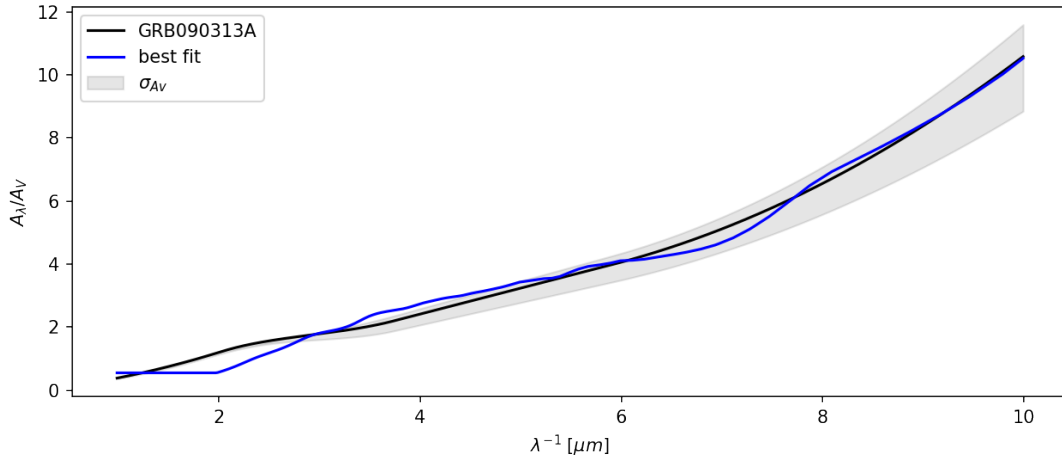


Figure 49: GRB 090313A silicate and carbon dust fit.

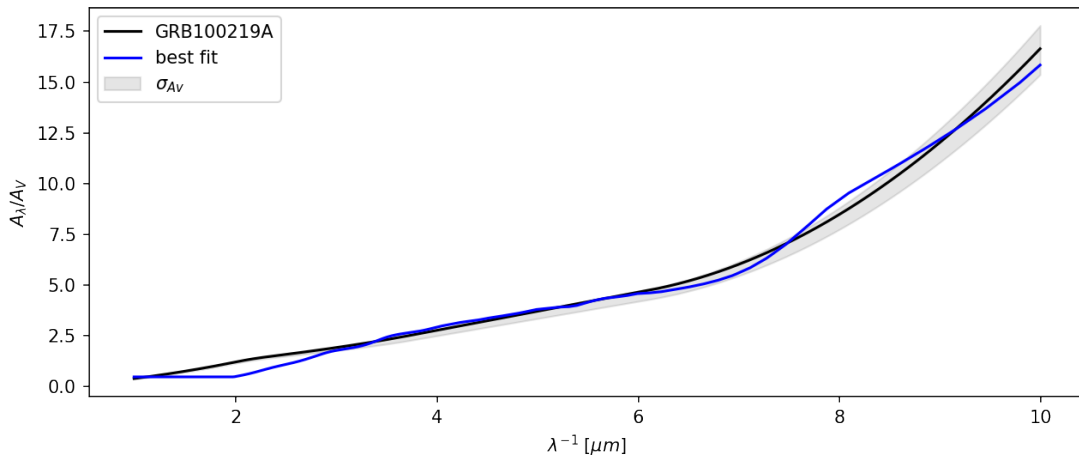


Figure 50: GRB 100219A silicate and carbon dust fit.

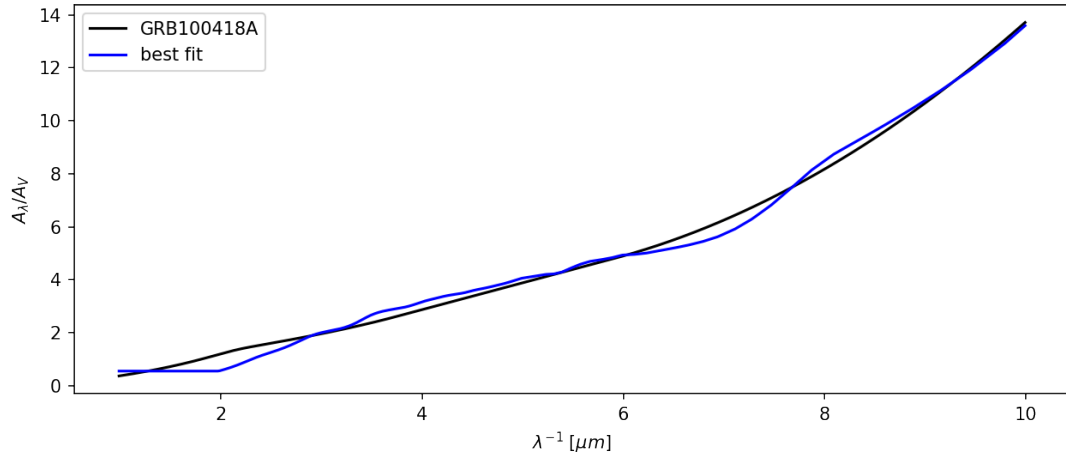


Figure 51: GRB 100418A silicate and carbon dust fit.

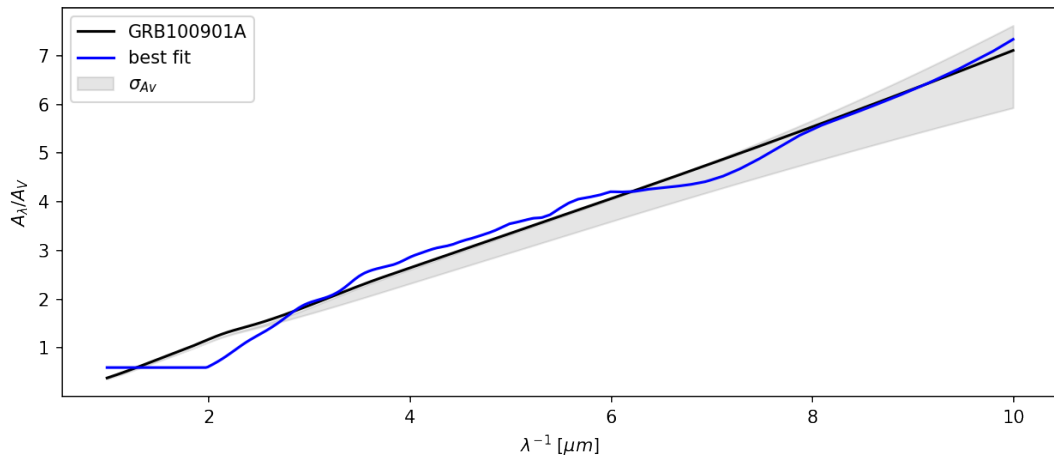


Figure 52: GRB 100901A silicate and carbon dust fit.

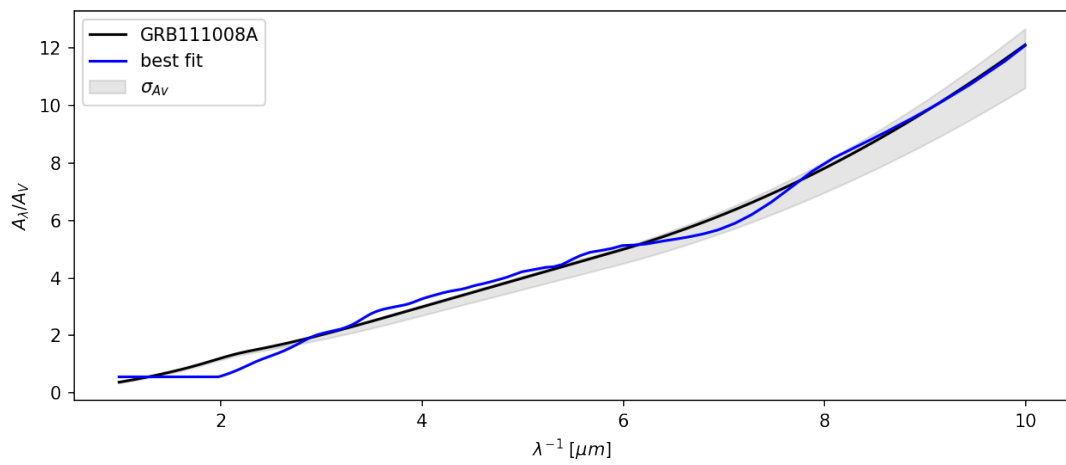


Figure 53: GRB 111008A silicate and carbon dust fit.

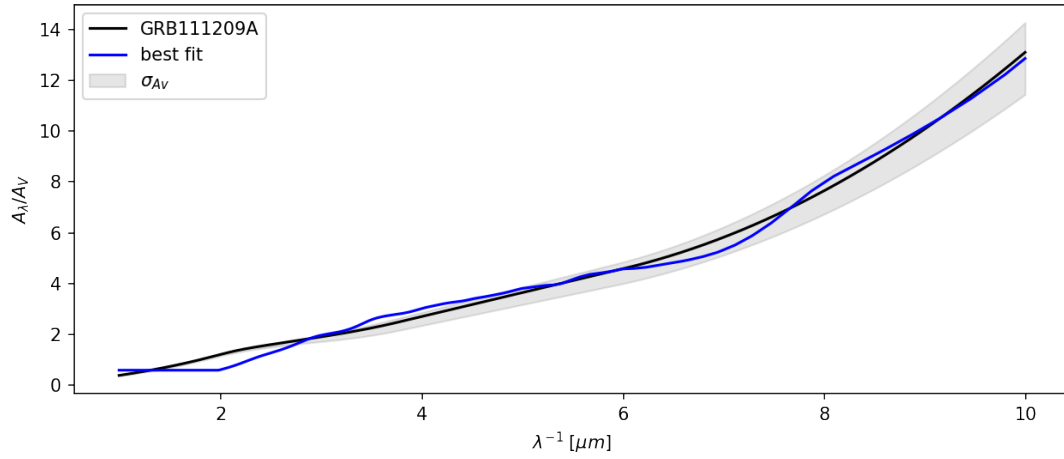


Figure 54: GRB 111209A silicate and carbon dust fit.

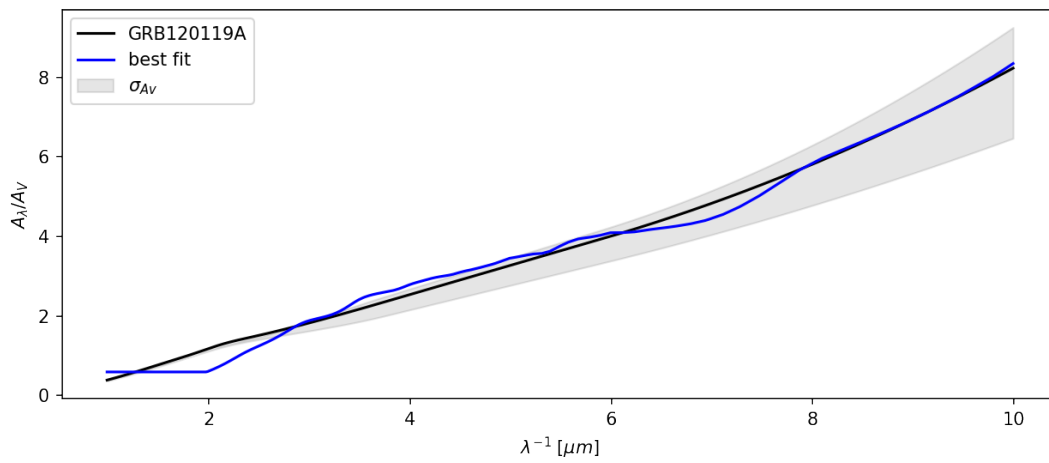


Figure 55: GRB 120119A silicate and carbon dust fit.

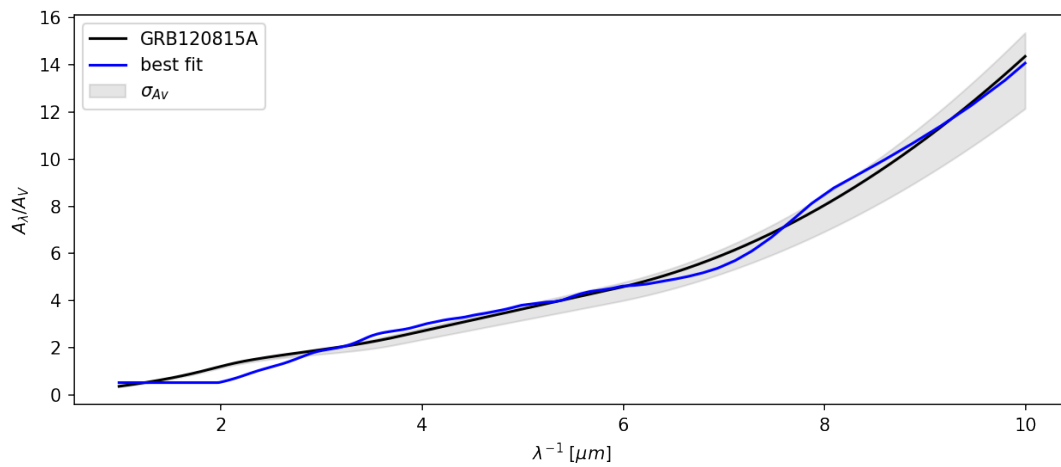


Figure 56: GRB 120815A silicate and carbon dust fit.

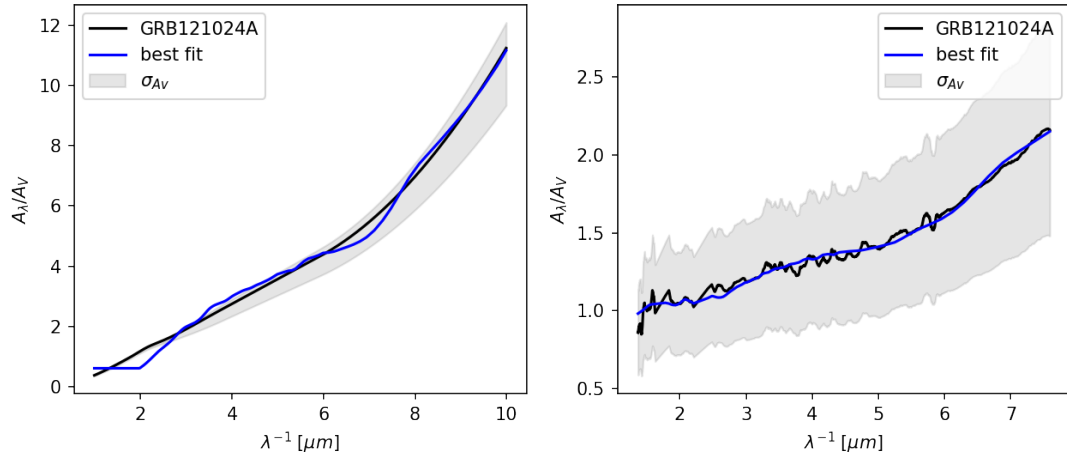


Figure 57: GRB 121024A silicate and carbon dust fit.

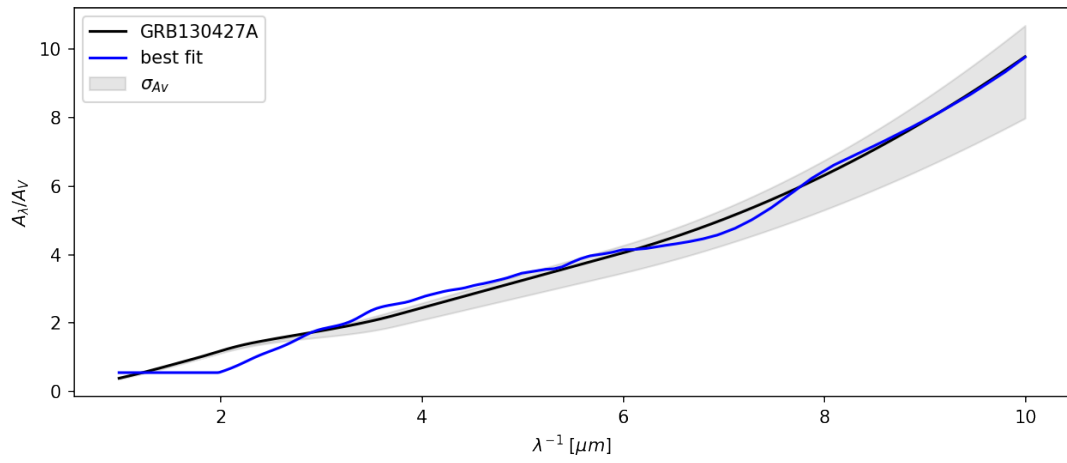


Figure 58: GRB 130427A silicate and carbon dust fit.

		GRB	GRB	GRB	GRB
		090313A	100219A	100418A	100901A
Bin 1	c: $0.04 - 0.20\mu m$	1.44%	0.41%	0.91%	3.29%
Bin 2	s: $0.01 - 0.20\mu m$	5.25%	3.20%	4.85%	10.47%
Bin 3	c: $0.001 - 0.009\mu m$	1.88%	5.78%	2.27%	0.35%
Bin 4	s: $0.001 - 0.009\mu m$	91.43%	90.61%	91.97%	85.89%
RMS		0.26	0.37	0.27	0.21
χ^2		15.86	21.26	14.52	10.76
		GRB	GRB	GRB	GRB
		111008A	111209A	120119A	120815A
Bin 1	c: $0.04 - 0.20\mu m$	1.11%	1.12%	2.47%	0.78%
Bin 2	s: $0.01 - 0.20\mu m$	6.35%	4.53%	7.68%	4.08%
Bin 3	c: $0.001 - 0.009\mu m$	1.72%	2.53%	1.00%	2.96%
Bin 4	s: $0.001 - 0.009\mu m$	90.81%	91.83%	88.85%	92.19%
RMS		0.25	0.27	0.21	0.29
χ^2		13.38	14.29	11.67	16.75
		GRB	GRB		GRB
		121024A	130427A		121024A
Bin 1	c: $0.04 - 0.20\mu m$	1.58%	1.65%	c: $0.01 - 0.06,$ $0.25 - 0.40\mu m$	4.76%
Bin 2	s: $0.01 - 0.20\mu m$	5.30%	6.07%	s: $0.01 - 0.06,$ $0.25 - 0.40\mu m$	7.83%
Bin 3	c: $0.001 - 0.009\mu m$	2.61%	1.43%	c: $0.001 - 0.009\mu m$	35.39%
Bin 4	s: $0.001 - 0.009\mu m$	90.51%	90.85%	s: $0.001 - 0.009\mu m$	52.02%
RMS		0.22	0.24		0.04
χ^2		10.97	14.70		3.08

Table 7: Overview of the different bins used in the silicate and carbon dust combination of the GRB host galaxies. S denotes that the sizes used are silicate dust and C similar is the carbon dust sizes used to make the combination. Included is also the RMS and χ^2 of each fit. For GRB 121024A the last entry in the table corresponds to the bins used to make the right plot of figure 57, whereas entry number 9 corresponds to the left plot of figure 57.